Thermochemistry of cyclic and acyclic radicals and kinetics of their recombination reactions

Thesis

Thermochemistry of Cyclic and Acyclic Radicals and Kinetics of Their Recombination Reactions

by

Steven Charles Guiver, B.Tech.

Faculty of Science
The Open University

October, 1986

Submitted as a partial requirement for the degree of
Doctor of Philosophy
in the discipline of Chemistry

Date of submission: October 1986
Date of award: 20 March 1987

Acknowledgements

The author wishes to express sincere thanks to the following people:

Professor L.J. Haynes for permission to work in the Chemistry Laboratories of the Open University.

Dr. C.J. Harding for his supervision, encouragement and invaluable discussion during the course of the work.

The technical staff of the Chemistry Department for their assistance in the construction of equipment, in particular Mr. J.E. Elliot, Mr. G. Jeffs and Mr. J. Gibb.

The Research Committee of the Open University and the Science and Engineering Research Council for the award of grants received during the course of the work.

Finally, to my wife, Kim, not only for her support, patience and encouragement, but also for the many hours spent typing this thesis. Thank you.

Abstract

The thermochemistry of a series of acyclic and cyclic hydrocarbon radicals has been studied using a radical buffer technique in solution. From these studies radical heats of formation and hydrocarbon carbon-hydrogen bond dissociation energies have been determined. These results are consistent with an increase in hydrocarbon bond dissociation energies over the previously accepted values with $D(C_2H_5\text{-}H)$ = 419 $kJmol^{-1}$, $D(n\text{-}C_3H_7\text{-}H)$ = 418 $kJmol^{-1}$, $D(i\text{-}C_3H_7\text{-}H)$ = 404 $kJmol^{-1}$, $D(c\text{-}C_5H_9\text{-}H)$ = 402 $kJmol^{-1}$, $D(c\text{-}C_6H_{11}\text{-}H)$ = 420 $kJmol^{-1}$ and $D(c\text{-}C_7H_{13}\text{-}H)$ = 400 $kJmol^{-1}$.

The work suggests typical primary carbon-hydrogen bond dissociation energies of 420 $kJmol^{-1}$ and typical secondary carbon-hydrogen bond dissociation energies of 400 $kJmol^{-1}$, although an anomalous result is obtained for cyclohexane. The high value obtained for $D(c\text{-}C_6H_{11}\text{-}H)$ is more typical of a primary than a secondary bond, a result which is considered in terms of ring strain and eclipsing interactions occurring upon formation of cycloalkyl radicals.

Further gas phase studies of the radical buffer reaction allowed relative radical recombination rate constants to be determined for cyclopentyl and cyclohexyl radicals. From these studies the rate constant for cyclopentyl radical recombination was determined as 2.4×10^9 $lmol^{-1}s^{-1}$ and the rate constant for cyclohexyl radical recombination as 1.6×10^9 $lmol^{-1}s^{-1}$, both at 430K.

These results are consistent with radical recombination in the gas phase being collision controlled and are considered in the context of previous suggestions that the cyclohexyl radical recombination rate constant is more than two orders of magnitude lower than that for cyclopentyl recombination.

Contents

Chapter 1

INTRODUCTION

For some time there has been uncertainty regarding the values of thermochemical and kinetic parameters for alkyl radicals. This chapter concerns the theories and experimental procedures employed to determine these quantities.

1.1 Free Radicals

Radicals are generally highly reactive species containing one or more unpaired electrons. The first reported discovery of a free radical was by Gomberg[1] in 1900 who observed a product with unexpected characteristics while attempting to synthesise hexaphenylethane from chlorotriphenylmethane and silver. The white crystalline product was rapidly oxidised by air and, in the absence of oxygen, reacted immediately with halogens. These observations led Gomberg to propose the compound isolated was the triphenylmethyl radical.

$$Ph_3CCl + Ag \longrightarrow Ph_3C\cdot + AgCl \qquad 1.1$$

This radical is an example of a persistent free radical in which the unpaired electron is delocalised over the aromatic rings. The majority of free radicals however, and particularly those of interest as intermediates in radical chain reactions, have a transient existence and, unless isolated in a matrix, react rapidly by a variety of routes. Such radicals were first accepted as intermediates in gas phase reactions following the experiments of Paneth and Hofeditz[2] in 1929. It was observed that a stream of certain metal alkyl vapours, when heated to temperatures in the range 750 - 1200K in a quartz tube, removed previously deposited metal mirrors from the tube downstream of the heat source. This was due to the formation and subsequent reactions of alkyl radicals, e.g.

$$Pb(CH_3)_4 \longrightarrow Pb + 4CH_3\cdot \qquad 1.2$$

$$Zn + 2CH_3\cdot \longrightarrow Zn(CH_3)_2 \qquad 1.3$$

Analysis of the volatile metal alkyl product enabled identification of the reacting radical. Observations of the rate of mirror removal as the furnace-to-mirror distance was varied allowed the first, albeit

crude, estimates of radical recombination rates.

Since these early experiments, free radicals have become increasingly important in explaining the mechanisms of many important industrial pyrolyses, atmospheric reactions and certain reactions of biological interest such as photosynthesis and ageing. Consequently a number of techniques have been developed to produce and detect free radicals and to study their thermochemistry and reaction kinetics.

Radicals may be produced directly by homolytic fission of a single bond. Once produced, these radicals provide indirect routes to other radicals by abstraction from or addition to molecules. Electron transfer to or from ions also yields radicals. Some examples are:

$$C_2H_6 \xrightarrow{\Delta} 2CH_3\cdot \qquad \text{Fission} \qquad 1.4$$

$$CH_3\cdot + C_2H_4 \longrightarrow C_3H_7\cdot \qquad \text{Addition} \qquad 1.5$$

$$CH_3^+ + e \longrightarrow CH_3\cdot \qquad \text{Reduction} \qquad 1.6$$

Of most interest to thermochemical and kinetic applications is bond fission as a primary source of radicals. This may be done either thermally or photolytically depending upon the functional groups present in the molecule. At sufficiently high temperatures all chemical bonds will be broken and so thermolysis may be an indiscriminate method of radical production. However, some bonds such as the single -O-O- bond in peroxides and the -C-N-bond in azo compounds, are readily broken at relatively low temperatures. Such compounds are often used to initiate free radical processes. For example, a useful source of $CH_3\cdot$ is the thermolysis of di^{t}butyl peroxide at T > 400K, when the ^{t}butyl peroxy radical is unstable and quickly yields CH_3:

$$((CH_3)_3CO)_2 \xrightarrow{\Delta} 2(CH_3)_3CO\cdot \xrightarrow{\Delta} 2CH_3\cdot + 2CH_3COCH_3 \qquad 1.7$$

Photolytic sources of free radicals also include peroxides and azo compounds as well as halogens, ketones and compounds containing metal - metal bonds, e.g.

$$(Me_3Sn)_2 \xrightarrow{h\nu} 2\ Me_3Sn\cdot \qquad 1.8$$

Once produced, radicals react rapidly with a variety of organic molecules, including alkanes which are generally resistant to ionic attack. The reactions of radicals, and in particular organic radicals, have been grouped into a small number of classes. Examples of these classes are given in Table 1.1.

Table 1.1

Classes of Radical Reactions

Type	Typical Example	log A	E	Ref
Combination	$2\cdot CH_3 \longrightarrow C_2H_6$	10.5	0	3
Disproportionation	$2\cdot C_2H_5 \longrightarrow C_2H_6 + C_2H_4$	9.6	0	4
Decomposition	$n\text{-}C_3H_7\cdot \longrightarrow C_2H_6 + \cdot CH_3$	13.5	131	5
Transfer	$\cdot CH_3 + C_2H_6 \longrightarrow \cdot C_2H_5 + CH_4$	11.7	90	6
Addition	$\cdot CH_3 + C_2H_4 \longrightarrow n\text{-}C_3H_7\cdot$	8.5	32	7

A / $lmol^{-1}s^{-1}$ or s^{-1} E / $kJmol^{-1}$

In general, the zero (or near zero) E of combination and disproportionation reactions are typical[73]. Thus, these reactions have a higher rate constant at a given temperature than other bimolecular radical reactions. However, radical reactivity usually ensures that radical concentrations are very low compared to molecular concentrations so that transfer and addition reactions usually

predominate. This often results in radical chain mechanisms in the gas phase and the growth of polymeric chains in solution.

The short lifetimes and low concentrations encountered for most free radicals makes them difficult to detect by conventional analytical techniques. The most useful technique for determining radical structures and concentrations is electron spin resonance (ESR) spectroscopy.

1.2 Electron Spin Resonance Spectroscopy

The ESR technique is dependent on the spin of the unpaired electron. In the presence of an applied magnetic field the magnetic spin vector of the electron may be aligned with or against the magnetic field vector. Thus, in the field, two spin states exist whose energy separation depends on the strength of the magnetic field. Transitions between these spin states occur upon irradiation with photons of resonant energy as given by[23]:

$$\Delta E = h\nu = g\beta H_0 \qquad 1.9$$

where g is the spectroscopic splitting factor, which has a value close to 2 for a free electron, β is the Bohr magneton and H_0 the applied field. Figure 1.1 shows splitting of electron spin states m_s in an applied magnetic field.

Figure 1.1

Splitting of Electron Energy Levels in a Magnetic Field

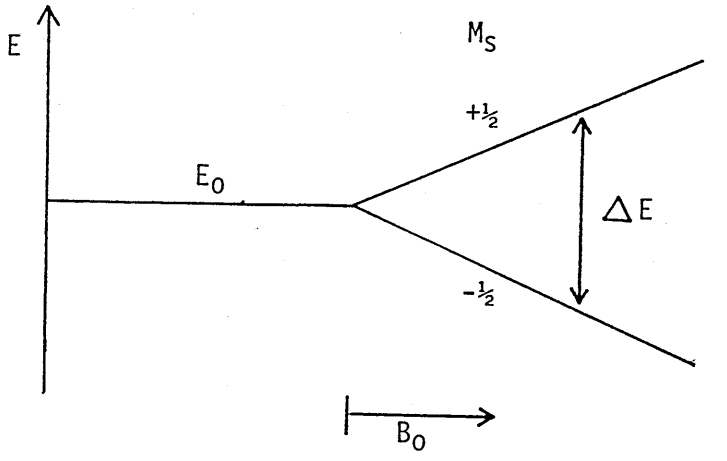

In practice, field strengths of a few kiloGauss are conveniently employed with an electromagnet, and the resulting spin states differ by the energy of a microwave photon. At a field of $H_0 \sim$ 3300Gauss the conditions of equation 1.9 are met for alkyl radicals by a microwave frequency in the X-band of $\nu \sim 9.5 GH_z$. By keeping the microwave energy fixed and scanning the magnetic field, microwave energy is absorbed and detected by a phase-sensitive detector which, after amplification, displays the derivative of the absorption signal. The area under the absorption curve in the spectra is proportional to the number of electron spin transitions and is therefore proportional to the radical concentration.

Structural information is obtained from ESR spectroscopy since the unpaired electron interacts with nearby magnetic nuclei (^1H, ^{13}C, ^{19}F, ^{17}O etc) to give hyperfine couplings. In the methyl radical for example, which is typical of most organic radicals, being planar with the unpaired electron in a p orbital, the unpaired electron interacts with three magnetically equivalent protons which have nuclear

spin, $M_I = \pm \frac{1}{2}$. The nuclear spin may be parallel or antiparallel to the electron spin and either add to or subtract from the local field at the electron, this results in a four line spectrum of relative intensities 1:3:3:1, as shown in Figure 1.2. The splitting between the lines is called the hyperfine coupling constant, 23.0 Gauss for the methyl radical[8].

Figure 1.2

ESR Spectrum of the CH_3 Radical

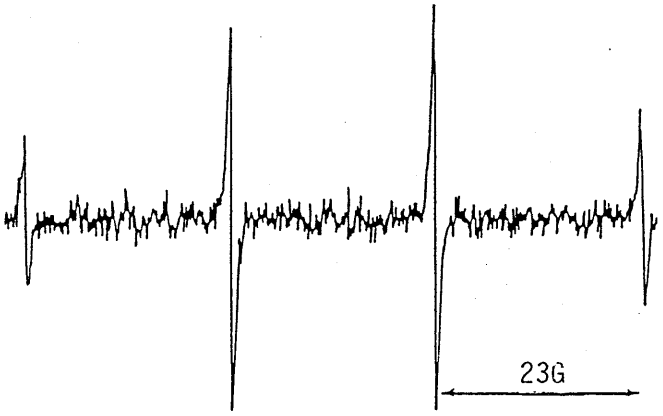

In general, interaction of the electron spin with N equivalent nuclei of spin $M_I = \frac{1}{2}$ results in N + 1 lines with binomial distribution, as demonstrated in Figure 1.2.

More complicated spectra are observed for larger radicals since the electron spin interacts strongly with magnetic nuclei on both the α and β carbon atoms. More distant couplings to γ protons are generally much weaker (1G or less compared to 20 - 40G for α and β couplings) and, under typical operating conditions, are frequently unresolved. Hence, in the n-propyl radical spectrum at low resolution only the two α and two β proton couplings are observed resulting in a triplet of triplets, a nine-line spectrum. This is represented diagrammatically in Figure 1.3.

Figure 1.3 demonstrates a phenomenon frequently encountered in ESR spectra of aliphatic radicals that, despite the fact that the β protons are more distant from the radical site than the α protons, larger coupling constants to β protons are observed[8].

Figure 1.3

Stick Diagram of the n-C_3H_7• ESR Spectrum

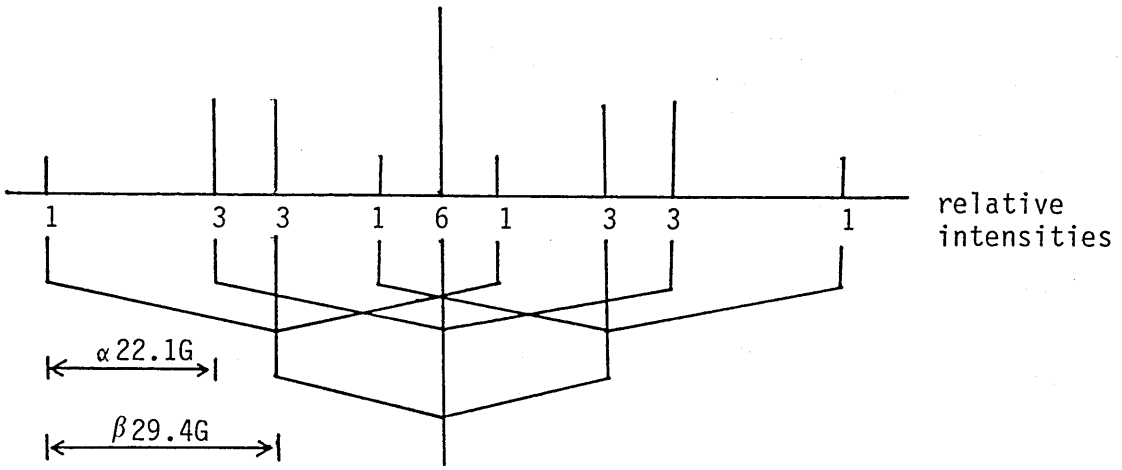

This effect may be qualitatively explained by consideration of the radical geometry and the orbital occupied by the unpaired electron[23]. In simple alkyl radicals the radical site is planar and the unpaired electron occupies a $2p_z$ orbital perpendicular to the plane. This electron cannot interact directly with electrons in the s orbital of the α proton. The α hyperfine coupling occurs by an effect called spin polarisation[9] in which arrangement (ii) of Figure 1.4 predominates slightly over arrangement (i), resulting in a net spin population in the hydrogen 1s orbital of opposite sign to that in the carbon $2p_z$ orbital and a net spin population in the carbon sp^2 orbital of like sign to that in the $2p_z$. In contrast the β coupling occurs through a hyperconjugation mechanism[9] in which the $2p_z$ orbital containing the unpaired electron overlaps with the β C-H bonding orbital. This results in a spin population in the 1s orbital of the β hydrogen. The β coupling is dependent on the angle between

the $2p_z$ orbital and β C-H orbital, being greatest when the angle is 0° and least when the angle is 90°. β coupling therefore provides information regarding radical conformations. Furthermore, the temperature dependence of the β coupling gives information about the rotational barrier about C_α - C_β bonds, an important quantity in determining radical heat capacities and entropies.

Figure 1.4

Orientation of Electron Spin

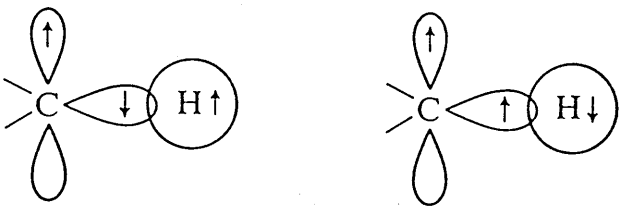

(*i*) (*ii*)

Structural information may also be gained from ^{13}C couplings which may be observed under favourable conditions. These couplings are very sensitive to the geometry about the radical centre and the coupling constant increases with the non-planarity of the radical site. This effect is demonstrated in Table 1.2 which shows increasing ^{13}C couplings with degree of fluorine substitution of methyl radicals as the pyramidal angle decreases from planar methyl through pyramidal fluoromethyls.

Table 1.2

Effect on ^{13}C Couplings of Increasing Fluorine Substitution

Radical	a(^{13}C) / Gauss
$\cdot CH_3$	38.3
$\cdot CH_2F$	54.8
$\cdot CHF_2$	148.8
$\cdot CF_3$	271.6

1.3 Bond Dissociation Energies

1.3.1 Definitions

The dissociation energy of a chemical bond is a measure of the bond strength between the two atoms constituting the bond. If A - B represents a molecule with a bond between fragments A and B, then the bond dissociation energy, (BDE), D(A - B), is the enthalpy change at 298K of the process

$$A - B \longrightarrow A\cdot + B\cdot \qquad 1.10$$

In the simplest case, where A and B are atoms, this process can be represented by Figure 1.5 which shows the variation of potential energy, E_{AB}, of A - B with interatomic distance, r_{A-B}.

Figure 1.5

Potential Energy Diagram for the Dissociation of A - B

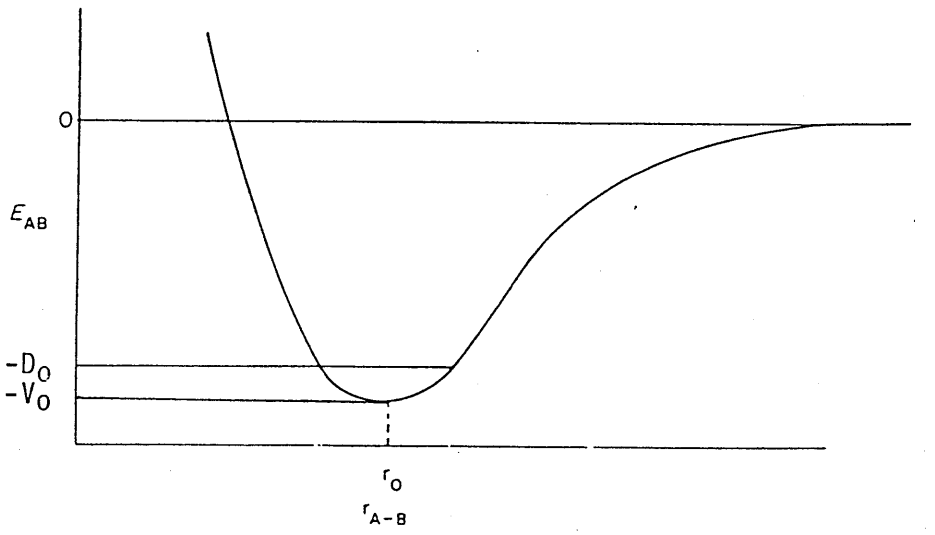

The minimum on the curve represents the equilibrium bond length in the A - B molecule, and the potential energy at this point is represented by V_0. The actual work required to completely separate A and B is less than this value by a quantity (V_0 - D_0) which is the zero point vibrational energy, $\frac{1}{2}h\nu$. The quantity D_0 differs

from D(A - B) because the latter is defined at 298K. In simple cases where the species are ideal gases and A - B has a high vibrational frequency, D(A - B) is 3/2RT greater than D_o[11].

Curves of the type shown in Figure 1.5 may be constructed by an analysis of electronic spectra of diatomic molecules and have provided accurate BDE values. For more complex molecules this approach is impractical due to the complexities of the spectra. Furthermore, the BDE is not only the energy involved in the breaking of the bond but also that involved in structural and electronic rearrangements upon formation of the resulting fragments. For example, D(CH_3 - H) includes the energy required for rearrangement of $\cdot CH_3$ from tetrahedral to planar[12]. These rearrangements may be inconvenient to theoreticians concerned with making accurate predictions of bond strengths, but are of interest to chemists concerned with radical properties.

To overcome these problems, different approaches have been made to the measurement of BDE's. These are generally based on equation 1.11 since, for the process given in 1.10

$$D(A - B) = \Delta H_f(A\cdot) + \Delta H_f(B\cdot) - \Delta H_f(AB) \qquad 1.11$$

If A or B is an atom, then its ΔH_f is generally known from spectroscopy. Also ΔH_f values for molecular species are usually available from calorimetry, particularly in the case of hydrocarbons for which values are well documented[13-15]. Hence the problem reduces to one of measuring the heat of formation of a radical. Consequently measurements of $\Delta H_f(R\cdot)$ and BDE's are usually complementary.

It is important at this stage to differentiate between BDE's derived from equation 1.11 which refer to a specific bond in a molecule,

and average bond dissociation energies which are the average BDE value of all such bonds in a compound. Consider for example the complete atomisation of methane.

$$CH_4 \longrightarrow C\cdot + 4H\cdot \qquad 1.12$$

The energy required for this process has been reported[12] as 1663 $kJmol^{-1}$. Since, due to the symmetry of methane, each bond may reasonably be considered to be of the same strength, simultaneous rupture of all four bonds implies a C - H bond energy of $\frac{1}{4} \times 1663 = 416$ $kJmol^{-1}$. However, the successive removal of hydrogen atoms from methane to form the radicals $\cdot CH_3$, $\cdot CH_2$, $\cdot CH$ and $\cdot C$ requires 432, 471, 422 and 339 $kJmol^{-1}$ respectively[12]. While the total energy requirements are the same in each case, the individual BDE's are not the average BDE, largely for reasons mentioned above, namely the geometrical and electronic rearrangements that occur in each step.

Radical thermochemistry and BDE's have been studied by a number of techniques, the most widely used of which have been based on kinetic studies[16-18]. These depend on the relationships between kinetic parameters and thermochemistry.

1.3.2 Relationships Between Kinetics and Thermochemistry

Since many determinations of BDE's rely on the kinetics of radical reactions, some kinetic relationships and their relationships to thermodynamics will be considered.

One of the most important effects studied in kinetics is that of temperature on the rate constant; in many reactions a 10K rise in temperature causes a doubling of the reaction rate. This effect was described quantitatively by Arrhenius[19] who found that the

variation of k with T could be expressed as

$$k = A \exp\left(\frac{-E}{RT}\right) \qquad 1.13$$

where A is the frequency factor or pre-exponential term and E the activation energy for the process.

This relationship is of particular importance in determining radical thermochemistry. For example, the principle of microscopic reversibility requires that for a process of the type

$$A \underset{-1}{\overset{1}{\rightleftharpoons}} B \qquad 1.14$$

the enthalpy change, ΔH, is given by

$$\Delta H = E_1 - E_{-1} + \Delta nRT \qquad 1.15$$

where E_1 and E_{-1} are the activation energies of the forward and reverse reactions respectively and Δn the difference in number of moles of products less number of moles of reactants.

Hence, experiments designed to measure the temperature dependence of forward and reverse reactions provide the enthalpy change of the reaction from which radical heats of formation and BDE's may often be obtained.

Even if the temperature dependence of the rate constants is unobtainable, useful information can still be gained by measuring the forward and reverse rate constants at the same temperature since

$$K = \frac{k_1 (R'T)^{\Delta n}}{k_{-1}} \qquad 1.16$$

where K is the equilibrium constant for the process, R' the gas constant in units of 1 atm mol^{-1} K^{-1}.

Measurements of equilibrium constants provide thermochemical quantities via the van't Hoff[20] equation

$$\ln K = \frac{-\Delta H}{RT} + \frac{\Delta S}{R} \qquad 1.17$$

From equation 1.17 the temperature dependence of the equilibrium constant yields enthalpy and entropy values. Alternatively if the equilibrium constant is available at only one temperature or the temperature range is limited, then ΔH may still be obtained since reasonably accurate values of ΔS may usually be estimated[4].

The pre-exponential term, A, in the Arrhenius equation is, for an equilibrium process such as Equation 1.14, related to the entropy change of the reaction via

$$\ln \frac{A_1}{A_{-1}} = \frac{\Delta S}{R} - \Delta n \ln(eR'T) \qquad 1.17a$$

1.4 Applications of Radical Thermochemistry and BDE s

One of the aims of chemists is to make accurate predictions as to the products and rates of chemical reactions. The majority of reactions in the gas phase consist of a number of elementary steps which often involve free radicals as intermediates, e.g. the pyrolysis of ethane in the range 800 - 1000K can be explained by a mechanism that consists of the steps[21]

$$C_2H_6 \longrightarrow 2\cdot CH_3 \qquad 1.18$$

$$\cdot CH_3 + C_2H_6 \longrightarrow \cdot C_2H_5 + CH_4 \qquad 1.19$$

$$\cdot C_2H_5 \rightleftharpoons C_2H_4 + H\cdot \qquad 1.20$$

$$H\cdot + C_2H_6 \rightleftharpoons \cdot C_2H_5 + H_2 \qquad 1.21$$

$$2\cdot C_2H_5 \longrightarrow C_4H_{10} \qquad 1.22$$

$$2\cdot C_2H_5 \longrightarrow C_2H_4 + C_2H_6 \qquad 1.23$$

The first general mechanism accounting for organic pyrolysis reactions was suggested by Rice and Herzfeld[22] who proposed an initiation step consisting of splitting the molecule at its weakest bond. Hence a knowledge of BDE's is required to identify likely initiating steps which determine the overall mechanism. Furthermore, from the thermochemistry of individual steps an equilibrium constant may be calculated for that step from which relative concentrations of species present may be estimated.

In many reversible reactions involving free radicals the reaction is more conveniently studied in one direction than the other, for example, the reaction of iodine with hydrocarbons involves the step[17]

$$I\cdot + RH \underset{-1}{\overset{1}{\rightleftharpoons}} R\cdot + HI \qquad 1.24$$

for which the Arrhenius parameters A_1 and E_1 are accessible from the rate of iodine depletion. The reverse parameters are less readily determined, however, and in such cases may be estimated from the thermochemistry of the reaction using the relationships given in equations 1.15 and 1.17a. Alternatively, radical thermochemistry may be determined from estimates of A_{-1} and E_{-1}[17].

Bond dissociation energies are also important in determining possible mechanisms of elimination reactions such as those occurring during the pyrolysis of alkyl halides. For example, a radical non-chain mechanism could be proposed for the pyrolysis of bromoethane. The most likely initiating step would be the homolysis of the weakest bond by reaction 1.26

$$C_2H_5Br \longrightarrow C_2H_5\cdot + Br\cdot \qquad 1.26$$

In a non-chain mechanism the following steps have been proposed[24]

$$C_2H_5Br + Br\cdot \longrightarrow C_2H_4Br + HBr \qquad 1.27$$

$$C_2H_4Br + C_2H_5\cdot \longrightarrow C_2H_5Br + C_2H_4 \qquad 1.28$$

The activation energy of this scheme is required to be at least that of the initiating step. However, the experimental activation energy for the overall reaction has been measured as 219 - 225 kJmol^{-1}[25,26] while $D(C_2H_5 - Br) \sim 284$ kJmol^{-1}[27]. Hence the non-chain mechanism can be rejected on energetic grounds. This reaction is believed to follow a radical chain mechanism.

Conversely the pyrolysis of 3-bromopropene has been proposed[28] to occur via the mechanism

$$C_3H_5Br \longrightarrow \cdot C_3H_5 + Br\cdot \qquad 1.29$$

$$Br\cdot + C_3H_5Br \longrightarrow \cdot C_3H_4Br + HBr \qquad 1.30$$

$$\cdot C_3H_4Br \longrightarrow \tfrac{1}{2}C_6H_6 + HBr \qquad 1.31$$

In this case, the overall activation energy has been measured as 190 kJmol^{-1}[28] which is in good agreement with the value $D(C_3H_5 - Br) \sim 190$ kJmol^{-1}[27] thus supporting a radical non-chain mechanism.

1.5 Entropy

The entropy of a substance can be related to its entropy at absolute zero if heat capacity data are available as a function of temperature since

$$S_T = S_0 + \int_0^T (C_p/T)dT \qquad 1.32$$

If phase changes occur between temperatures 0 and T, then these must also be included in the calculation. Equation 1.32 is represented graphically in Figure 1.6.

Figure 1.6

Entropy Calculations From Heat Capacity Data

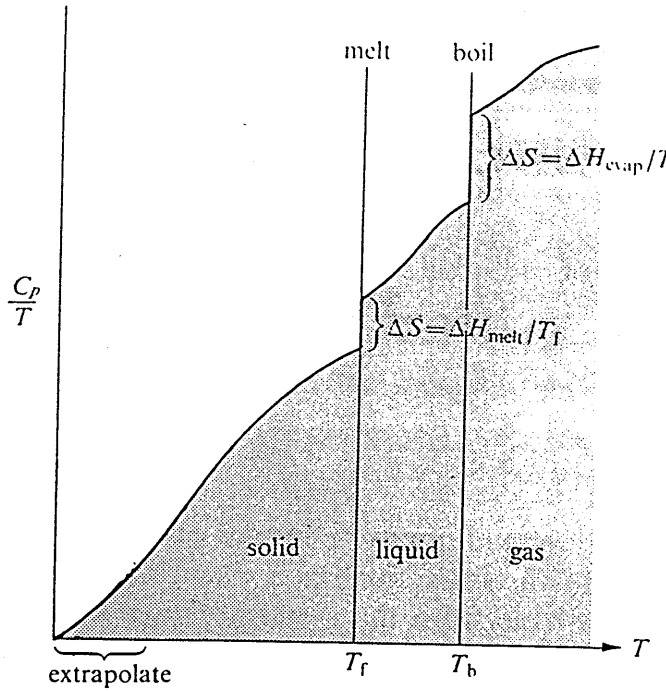

Experimentally it is difficult to measure heat capacities in the vicinity of absolute zero and extrapolations are necessary in this region. The desired entropy, S_T, is available from Equation 1.32 since, according to the Third Law of thermodynamics, at absolute zero the entropy of a perfect crystal is zero.

This method of determining entropies is only applicable to stable species whose heat capacities may be measured. For highly reactive species such as free radicals, entropies must be calculated using statistical thermodynamics.

The partition function, Q, arises from the Boltzmann distribution law and may be defined as

$$Q = \sum_i p_i \exp(-E_i/RT) \qquad 1.33$$

where p_i is the number of discrete states of the molecule with energy E_i. The partition function is related to the entropy of the species as follows:

$$S = R\ln Q + RT\left(\frac{d\ln Q}{dT}\right) \qquad 1.34$$

For ideal gases the partition function can be factorized into a product of the partition functions for each degree of freedom

$$Q = q_{trans} \times q_{rot} \times q_{vib} \qquad 1.35$$

If low lying electronic states are accessible or there is a non-zero spin, as in free radicals, then the additional factor, q_{elect} is required in equation 1.35 for the electronic degrees of freedom.

Since the entropy is related to the logarithm of the partition function, it can be expressed as the sum of the various terms. Thus

$$S = S_t + S_r + S_v + S_e \qquad 1.36$$

Translational energy levels are very closely spaced, hence the summation of Equation 1.33 may be replaced by an integral. This leads to the Sackur-Tetrode[29,30] equation for the translational entropy which, for an ideal gas at temperature, T, and pressure, p, becomes

$$S_t = R\ln\left[e^{5/2}\left(\frac{2\pi mkT}{h^2}\right)^{3/2}\left(\frac{kT}{P}\right)\right] \qquad 1.36a$$

At a pressure of 1 atmosphere and if m is stated in atomic mass units, then

$$S_t = R[{}^3/_2 \ln M + {}^5/_2 \ln T] - 9.686 \text{ JK}^{-1}\text{mol}^{-1} \quad 1.37$$

For the rotational contribution to entropy it may be shown that

$$S_r = R({}^1/_2 \ln D \times 10^{117} + {}^3/_2 \ln T - \ln \sigma) - 0.141 \text{ JK}^{-1}\text{mol}^{-1} \quad 1.38$$

where D is the product of the three principle moments of inertia and σ the external symmetry of the species. The moments of inertia are available either from microwave spectroscopy or via calculations using structural data for the species.

Vibrational contributions to entropy must be calculated by direct summation of the contribution to each vibrational energy level given by

$$S_V = R[-\ln(1 - e^{-x}) + \frac{x}{e^x - 1}] \quad 1.39$$

where

$$x = \frac{ch\tilde{\nu}}{kT} \quad 1.40$$

in which $\tilde{\nu}$ is the wavenumber of the vibration. Vibrational frequencies for free radicals may be estimated by analogy to alkanes [32] or measured spectroscopically by isolating the free radical in a solid matrix of an inert gas[33-35]. If vibrational frequencies cannot be determined experimentally, then sufficiently accurate estimates can sometimes be obtained from theoretical calculations[36,37].

In a complex molecule there are (3N -5) or (3N - 6) fundamental vibrational modes for linear and non-linear species respectively. One or more vibrational modes may be a hindered or free rotation about a single bond. The entropy contributions of such rotations depend upon the moment of inertia of the rotation and the energy barrier

to rotation. For a free rotation the entropy contribution is given by[31]

$$S_{ir} = R(\tfrac{1}{2}\ln I_r T - \ln n) + 376.427\ JK^{-1}mol^{-1} \qquad 1.41$$

where I_r is the moment of inertia of the barrier and n the symmetry of the rotation. If a barrier exists to internal rotation, then the entropy contribution is reduced from that of a free rotor. The reduction may be calculated from standard tables[31] giving the variation of $^{1}/_{Q_{ir}}$ with $^{V}/_{RT}$ values where V is the barrier to internal rotation. Barriers to internal rotation of molecules may be obtained from NMR spectroscopy[82] and those for radicals from ESR spectroscopy (see section 1.1.2).

Finally, the electronic contribution to entropy, in the case of free radicals with one unpaired electron, spin ½, is given by

$$S_e = R\ln 2 \qquad 1.42$$

The relative magnitudes of the contributions towards radical entropies may be exemplified by the entropy of the i-propyl radical at 300 and 1000K, as shown in Table 1.3.

Table 1.3 demonstrates that at low temperatures only the low vibrational frequencies contribute significantly to the entropy and these, together with uncertainties in barriers to internal rotation, (4 $kJmol^{-1}$ uncertainty in V represents 1 - 2 $JK^{-1}mol$ uncertainty in S), are the main sources of error in calculating radical entropies.

Table 1.3

Contributions Towards $S(i\text{-}C_3H_7\cdot)$ at 300 and 1000K

Mode			Temperature/K 300	1000
Translation			155.8	189.3
External Rotation[a)]			88.5	108.5
Internal Rotation[b)]			28.2	41.6
Vibration				
	Wavenumber[38]	Degeneracy		
	3100	1	0	1.77
	2960	6	0	11.82
	1440	6	0.40	37.58
	1300	1	0.12	7.00
	1200	1	0.18	7.59
	990	4	1.68	36.22
	950	1	0.49	9.37
	397	1	4.12	16.40
	367	1	4.61	17.04
Total Vibration			11.60	144.79
Electronic			5.76	5.76
Total			289.8	489.9

$S/JK^{-1}mol^{-1}$, wavenumber $/cm^{-1}$

a) Moment of Inertia, D = 2.67×10^{-115} gcm^2, σ = 2 (ref. 38)

b) Two free rotors, I_r = 4.2×10^{-40} gcm^2, n = 3 (ref. 38)

1.6 Measurement of Radical Heats of Formation and BDE s

1.6.1 Bond Fission

As stated earlier (section 1.3.2), the pyrolysis of a hydrocarbon is initiated by the breaking of the weakest bond. Also Equation 1.15 relates the enthalpy change of such a reaction to the difference in forward and reverse activation energies for the reaction. Since it is now generally accepted that the majority of alkyl radical recombinations have near-zero activation energy[27], the measurement of the activation energy for bond fission provides a measure of the enthalpy change for the reaction. Thus for pyrolysis of an alkane, RR' the quantity sought is the activation energy E_1.

$$RR' \underset{-1}{\overset{1}{\rightleftharpoons}} R\cdot + R'\cdot \qquad 1.43$$

If R· = R'· as in pyrolysis of a symmetrical alkane such as ethane or 2,3-dimethylbutane then

$$\Delta H_1 = 2\Delta H_f(R\cdot) - \Delta H_f(RR) \qquad 1.44$$

and, since $\Delta H_f(RR)$ values are generally available, $\Delta H_f(R\cdot)$ is determined.

However, determination of E_1 is seldom straightforward since such pyrolyses usually proceed via a radical chain mechanism and the overall activation energy for the reaction does not equate to that of initiation. Bond fission experiments have therefore been designed in which the radical chain mechanism is suppressed; by employing very short reaction times, or operating at low pressures, which essentially eliminates bimolecular chain propagating steps, or removing propagating radicals such as H· and CH_3· by use of a radical scavenger.

Historically the most important of these techniques have been flow experiments in which pyrolysis occurs in a stream of toluene[39] or aniline[40]. Such experiments suppress chain reactions by removing propagating radicals from the system, as demonstrated in the pyrolysis of cumene in a flow of toluene[16].

$$C_6H_5CH(CH_3)_2 \longrightarrow C_6H_5\dot{C}H(CH_3) + CH_3\cdot \qquad 1.45$$

$$CH_3\cdot + C_6H_5CH_3 \longrightarrow CH_4 + C_6H_5CH_2\cdot \qquad 1.46$$

In this scheme the reaction kinetics may be monitored by the rate of formation of methane. The benzyl radical formed is resonance stabilised and, at temperatures below 670K, does not propagate chain reactions. A drawback to this method is that at higher temperatures the following reactions may occur

$$C_6H_5CH_3 \longrightarrow C_6H_5CH_2\cdot + H\cdot \qquad 1.47$$

$$H\cdot + C_6H_5CH_3 \longrightarrow C_6H_6 + CH_3\cdot \qquad 1.48$$

thus providing an additional source of $CH_3\cdot$ radicals, and hence CH_4 via Equation 1.46. This may lead to errors in the kinetic conclusions when compounds with labile R - CH_3 bonds are studied unless these additional reactions are considered. Also it has been shown that at temperatures above 670K benzyl radicals can abstract hydrogen and therefore initiate chain processes[41]. Pyrolyses carried out at above 670K generally include some component of chain decomposition. Finally, it has been shown that the majority of pyrolysis reactions using carrier techniques give activation energies 20 - 40 $kJmol^{-1}$ lower than values calculated from the data for individual steps obtained from other well established techniques[38]. Hence the heats of formation and BDE's derived will also be lower than expected.

A more recent technique which has been developed to suppress secondary reactions in pyrolysis mechanisms is the pyrolysis of hydrocarbons in the presence of low concentrations of oxygen[42-44]. In a KCl coated reaction vessel the basic mechanism is

$$RR' \xrightarrow{1} R\cdot + R'\cdot \qquad 1.49$$

$$R\cdot(R'\cdot) + O_2 \longrightarrow \text{alkene} + HO_2\cdot \qquad 1.50$$

$$HO_2\cdot \xrightarrow{\text{surface}} \tfrac{1}{2}H_2O + \tfrac{3}{4}O_2 \qquad 1.51$$

$$2HO_2\cdot \longrightarrow H_2O_2 + O_2 \qquad 1.52$$

$$H_2O_2 \xrightarrow{\text{surface}} H_2O + \tfrac{1}{2}O_2 \qquad 1.53$$

The kinetics of the reaction is followed by measuring alkene yields at various O_2 and alkane pressures from which k_1 values are determined. The temperatures at which the reaction may be studied are limited since in the case of dimethylbutane pyrolysis[44] low rates are encountered below 750K while above 810K OH radicals resulting from H_2O_2 decomposition complicate the mechanism. This limits the accuracy with which A_1 and E_1 may be determined. Greater accuracy is achieved by combining the results with those obtained from shock tube studies[45] in the region 1000 - 1200K.

From the activation energy obtained for the symmetrical decomposition of dimethylbutane using this method and the assumption that i-propyl recombination has zero activation energy, the values $\Delta H_{f298}(i\text{-}C_3H_7) = 79.6 \pm 1.8$ kJmol^{-1} and $D(iC_3H_7 - H) = 401.3 \pm 1.8$ kJmol^{-1} are obtained. These values are in excellent agreement with the most recent determinations and support the use of the method.

Another technique which allows the measurement of bond fission rates is the single pulse shock tube developed by Tsang[46]. The apparatus is shown schematically in Figure 1.7.

Figure 1.7

The Single Pulse Shock Tube

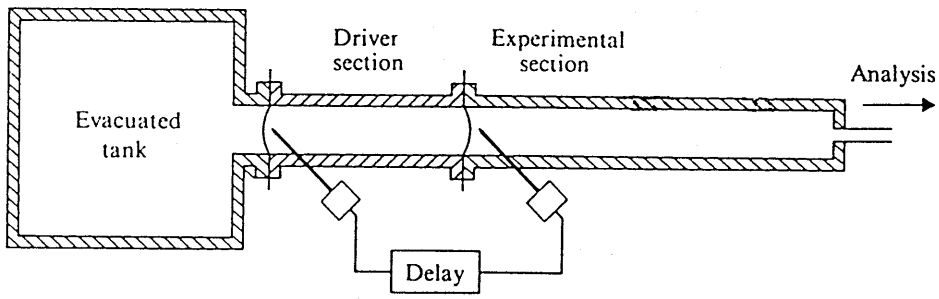

The driver section contains an inert gas at high pressures and is separated from the experimental section containing the sample gas at low pressure by a diaphragm. On piercing the diaphragm a shock wave propagates through the sample causing an increase in temperature, typically of the order of 1000K, in a timescale which is typically milliseconds. Following the puncture of the first diaphragm, the second is punctured which causes a rarefaction wave which quenches the reaction by rapid cooling. The resultant short reaction time effectively prevents diffusion to the reactor walls and is also short compared to the lifetime of free radical reactions. Thus, secondary reactions do not occur to complicate the reaction scheme and, therefore, the rates observed via product analysis are those corresponding to the bond fission reaction alone.

The difficulties encountered in this technique are that the reaction times and temperatures are uncertain. This is overcome by using

the shock tube in a comparative mode whereby the sample is pyrolysed in the presence of another compound, such as cyclohexene, for which Arrhenius parameters have been determined by other techniques. In this way a knowledge of the exact temperature and reaction times are unimportant since

$$\log k = [\log A - (E/E_s) \log A_s] + (E/E_s) \log k_s \qquad 1.54$$

where k and k_s are the measured rate constants for the substance under study and standard respectively. By repeating the experiment with varying shock velocities and measuring the overall rate constants k and k_s by product analysis, the required Arrhenius parameters are available from a plot of log k against log k_s. The radical thermochemistry is then calculated in the usual way from the assumptions regarding radical recombination and the heat of formation of the parent molecule.

Among the radicals studied by this technique are ethyl, i-propyl and t-butyl from the pyrolyses of butane[47], 2,3-dimethylbutane[45] and 2,2,3,3-tetramethylbutane[48] respectively. The activation parameters determined led to radical heats of formation which were shown to be incompatible with results derived from radical buffer studies[50-53], unless the previously accepted values were increased by 10 $kJmol^{-1}$ for ethyl and i-propyl and 20 $kJmol^{-1}$ for t-butyl. Used in the comparative mode the single pulse shock tube has provided much impetus for the reinvestigation of alkyl radical thermochemistry.

1.6.2 Halogenation Kinetics

The gas phase reaction of iodine with hydrocarbons in the region of 570K follows the general stoichiometry

$$RH + I_2 \longrightarrow RI + HI \qquad 1.55$$

and the following mechanism has been found applicable in the vast majority of cases[17]

$$I_2 + M \underset{-1}{\overset{1}{\rightleftharpoons}} 2I\cdot + M \qquad 1.56$$

$$I\cdot + RH \underset{-2}{\overset{2}{\rightleftharpoons}} R\cdot + HI \qquad 1.57$$

$$R\cdot + I_2 \underset{-3}{\overset{3}{\rightleftharpoons}} RI + I\cdot \qquad 1.58$$

In the early stages reaction -3 is unimportant and

$$\frac{-d[I_2]}{dt} = k_2\left(\frac{k_1}{k_{-1}}\right)^{\frac{1}{2}} [I_2]^{\frac{1}{2}} [RH] \qquad 1.59$$

The depletion of I_2 may be followed spectroscopically and the results fitted to an integrated form of Equation 1.59 to yield $k_2\left(\frac{k_1}{k_{-1}}\right)^{\frac{1}{2}}$. The term in brackets is the equilibrium constant for iodine dissociation, which is known. Hence k_2 is obtained, the temperature dependence of which yields E_2. If the activation energy E_{-2} was also available then $\triangle H_2$ could be determined and, since

$$\triangle H_2 = D(R - H) - D(H - I) \qquad 1.60$$

the hydrocarbon BDE could be calculated since D(H - I) is accurately known from spectroscopy.

However, the radical trapping reaction, -2, is a very fast process for which the Arrhenius parameters are difficult to determine. For this reason the assumption

$$E_{-2} = 0 \pm 4 \text{ kJmol}^{-1} \qquad 1.61$$

has been generally applied[17]. This assumption has been validated using very low pressure pyrolysis for a small number of radicals

including CH_3[54] and tC_4H_9[55].

In cases where the iodoalkane formed is unstable at the operating temperature the mechanism is complicated by the reaction

$$RI \underset{-4}{\overset{4}{\rightleftharpoons}} \text{Olefin} + HI \qquad 1.62$$

and the overall stoichiometry becomes

$$RH + I_2 \rightleftharpoons \text{Olefin} + 2HI \qquad 1.63$$

Although this leads to a more complicated rate expression than that given in Equation 1.59 the desired thermochemical parameters may still be extracted from the data.

The reaction may also be studied by the addition of HI to RI and by following the appearance of I_2 in reaction -3. In this approach the activation energy E_{-3} is obtained and the assumption that

$$E_3 = 4 \pm 4 \text{ kJmol}^{-1} \qquad 1.64$$

has been made. Where BDE s have been determined from measurements of both E_2 and E_{-3} reasonably good agreement has been obtained[17].

Since its introduction in 1961 the iodination technique has been widely applied to determine BDE s in the range 300 - 450 $kJmol^{-1}$. Its main use has been the determination of radical thermochemistry for hydrocarbons[17] although it has also been applied to silicon compounds by Walsh and Doncaster[56] and fluorocarbons by Rodgers[57].

Recently, however, the technique has been questioned[49] since the results obtained for many alkyl radicals are in disagreement with those obtained by newer methods. These discrepancies will be considered in more detail later.

1.6.3 Very Low Pressure Pyrolysis (VLPP)

This technique was developed in the mid 1960 s by Spokes and Benson[58] as another method designed to eliminate secondary reactions from bond fission studies. At the low pressures employed, typically in the region 4 x 10^{-3} torr, the vast majority of collisions of reactants and products are with the walls of the reactor thus allowing the observation of unimolecular decomposition processes.

The simplest form of the VLPP reactor is shown schematically in Figure 1.8.

Figure 1.8

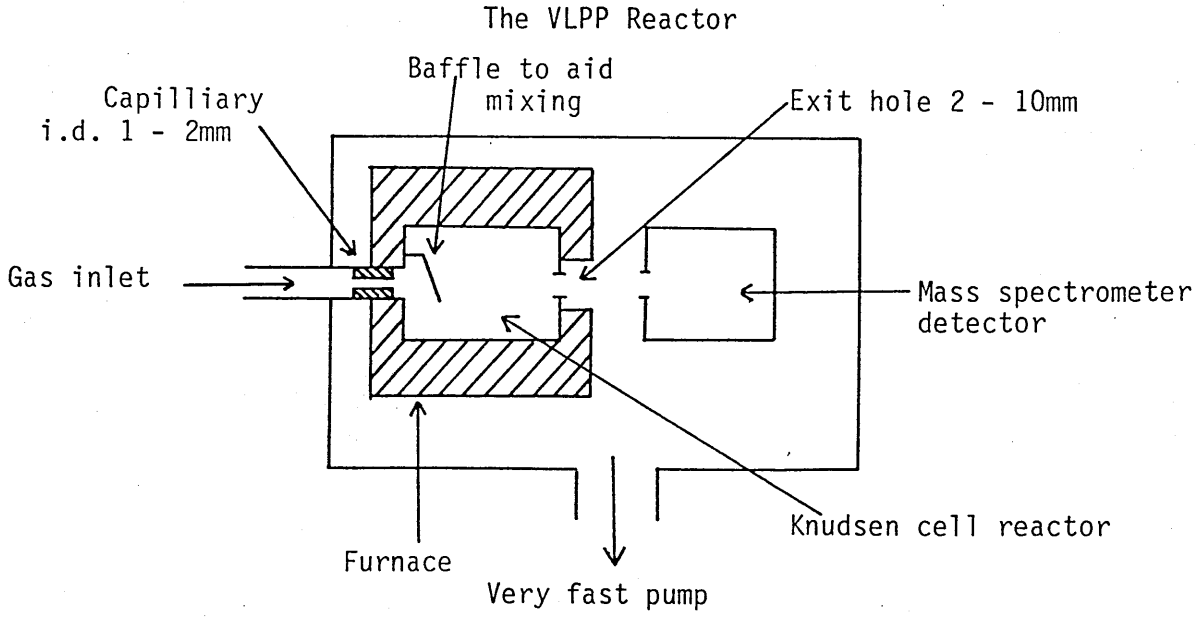

The principle of the technique is that reactant gas flows into a heated Knudsen cell in which reaction occurs. The gaseous products then exit via a larger aperture to a mass spectrometer detector for analysis. The VLPP method has advantages over the shock tube since the gas is heated by the reactor walls thus removing uncertainty regarding temperature.

If we consider the unimolecular decomposition of a molecule, A, to

yield products B and C

$$A \xrightarrow{1} B + C \qquad 1.65$$

and k_1 is the first order rate constant for the process and k_e the rate of escape of A from the reactor, then the specific flux, R_A, of A into the reactor is given by

$$R_A = k_1[A]_{ss} + k_e [A]_{ss} \qquad 1.66$$

where $[A]_{ss}$ is the steady state concentration of A in the reactor.

Defining $[A]_o$ as the concentration of A in the reactor when no reaction occurs, i.e. if the cell was bypassed, we have

$$[A]_o = \frac{R_A}{k_e} \qquad 1.67$$

From 1.66 and 1.67

$$\frac{[A]_o - [A]_{ss}}{[A]_{ss}} = \frac{k_1}{k_e} \qquad 1.68$$

The left hand side of Equation 1.68 is experimentally determined from the relative intensities of mass spectrometer signals, and k_e may be calculated from kinetic theory and reactor geometry. Thus k_1 may be determined.

The technique has been applied to a number of reactions[59] including the pyrolyses of 2,3-dimethylbutane and 2,2,3,3-tetramethylbutane to yield i-propyl and t-butyl radicals respectively. The rate parameters derived from these studies agree well with those obtained from the shock tube technique[45,48].

Among the advantages of VLPP are the range of rate constants that

may be measured for fast unimolecular reactions (between 10^{-1} and $10^{4}s^{-1}$) and the accuracy with which the temperature, which may be varied between ambient and 1900K, is known. However, the technique suffers a disadvantage as a result of the low pressures employed, namely a number of unimolecular pyrolyses are not at their high pressure limits and rate data must be treated by unimolecular theories[60]. This poses a problem since the temperature dependence of the rate constant no longer follows the Arrhenius equation under fall-off conditions. Hence, to obtain a value for the activation energy it is necessary to specify the A factor. In the majority of cases these may be calculated with reasonable accuracy[4] from estimates of the entropy of activation, although this is an added source of uncertainty in the results obtained.

The VLPP apparatus is versatile in also being suitable for the study of radical-radical and radical-molecule reactions. When used to study radical recombinations a suitable radical precursor is pyrolysed and the resulting radical recombination product and unreacted precursor detected by the mass spectrometer. For example, to study ethyl recombination azoethane was pyrolysed[46] giving the following reaction scheme

$$(C_2H_5)_2N_2 \longrightarrow 2C_2H_5\cdot + N_2 \qquad 1.74$$

$$2C_2H_5\cdot \longrightarrow C_4H_{10} \qquad 1.75$$

$$2C_2H_5\cdot \longrightarrow C_2H_6 + C_2H_4 \qquad 1.76$$

The reaction was followed by monitoring peaks at 86 and 43 amu corresponding to azoethane and butane respectively. Alternatively, by lowering the ionisation energy of the detector it was possible to obtain a measure of the radical concentration from the peak at 29 amu, the ethyl radical ion.

The results of these studies suggested an ethyl radical recombination rate in the region of 10^{10} $lmol^{-1}s^{-1}$ which, as will be demonstrated later, supports a higher $\Delta H_f(C_2H_5\cdot)$ value than previously accepted.

The apparatus has been used in a slightly modified form to study radical-molecule equilibria and has yielded accurate data for radical heats of formation. An example of this application is a study by Benson and co-workers[62,63] of the equilibrium.

$$Cl\cdot + CH_4 \underset{-1}{\overset{1}{\rightleftharpoons}} CH_3\cdot + HCl \qquad 1.77$$

The modifications to the apparatus shown in Figure 1.8 included the addition of two sample inlets, one equipped with a microwave discharge tube to supply a source of $Cl\cdot$ atoms from Cl_2. In this experiment the variation of concentration of $Cl\cdot$ atoms escaping from the reactor was monitored at various flow rates of CH_4 entering via a separate inlet. This provided information from which k_1 was calculated. The reaction was then studied in the reverse direction by monitoring the effect of varying HCl flow rates on $[Cl\cdot]$. This allowed k_{-1} to be determined and hence the equilibrium constant for the reaction. From the entropies of all the species and heats of formation of $Cl\cdot$, CH_4 and HCl a value of $\Delta H_f(CH_3\cdot) = 146.9 \pm 0.4$ $kJmol^{-1}$ was obtained.

This was the first case in which a free radical heat of formation had been determined with a precision approaching that of stable species and demonstrates the usefulness of the technique in appropriate circumstances.

1.6.4 Evans Polanyi Relationships

Consideration of the shapes of potential energy curves for the reaction of sodium atoms with alkyl halides led Evans and Polanyi[64] to deduce a linear relationship between the activation energy and enthalpy

change.

For a series of metathesis reactions of saturated hydrocarbons of the type

$$X\cdot + RH \rightleftharpoons HX + R\cdot \qquad 1.78$$

the same bond is being formed, regardless of the nature of R. Observations have shown that within such a series, a relationship of the form given in Equation 1.79 holds.

$$E = a[D(R - H) - c] \qquad 1.79$$

where a and c are constants for a given $X\cdot$.

This method greatly simplifys the experimental procedures required to determine D(R - H) values since it is sufficient to study the overall kinetics of reaction 1.78, and so activation energies for individual steps are not required. Furthermore, the kinetic experiments may be performed in a competitive manner allowing accurate determinations of activation energies and providing a check on internal consistency.

An example of the technique is given in Table 1.4 which gives activation energies for hydrogen abstraction by various radicals from a series of alkanes. These data are plotted against D(R - H) in Figure 1.9.

Although this treatment has been applied to a number of reactions there are certain limitations in predicting BDE s. In cases where the slope of the plot has a low value, as in abstraction by $CH_3\cdot$, small errors in E result in relatively large errors in D(R - H). Furthermore, the technique requires a knowledge of some BDE s within a series to provide the constants a and c of Equation 1.79. Since

the technique is only valid within a closely related series this means that any BDE s derived by the method will usually be reasonably well known anyway.

For these reasons, results obtained from Evans-Polanyi relationships are best considered as giving support to other techniques, rather than definitive.

Table 1.4

Activation Energies for $X\cdot + RH \rightleftharpoons XH + R\cdot$ (a,b)

R· \ X·	I·	Br·	CH_3·	NF_2·	D(R - H)
CH_3·	142.7	76.6	60.7		435
C_2H_5·	116.7	56.1	49.8		410
i-C_3H_7·	104.6	42.7	43.1		395
sec-C_4H_9·		42.7	40.6	88.7	396
t-C_4H_9·	89.5	31.4	34.3	73.2	381
neo-C_5H_{11}·		59.8		111.7	416
c-C_5H_9·			38.1	83.3	389

a) Units $kJmol^{-1}$, b) Data from reference 16

Figure 1.9

Evans - Polanyi Plots of E vs D(R - H)

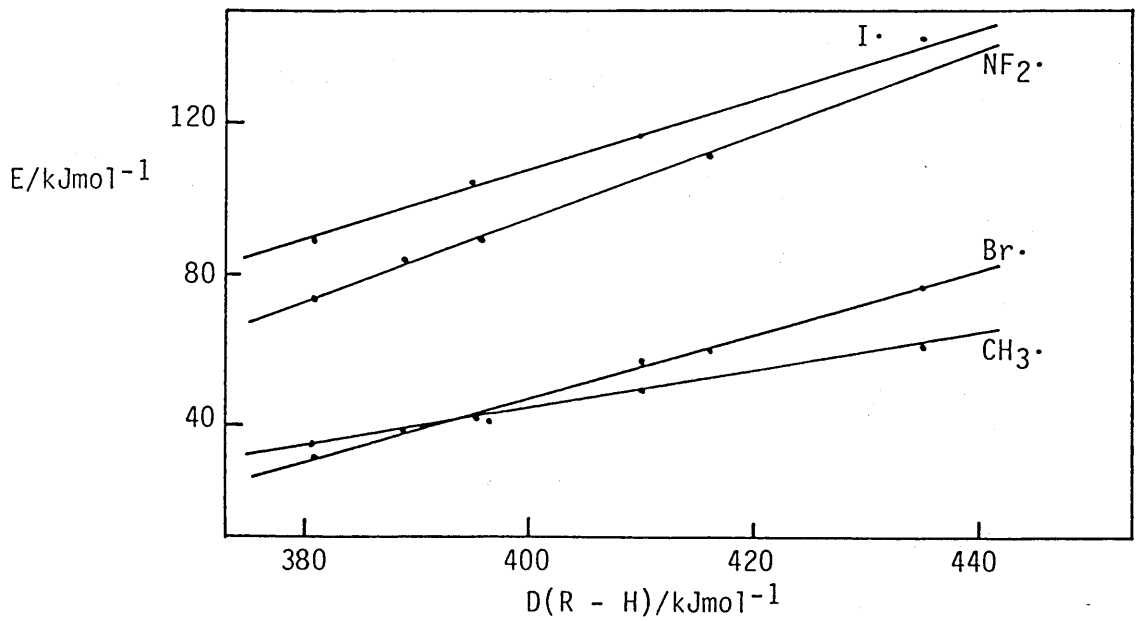

1.6.5 Radical Buffer Technique

Studies of gas phase iodine atom metathesis reactions of alkyl radicals led Benson to the conclusion that, under typical reaction conditions where [RI] >> [R·], the rate of iodine metathesis is orders of magnitude greater than the radical recombination rate[50]. This process, represented by Equation 1.80, has been described as a radical buffer because the values of k_{80} and k_{-80}, together with the high [RI]/[R·] ratios, ensure that the ratio [R·]/[R'·] is not much affected by disturbances caused by the self reactions and other reactions of these radicals.

$$R\cdot + R'I \rightleftharpoons R'\cdot + RI \qquad 1.80$$

In its original application the technique was used to obtain radical recombination rates by measuring the radical recombination products occurring from the reactions

$$R\cdot + R\cdot \xrightarrow{1} R_2 \qquad 1.81$$

and

$$R\cdot' + R\cdot' \xrightarrow{1'} R'_2 \qquad 1.82$$

The ratios of the rates of formation of R_2 and R_2' is given by

$$\frac{d[R_2]}{d[R'_2]} = \frac{k_1[R\cdot]^2}{k_1'[R'\cdot]^2} \qquad 1.83$$

Since the equilibrium constant, K, for reaction 1.80 is given by

$$K = \frac{[R'\cdot]}{[R\cdot]} \cdot \frac{[RI]}{[R'I]} \qquad 1.84$$

From equations 1.83 and 1.84 we obtain

$$K\left(\frac{k_1'}{k_1}\right)^{\frac{1}{2}} = \frac{[R_2']_t^{\frac{1}{2}}}{[R_2]_t^{\frac{1}{2}}} \cdot \frac{[RI]_{av}}{[R'I]_{av}} \qquad 1.85$$

where $[R_2]_t$ is the concentration at time t and $[RI]_{av}$ the average concentration over time t.

The right hand side of Equation 1.85 is determined experimentally, and K obtained from the thermochemistry of the buffer reaction. Hence, if the recombination rate of one radical has been determined by an absolute technique, the recombination rate of the other radical is obtained.

When this technique was used to determine the ^{t}butyl radical recombination rate, a value of $10^{5.4}$ $lmol^{-1}s^{-1}$ was obtained[68], about 4 orders of magnitude less than that obtained by direct methods[69]. This low value suggested an error in the ^{t}butyl radical thermochemistry and provided an impetus for the re-investigation of radical thermochemistry[119].

The radical buffer technique has been applied to a number of alkyl radical recombination reactions[50-54,65] but has generally provided results that have been inconsistent with absolute methods. It will be demonstrated later that revisions of radical thermochemistry reconcile the differences.

Having provided an impetus for revising radical thermochemistry the buffer technique has more recently been reversed to obtain thermochemical data. This approach by Griller and co-workers[66,67] was carried out in iso-octane solution and involved direct measurement of radical concentrations using electron spin resonance spectroscopy.

Since the relative concentration of iodoalkanes remains essentially constant during the experiment the equilibrium constant is obtained from Equation 1.84. From this equilibrium constant and the thermochemistries of the iodoalkanes and one radical, the heat of formation of the other radical is determined. Data obtained using this method based on $\Delta H_f(CH_3\cdot) = 143.9\ kJmol^{-1}$ are given in Table 1.5.

Table 1.5

Thermochemical Data Obtained From Radical Buffer Studies[67]

R·	$\Delta H_f(R\cdot)/kJmol^{-1}$	$D(R - H)/kJmol^{-1}$
$C_2H_5\cdot$	117.2	419.7
$n\text{-}C_3H_7\cdot$	95.4	417.1
$i\text{-}C_3H_7\cdot$	80.3	402.1
$s\text{-}C_4H_9\cdot$	62.8	407.9
$t\text{-}C_4H_9\cdot$	39.3	392.9
$c\text{-}C_5H_9\cdot$	105.0	400.0

The data in Table 1.5 are in good agreement with those obtained by other recent techniques, thus supporting the method. Also this method is a departure from the majority of other methods giving radical thermochemistry since it does not require kinetic measurements.

There are some limitations to the use of the radical buffer technique however. For reaction 1.80 to be in equilibrium the rate of iodine metathesis must be much greater than the rate of removal of radicals from the system. This requirement is supported by CIDNP experiments for a few unstabilised radicals. Where the radicals are stabilised,

as in benzyl or allyl, the equilibrium requirement is not met and the technique is inapplicable.

Furthermore, the experiments are carried out in solution whereas the standard state for measuring BDE s is the gas phase. It is assumed that the difference between the heats of mixing of the two radicals is similar to the difference between those of their parent alkanes. In any case, both types of substance are weakly solvated in non-polar solutions[70]. Thus, any corrections required for heats of mixing are likely to be small and, to a large extent, self cancelling.

1.7 Group Additivity

A number of molecular properties of larger molecules approximate to additive contributions due to individual atoms or bonds within the molecule. Thus, such physical properties as refractive index, ultraviolet and infrared absorption spectra, magnetic susceptibility and some thermodynamic functions such as entropy, heat capacity and heat of formation may be estimated from contributions due to individual components within the molecule[4]. This empirical observation has been justified on the basis that intermolecular and intramolecular forces are short-range , appreciable over a distance of 0.1 - 0.3nm, i.e. typical interatomic distances.

To a first approximation an additivity scheme could be developed where contributions due to partial atomic properties were summed to give the molecular property. Such a scheme would be of limited use in determining changes in thermodynamic functions however, since the conservation of atoms in a chemical reaction would mean zero change in the thermodynamic function for the reaction, i.e. $\Delta H = 0$ and $\Delta S = 0$.

The principle of additivity was refined by Benson and Buss[71] into an additivity of bond as opposed to atomic properties, since this was found to provide more reliable data. Hence all hydrocarbon thermochemistry may be obtained from partial C - C and C - H values, which are assigned using known thermochemistry for prototypical compounds. Thus, by assigning ΔH_f(C - C) = 11.4 kJmol^{-1} and ΔH_f(C - H) = -16.0 kJmol^{-1} [4], we find $\Delta H_f(C_3H_8)$ = -105.2 kJmol^{-1}, in good agreement with the accepted value of -103.8 kJmol^{-1} [15]. Partial bond values have been assigned to a number of bonds, and thermochemical data can usually be estimated to within 8 kJmol^{-1} for ΔH_f and 4 JK^{-1}mol^{-1} for S^o and Cp, although larger errors may be encountered for heavily branched compounds. The major limitation of a bond additivity method is the inability to distinguish between isomeric species, such as n-butane and iso-butane and cis and trans olefins.

These problems are in part overcome by a further refinement of the method in which properties of individual groups within a molecule are assigned. A group for these purposes is defined as a polyvalent atom with at least two attached ligands. For example, C - $(H)_2(C)_2$ represents a carbon atom bonded to two hydrogens and two other carbons i.e. a secondary carbon as in propane. Various corrections are applied to the method to allow for such factors as cis isomers in olefins, ring strain in cyclic compounds and symmetry contributions to entropy[4]. The method generally allows estimation of S^o and Cp to within 1.5 JK^{-1}mol^{-1} and ΔH_f to within 2 kJmol^{-1}, although the uncertainties may increase to 6 JK^{-1}mol^{-1} and 12 kJmol^{-1} respectively where heavily substituted species are involved. The generally good agreement between estimated and observed thermodynamic parameters for a wide variety of molecular species has been demonstrated in a detailed review of the method[72].

The group additivity method may also be applied to free radicals by assigning group values for the radical centres ·C - $(C)(H)_2$, ·C - $(C)_2(H)$, C - (·C)$(H)_3$ etc. The data obtained are less reliable than those obtained for molecular species however, particularly in the case of $\Delta H_f(R\cdot)$ values. This is primarily due to uncertainties in the measured heats of formation of the free radicals from which the group contributions are derived.

Estimating thermodynamic parameters using group additivity is particularly valuable in cases where very little or unreliable experimental data exist.

1.8 Typical Values of Hydrocarbon BDE s

There is currently a good deal of disagreement over the absolute values for hydrocarbon BDE s with some workers favouring lower values than others. However, the relative values of BDE s are well established, as shown by the prototypical values given in Table 1.6.

Table 1.6

Prototypical Values of Hydrocarbon BDE s[27]

R·	D(R - H)/kJmol^{-1}
CH_3·	439.7
C_2H_5·	410.9
i-C_3H_7·	397.9
t-C_4H_9·	389.9
benzyl·	368.2
allyl·	361.1

The values of D(R - H) for ethyl, i-propyl and t-butyl are the typical values for primary, secondary and tertiary C - H bonds. The values given are those contained in the recent review by McMillan and Golden[27] which recommends somewhat lower values than those favoured by other workers[38,49,67]. The impact of these revisions will be discussed later. The low D(R - H) values for benzyl and allyl arise from radical stabilisation due to delocalisation of the unpaired electron. Thus the overall trend in BDE s for hydrocarbons is

$$D(CH_3 - H) > D(RCH_2 - H) > D(R_2CH - H) > D(R_3C - H) > D(\text{allyl, benzyl} - H) \qquad 1.86$$

For cyclic radicals deviations from typical secondary BDE values occur due to ring strain and conformational changes upon radical formation. Table 1.7 gives recent values of cyclic R - H BDE s for a series of cycloalkanes.

Table 1.7

BDE Values for Cycloalkanes[27]

R•	D(R - H)/kJmol^{-1}
cC_3H_5	445
cC_4H_7	404
cC_5H_9	395
cC_6H_{11}	400
cC_7H_{13}	387

These values have been determined from Evans-Polanyi relationships with the exception of cyclopropyl which was obtained using a VLPP technique. The value obtained for D(c - C_3H_5 - H) is the highest

C - H BDE for any saturated alkane and is associated with the high strain energy within the ring and the olefinic nature of the bonding[84].

C - H BDE values for C_5 - C_7 cycloalkanes are investigated in this work and considered in detail in a later section.

1.9 Kinetics of Radical Termination Reactions

1.9.1 Disproportionation and Recombination

Many reactions occur via free radical chain mechanisms in which disproportionation and recombination of radicals are the termination reactions in the mechanism. Thus a knowledge of these rates is important in fully understanding the mechanisms of these reactions. Also, the kinetics of a number of radical reactions have been studied by measuring the reaction rate relative to the rate of radical recombination[73]. For example, two of the steps occurring during the reaction of alkyl radicals with carbon tetrachloride are

$$RH + \cdot CCl_3 \longrightarrow R\cdot + HCCl_3 \qquad 1.87$$

and

$$\cdot CCl_3 + \cdot CCl_3 \longrightarrow C_2Cl_6 \,. \qquad 1.88$$

It was shown[74] that the rate constants for the two reactions were related via

$$\frac{R_{HCCl_3}}{R_{C_2Cl_6}^{\frac{1}{2}}\,[RH]} = \frac{k_{87}}{k_{88}^{\frac{1}{2}}} \qquad 1.89$$

where $R_{C_2Cl_6}$ and R_{HCCl_3} are the rates of formation of the respective products. The left hand side of Equation 1.89 was determined experimentally, thus the recombination rate constant for the trichloromethyl radical, k_{88}, is required to determine the rate

constant for hydrogen abstraction by trichloromethyl radicals from alkanes.

Accurate values for radical recombination rates are also required to determine radical reaction thermochemistry when combined with data from pyrolysis reactions, as described in section 1.6.1.

Experiments designed to measure radical recombination rates by monitoring the concentration of alkyl radicals generally measure the radical termination rate constant, k_t, which is the sum of the recombination rate constant, k_c, and disproportionation rate constant, k_d.

$$k_t = k_c + k_d \qquad 1.90$$

Fortunately, measurement of disproportionation/recombination ratios are relatively straightforward from measurements of recombination and disproportionation products, and values are generally available[75].

Two approaches exist to studying the kinetics of radical-radical reactions. In absolute methods the radical concentration is measured directly by a technique such as mass spectrometry or absorption spectroscopy. Indirect methods depend upon the thermochemistry of the reaction studied, such as radical buffer and pyrolysis techniques. The various methods are described briefly in the following sections.

In general, the methods indicate that disproportionation and recombination reactions are very fast reactions with small or zero activation energies[73]. In the gas phase the rate constants for these reactions are typically 10^8 - 10^{10} $lmol^{-1}s^{-1}$, suggesting they are collision controlled. These reactions also occur with similar rate constants in solution, suggesting diffusion control.

1.10 Absolute Methods for Determining Recombination Rates

1.10.1 Rotating Sector

Historically this is the most important method used to study termination reactions. The technique is based on the kinetic behaviour of photochemical reactions involving radical recombination when the photolysis is intermittent. A rotating disc in which a sector is cut out is placed between the light source and the sample thus modulating the photolysis. The reaction rate is observed to depend upon the duration of each light flash and therefore on the speed of rotation of the disc.

A simple photo-initiated chain reaction, in which reactant A is transformed into a product B, may be represented schematically by

$$\text{Initiation, I} \qquad A \xrightarrow{h\nu} 2R\cdot \qquad 1.91$$

$$\text{Propagation, kp} \qquad R\cdot + A \longrightarrow B + R\cdot \qquad 1.92$$

$$\text{Termination, } k_t \qquad R\cdot + R\cdot \longrightarrow R_2 \qquad 1.93$$

When a steady state is established, the radical concentration is given by

$$\frac{d[R\cdot]}{dt} = 0 = I - k_t[R\cdot]^2 \qquad 1.94$$

Where I is the rate of initiation, dependent on light intensity. The overall reaction rate is given by

$$\frac{-d[A]}{dt} = \frac{d[B]}{dt} = kp[R\cdot][A] = \frac{kp(I)^{\frac{1}{2}}[A]}{kt^{\frac{1}{2}}} \qquad 1.95$$

Many kinetic methods do not allow separation of the rate constants kp and k_t. Both constants can be determined by the rotating sector technique, however, since the establishment of a steady radical concentration can be prevented.

Under steady state conditions, a mean lifetime τ for the radicals may be defined as the concentration of radicals divided by their rate of removal, thus from above

$$\tau = \frac{[R\cdot]}{k_t[R\cdot]^2} = \frac{1}{k_t[R\cdot]} \qquad 1.96$$

Combining this with Equation 1.95 gives

$$-\frac{d[A]}{dt} = \frac{kp}{k_t} \cdot \frac{[A]}{\tau} \qquad 1.97$$

Thus a measure of τ together with the steady state propagation rate given by Equation 1.95 allows separation of kp and k_t. τ is determined by varying the speed of rotation of the disc.

At a slow rotation speed where the period of illumination is much longer than τ, a steady state concentration of radicals builds up in the light period and effectively decays to zero in the dark period. Consider a sector angle of 90°. In this case the rate of reaction observed will be ¼ that observed under continuous photolysis, i.e. from Equation 1.95.

$$R_{slow} = (\tfrac{1}{4}) \cdot \frac{kp(I)^{\frac{1}{2}}[A]}{k_t^{\frac{1}{2}}} \qquad 1.98$$

On the other hand, if the illumination period is short with respect to τ, then the radical concentration changes very little between

the light and dark periods. These two situations, slow and fast rotation, are represented diagrammatically in Figure 1.10. Under fast rotation a quasi-stationary state radical concentration is established, corresponding to reducing the initiating light intensity by a factor of 4. Thus

$$R_{fast} = \frac{kp(I/4)^{\frac{1}{2}}[A]}{k_t^{\frac{1}{2}}} \qquad 1.99$$

Figure 1.10

Build-up and Decay of Radicals at High and Low Rotation Speeds

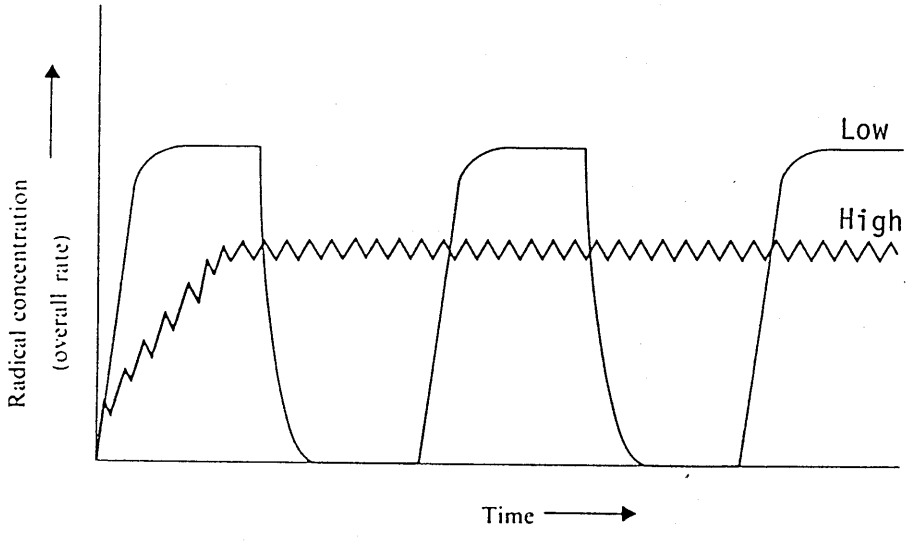

The ratio of the reaction rates at fast and slow rotation speeds is related to the desired quantity τ and is approximately equal to the turning point shown in Figure 1.11. The theoretical relationship between the ratio of reaction rates and flash duration t_1 has been derived, and τ tabulated for various sector angles[76].

Figure 1.11

Dependence of Reaction Rate on Duration of Light Pulse

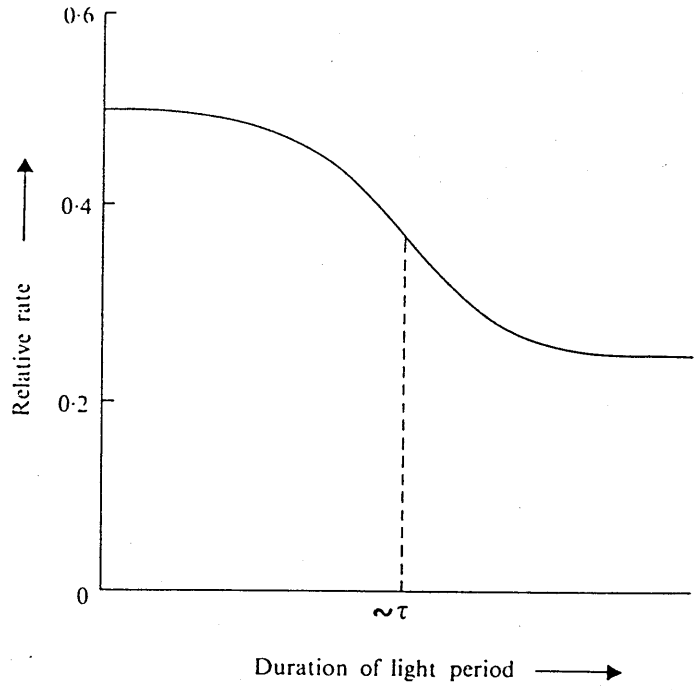

An example of the technique is the measurement of the methyl radical recombination rate by Shepp[77] using acetone as a photolytic source of methyl radicals. Above 400K using 250nm radiation the reaction scheme is

$$CH_3COCH_3 \xrightarrow{I} 2CH_3\cdot + CO \qquad 1.100$$

$$CH_3\cdot + CH_3COCH_3 \xrightarrow{k_p} CH_4 + \cdot CH_2COCH_3 \qquad 1.101$$

$$2CH_3\cdot \xrightarrow{k_t} 2C_2H_6 \qquad 1.102$$

$$2CH_3COCH_2\cdot \longrightarrow (CH_3COCH_2)_2 \qquad 1.103$$

$$CH_3\cdot + CH_3COCH_2\cdot \longrightarrow CH_3COCH_2CH_3 \qquad 1.104$$

The rate of the propagation reaction was followed by the production of methane since the acetone concentration is virtually constant. The initiation rate is obtained from the carbon monoxide yield. This gave a value for the methyl radical recombination rate constant of

2.2×10^{10} $lmol^{-1}s^{-1}$, in good agreement with that obtained by the more recent technique of molecular modulation spectroscopy[78]. However, for larger radicals the technique is not very accurate, with errors in excess of 20% not uncommon[73]. It is therefore not the technique most suited to measuring temperature coefficients of reactions with low activation energies since correspondingly high errors in Arrhenius parameters will be obtained.

1.10.2 Flash Photolysis

This technique, first reported by Norrish and Porter[79] in 1949, is one of the best known techniques for studying fast reactions. The reactions are initiated by a very short intense flash of light which produces a high concentration of radicals. The disappearance of the radicals after the initial flash is then followed spectroscopically, often using a delayed second flash as a spectrophotometric light source. Using modern laser sources, time resolution to 10^{-8}s has become possible.

The basic experimental arrangement is illustrated in Figure 1.12

Figure 1.12

Flash Photolysis Apparatus

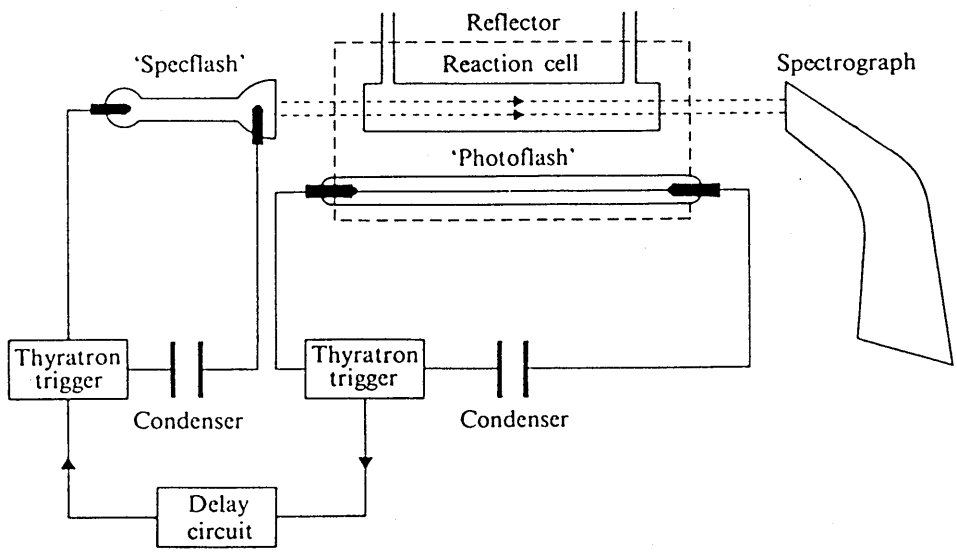

Basically, the photolysis is initiated by discharging a capacitor through the photolysis source which transmits an energy in the region of 25kJ to the sample gas in a few microseconds. At some short period after photolysis, typically 0 - 10 milliseconds, the 'specflash' is triggered which generates a much lower energy than the original flash, and the light absorption by the reactive species is then recorded by the spectrometer. In a variation of the technique, known as kinetic spectroscopy, the time delay between the two flashes is varied allowing a profile of the radical decay to be determined. The rate constant for radical-radical reactions is determined by analysis of the decay curve.

Flash photolysis is applicable to bimolecular reactions with rate constants up to 10^{11} $lmol^{-1}s^{-1}$. The short timescales employed ensure that fast reactions occur before diffusion to the reactor walls, thus eliminating heterogeneous effects.

An example of the technique is a study of the recombination of methyl radicals produced by the photolysis of azomethane[80].

$$CH_3 - N = N - CH_3 \xrightarrow{h\nu} 2CH_3\cdot + N_2 \qquad 1.105$$

$$2CH_3\cdot \xrightarrow{k_t} C_2H_6 \qquad 1.106$$

The azomethane (about 5torr) was photolysed in an excess of nitrogen to reduce the heating effect due to photolysis. The methyl radical decay was then followed at intervals up to 100 microseconds after photolysis by monitoring the methyl absorption at 216nm. The decay of the absorbance A was found to be second order i.e. a plot of $1/A$ against time was linear.

Since A is proportional to $[CH_3\cdot]$ via

$$A = \varepsilon l[CH_3\cdot] \qquad 1.107$$

where ε is the extinction coefficient and l the cell length.

This demonstrated that all methyl radicals reacted by recombination. Furthermore the second order rate law implies

$$\varepsilon l \, d(1/A)/dt = 2k_t \qquad 1.108$$

Thus k_t is available from the slope of the plot of $1/A$ against time and the value of ε . The determination of ε was achieved by measuring the absorbance as a function of time as it rose during the photoflash and began to decline. The initial absorbance that would have been observed if no recombination occurred and if the photolysing flash was instantaneous was calculated from the decay after the flash. The total number of radicals generated was taken as twice the number of ethane molecules generated at the end of the experiment. Thus ε was determined via

$$\varepsilon = \frac{A_T}{2[C_2H_6]l} \qquad 1.109$$

where A_T is the total absorbance. Substituting ε into Equation 1.108 enabled k_t to be determined as 2.6×10^{10} $lmol^{-1}s^{-1}$, in good agreement with the value obtained by the rotating sector method[77] and another flash photolysis study[81] using dimethyl mercury as a radical source.

The main disadvantage of the technique is the need to follow the radical concentration spectroscopically since absorption bands for some radicals are weak[69] and radical absorption spectra are not generally known.

1.10.3 Molecular Modulation Spectrometry

The application of molecular modulation spectrometry to the determination of alkyl radical recombination rates was first reported in 1976 by Parkes and Quinn[69,78].

The apparatus consists of a quartz reaction cell, about 60cm long and 4cm diameter, which is surrounded by fluorescent tubes. Radicals are generated by photolysis of a suitable precursor by applying square wave modulation to the fluorescent tubes which allows them to be switched on and off at frequencies between 10^2 and 10^{-2} Hz. The modulated radical concentration is detected by measuring the ultraviolet absorption due to the radicals along the axis of the cell. This signal lags behind the photolysis lamp modulation by an amount which depends on the radical removal rate and the modulation frequency. The absorption signal is digitised and recorded by two up-down counters. The first of these counts up when the lamps are on and down when they are off (in-phase). The second count lags the first by 90° (in-quadrature). The timing relationships are demonstrated in Figure 1.13.

Data are collected over a range of modulation frequencies and substrate pressures. From the relationship between the in-phase and in-quadrature counts the radical termination rate constant can be determined. At relatively low modulation frequencies the radical concentration closely follows the square wave pattern of the photolysis. At higher frequencies the time constant of the reaction leads to a phase shift between the photolysis frequency and the radical concentration. With the detection and counting system employed, this results in an in-phase signal which rises to a value related to the steady state radical concentration. The in-quadrature signal also

Figure 1.13

Timing Relationships in Molecular Modulation Spectrometry

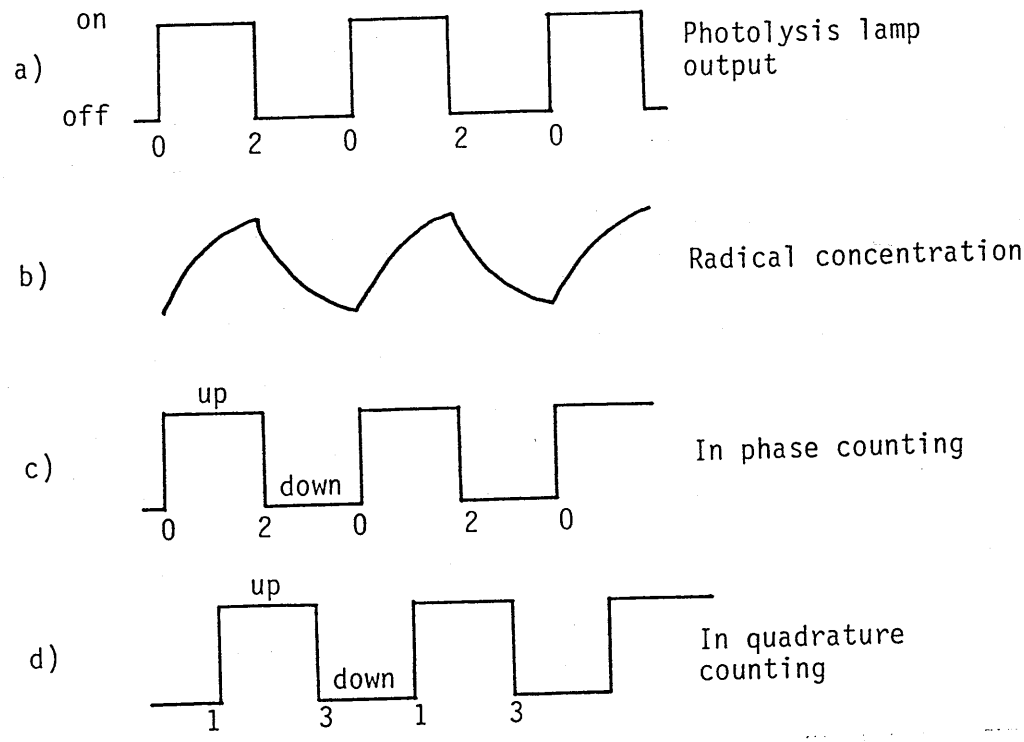

Figure 1.14

Radical Signals from Molecular Modulation Spectrometry

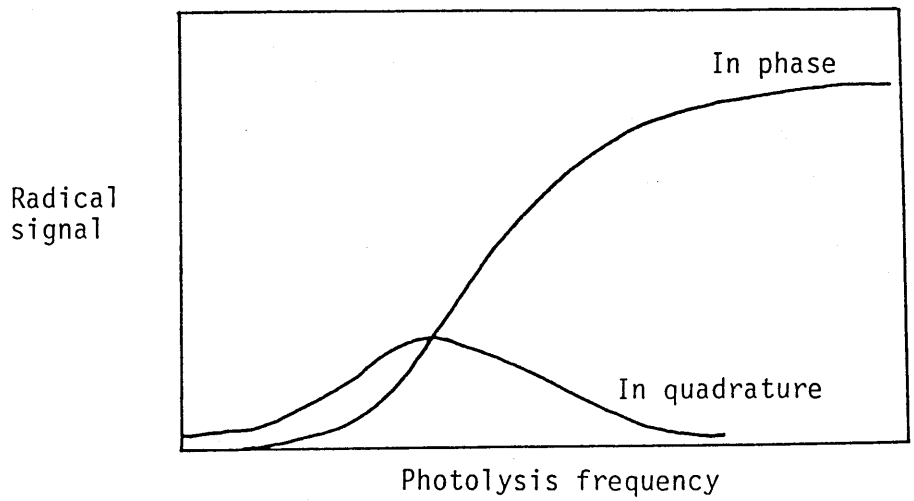

rises as the phase shift becomes apparent. At very high frequencies the radical concentration becomes a sawtooth waveform and both signals drop, the in-quadrature more quickly. The form of the signal variations is shown in Figure 1.14.

For a process of the type

$$2R\cdot \xrightarrow{k_t} R_2 \qquad 1.110$$

it has been shown[78] that the photolysis frequency at which the curves intersect, t_o, is given by

$$1/t_o = (Bk_t)^{\frac{1}{2}} / 2.2 \qquad 1.111$$

where B is the photolytic rate of radical production. B may be calculated by following the decline in radical intensity with experimental time thus allowing calculation of k_t from Equation 1.111.

The technique has been used to study the recombination rates of CH_3 and CD_3 radicals[78] as well as ethyl, i-propyl and t-butyl[69]. The data obtained are generally considered to be among the most reliable to date.

The other major technique applied to obtain absolute rates for radical recombination is that of very low pressure pyrolysis. The technique uses mass spectrometry to detect the radical products and precursors and is described in section 1.6.3. The major drawback of the VLPP technique is the necessity to correct data for fall-off effects due to reactions not being at their high pressure limits under the experimental conditions.

Indirect methods for obtaining radical recombination rates have been discussed earlier since they depend upon the reaction thermochemistry

and therefore provide radical thermochemistry if recombination data are available. The major techniques in this category are the shock tube method described in section 1.6.1 and the radical buffer technique described in section 1.6.5. In the former technique the recombination rate constant is determined from the kinetics of the reverse reaction, bond fission. The latter technique provides relative data for the recombination of two alkyl radicals produced during iodine metathesis reactions.

1.11 Typical Values of Recombination Rate Constants

Rate constants for the recombination of prototypical alkyl radicals in the gas phase are well established by the molecular modulation technique[69,78]. These values are given in Table 1.8.

Table 1.8

Radical Recombination Rate Constants

R·	10^{-9} k_r/lmol^{-1}s^{-1}	T/K
CH_3·	24	250 - 900
C_2H_5·	8.4	300 - 850
i-C_3H_7·	4.8 $(T/300)^{-0.5}$	300 - 800
t-C_4H_9·	2.4 $(T/300)^{-1.5}$	300 - 650

The temperature dependencies of the recombination rate constants are zero for methyl and ethyl radicals. However, i-propyl and t-butyl show a slightly negative temperature dependency, i.e. rate constant decreases as temperature increases. Interpreted as an Arrhenius activation energy i-propyl and t-butyl recombinations have energy barriers of -2 and -5 kJmol^{-1} respectively which, to within the error limits involved, is in reasonable accord with the assumption of zero

activation energy for radical recombination[27].

It is interesting to compare the rate constants with the collision frequency in the gas phase which is approximately 1×10^{11} $lmol^{-1}s^{-1}$ for methyl radicals. This implies a very high efficiency for methyl radical recombination, with about one in five collisions resulting in reaction. Rate constants close to the collision frequency are generally obtained for alkyl radicals in the gas phase[73] and these are usually termed collision controlled reactions.

In solution recombination rate constants are generally of the same order of magnitude as those obtained in the gas phase[75], although slightly lower values are observed due to reduced encounter frequencies due to solvent effects. Radical recombination in solution usually proceeds at the diffusion controlled rate.

The only exceptions to diffusion or collision controlled rates are observed in spin-forbidden recombinations involving electronically excited states[83], although Tedder[124] has reported a rate constant for cyclohexyl recombination of $< 1 \times 10^{7}$ $lmol^{-1}s^{-1}$. This anomalous value is investigated in this work by a study of cyclopentyl and cyclohexyl recombination using the radical buffer technique.

Chapter 2

EXPERIMENTAL

This chapter describes the apparatus and techniques employed to determine thermochemical and kinetic parameters for alkyl radicals using the radical buffer technique.

2.1 Thermochemical Experiments

This section deals with the study of the radical buffer reaction and gives the techniques employed to generate and determine relative concentrations of alkyl radicals from their corresponding iodoalkanes under equilibrium conditions.

2.1.1 Apparatus

a) Electron Spin Spectroscopy (ESR)

Radical concentrations were determined by ESR spectroscopy using a Varian E109 spectrometer equipped with an E231-2 rectangular microwave cavity and an E102 9.5GHz microwave bridge. Temperature was controlled by flowing nitrogen gas through the microwave cavity. The gas temperature was regulated by a Varian Variable Temperature Controller and measured to 0.1°C by a Comark Microprocessor Thermometer using a copper/copper nickel thermocouple inserted into the cavity. For operation at temperatures of less than 35°C the nitrogen gas was precooled by flowing through a heat exchanger coil immersed in liquid nitrogen, prior to subsequent heating to the required temperature by the control apparatus.

Microwave power level was varied according to the system under investigation such that maximum signal intensity was obtained without saturation. For a non-saturated ESR signal the amplitude increases in direct proportion to the square root of the incident microwave power[23]. The effect of microwave power on the radicals investigated in this work was checked to ensure power levels employed were well within this relationship. Typically the incident microwave power was in the region of 1 - 2 milliwatts.

Modulation amplitude was chosen to give maximum signal amplitude

without excessive broadening of the lines of interest. Generally, the modulation amplitude chosen also prevented the resolution of additional fine structure due to any possible γ(H) couplings. Typical values were in the region of 0.5 - 2 Gauss.

b) Photolysis

Reactions were initiated by continuous ultraviolet photolysis from a Hanovia 977B-1 1000 watt high pressure mercury-xenon arc lamp. The housing of this lamp is fitted with a spherical mirror behind the lamp to increase the light intensity in the forward direction by reflecting back light leaving the rear of the lamp. At the front of the housing a silica lens collimates the beam which is then focussed into the microwave cavity by a 75mm silica lens. The optical system was carefully aligned by placing a light-sensitive cell in the microwave cavity and optimising its output.

In the light path, between the collimating and focussing lenses, a filter containing distilled water of 10cm path length reduced the heating effect at the microwave cavity, due to photolysis, to less than 1°C by removing most of the infrared radiation from the beam. This filter was constructed from two 75mm diameter silica windows and was cooled by circulating water through a surrounding external jacket.

A hinged gate located in the beam path enabled the termination of photolysis without switching off the lamp which took 10 minutes to reach steady operating conditions.

2.1.2 Determination of Radical Concentrations in a Static System

The first system investigated in this work was the equilibrium between

iodoethane and 1-iodopropane and their corresponding radicals when an initiator was photolysed in the presence of the iodoalkanes in an ESR tube situated in the microwave cavity. In such an experiment the iodoalkanes may be consumed at differing rates. Therefore, to determine the equilibrium constant for the reaction, it was necessary to determine the relative alkyl radical concentrations at the start of the experiment, i.e. the commencement of photolysis. As the lines of the ESR spectrum of each radical could not be recorded simultaneously, this was achieved by recording the variation of intensity with time of a line from each radical and extrapolating back to the start of the experiment. The output obtained from the ESR spectrometer is the derivative of the absorbtion curve and lines from each radical were alternately scanned from peak to peak. The output was recorded on a chart recorder, an example of which is given in Figure 2.1.

Figure 2.1

Peak Heights from a Static Experiment

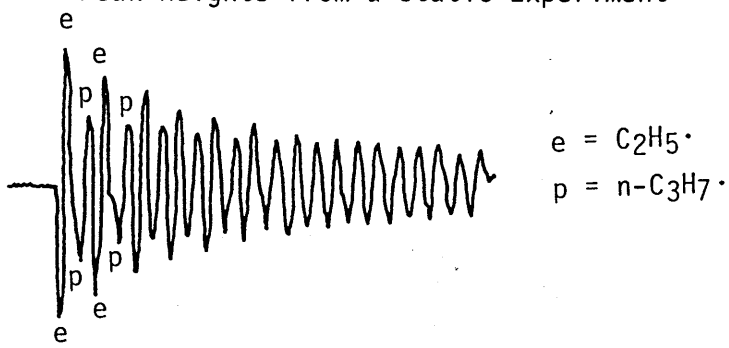

Ideally the lines recorded for each radical would have been integrated twice to give the area under the absorption curve, prior to extrapolation. However, as it is necessary to scan the lines slowly over a narrow scan range to obtain accurate second integrals, it was only possible to obtain about four measurements for each radical before the initiator became exhausted, typically about 15 minutes under the conditions used. This obviously led to greatly increased

errors in extrapolation. By scanning the lines peak to peak it was usually possible to obtain at least 10 measurements for each radical in the same timescale. This technique is only valid if the lines have the same peakshapes[23], which was shown to be the case for ethyl and n-propyl radicals.

To overcome the problems arising from extrapolation the flow technique was developed.

2.1.3 Determination of Radical Concentrations in a Flow System

To enable the observation of a steady concentration of radicals during photolysis the reactants were driven at a constant rate through a flow cell in the ESR cavity.

Figure 2.2

The Flow Cell

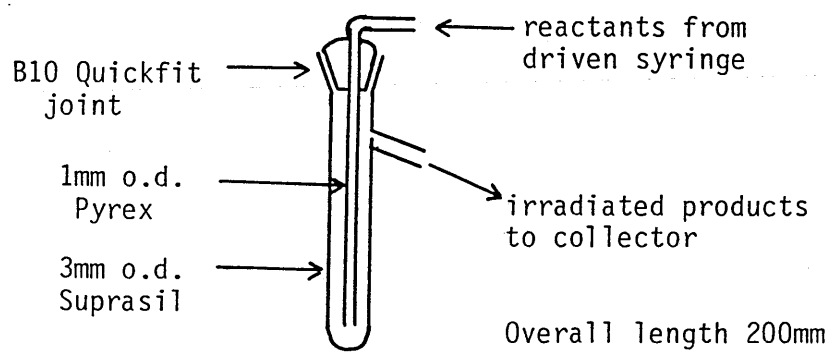

Constant flow was achieved by passing the reactants through the cell from a $20cm^3$ glass syringe driven by a Sage Instruments model 341A syringe pump. The syringe was connected to the inlet of the cell via a 3 way tap and narrow bore Teflon tubing.

The temperature of the solution was measured using a thermocouple placed directly in the solution, just above the photolysed region of the cavity. As the inner capilliary and sample tube were concentric

the reactants were precooled or heated to the desired temperature by the outgoing solution, prior to photolysis.

Typical flow rates were in the region of 1 ml/minute thus giving an average residence time in the photolysed region of about 12 seconds. In determining the equilibrium constant by this technique it is essential that the relative iodoalkane ratio is constant throughout the experiment. This was tested by gas chromatographic analysis of the irradiated products from a few experiments involving 1-iodopropane and iodocyclopentane. The results shown in Table 2.1 show this condition is met to within the experimental limits of the analysis.

Table 2.1

Iodoalkane Ratios Before and After Photolysis

		$[nC_3H_7I]/[cC_5H_9I]$	
Run	Temp./°C	Initial	After Photolysis
R160	44.5	15.75	17.46
R161	44.7	15.73	18.26
R162	44.7	14.50	14.55
R163	- 42.8	14.67	13.86
R164	- 42.3	14.62	13.89
R165	- 41.7	14.76	13.54

A problem occasionally encountered in flow experiments was blocking of the inner capilliary of the flow cell. This was particularly apparent at low temperatures where the solubility of the initiator was limited, and was overcome by passing smaller volumes (typically 8 - 10 ml) of solution through the flow cell. Under these conditions any partial crystallisation of solute did not cause total blockage.

2.1.4 Computing

Signals from the ESR spectrometer were processed using a Digital Corporation MINC computer equipped with a MINC Basic /03 V.3.0 operating system. To remove high frequency interference which was occasionally observed, the spectrometer output was fed to the computer's analogue-to-digital converter via a 45 Hz low pass filter. Each spectrum was sampled and stored as 2048 data points.

The ESR spectrometer employs a phase sensitive detection system and the output obtained is the derivative of the absorption curve, thus two integrations are necessary to obtain radical concentrations. This was accomplished numerically by the following procedure:

1) The data points collected over the width of the line were summed and divided by the number of points, thus determining the average baseline offset. This offset was then subtracted from each point to zero the baseline.
2) The first integration was performed by progressive summation of each point of the line of interest, yielding the absorption curve which could be displayed for inspection.
3) Procedure 2 was repeated to yield the area under the absorption curve.

Figure 2.3 illustrates the typical output obtained at each stage of the integration procedure.

Typically integrations were performed over 150 to 500 data points, depending upon line width and scan range.

Figure 2.3

Computer Integration of ESR Signals

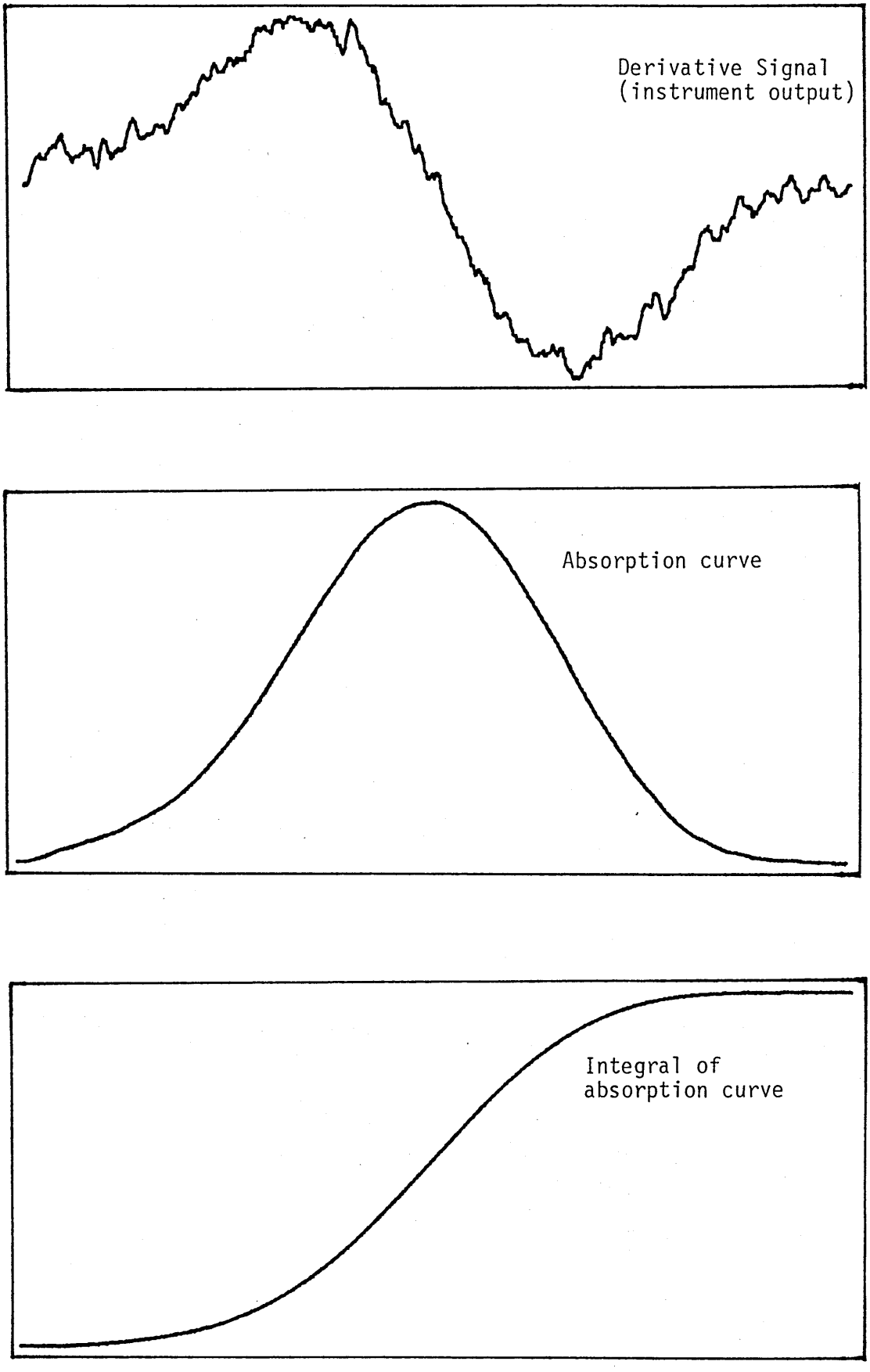

2.1.5 Materials

a) Iodoalkanes

With the exception of iodocycloheptane the iodoalkanes used in this work were commercially available and obtained from the following suppliers

iodomethane iodoethane 1-iodopropane 2-iodopropane 1-iodopentane iodocyclohexane	Aldrich Chemical Co. Ltd.
iodocyclopentane	Lancaster Synthesis

The above iodoalkanes were repeatedly distilled trap-to-trap on a vacuum line with the middle fraction being retained each time until GC analysis indicated a purity of >99%. They were then stored in the dark over copper turnings.

Iodocycloheptane was prepared from the corresponding alcohol (obtained from Aldrich) following the procedure of Olah et al[85]. Thus cycloheptanol (11.4g, 100mmol) and sodium iodide (30g, 200mmol) were dissolved in acetonitrile (130ml) and purged with nitrogen. Chlorotrimethylsilane (21.7g, 200mmol) was added dropwise with rapid stirring at room temperature and reaction followed by monitoring the alcohol by GC. After 4 hours some alcohol remained and the reaction was brought to completion by heating to 50°C for 1 hour. Water (50ml) was added and the reaction mixture taken up in ether. The ether layer was washed with water followed by 10% sodium thiosulphate then saturated brine and finally water and then dried

over magnesium sulphate. Evaporation of the ether yielded the iodocycloheptane (17.1g, 76%) which was distilled and stored as above.

b) Initiator

The initiator used in this work was hexamethylditin, obtained from Alpha Inorganics. Prior to use it was distilled trap-to-trap on a vacuum line and stored under nitrogen in a tube sealed with a septum cap.

c) Solvents

2,2,4-Trimethylpentane (iso-octane) was the solvent of choice for all experiments. Aldrich spectrophotometric grade, Gold Label with a stated purity of >99% was used as received other than degassing by a stream of nitrogen gas to remove dissolved oxygen. This solvent was chosen as it has a particularly wide liquid range (-112 to +98°C and was inert to hydrogen abstraction in the systems studied other than where methyl radicals were produced at temperatures >20°C. A few control experiments were run on the ethyl/n-propyl system to investigate the effects of a change of solvent to either cyclohexane or n-hexane, the results of which are given in Table 2.2.

Table 2.2

Effect of Solvent on K

Run	Solvent	Temperature/°C	K
53	Isooctane	21°	0.42
54	Hexane	19°	0.43
55	Cyclohexane	19°	0.44

Thus a change in solvent had no effect on the measured equilibrium constant to within the experimental errors.

2.1.6 General Procedure for a Thermochemical Experiment

The two iodoalkanes were weighed into a conical flask of suitable capacity and the appropriate volume of solvent added. The mixture was then degassed by bubbling oxygen-free nitrogen through it for 2 minutes before adding the initiator which was transferred via a gas tight syringe from a septum capped tube containing a positive pressure of nitrogen. It was necessary to warm the initiator and syringe in a hot air stream for a few minutes prior to transfer as the hexamethylditin, m.p.23°C, was often solid. The flask contents were then mixed and transferred to the syringe via a 3 way tap. After starting the syringe drive and waiting for the flow to reach the cavity, the gate between the lamp and cavity was opened, commencing the photolysis. Spectra were only recorded after the temperature of the solution had stabilised, typically 1 - 2 minutes after the start of photolysis.

2.2 Kinetic Experiments

This section deals with the experimental techniques developed to obtain radical recombination rate constants from a gas phase study of the radical buffer reaction.

2.2.1 Apparatus

a) The Vacuum Line

A diagram of the vacuum line used in this work is given in Figure 2.4. The line was constructed of pyrex glass tubing and greaseless rotaflow taps, with the exception of taps T_1, T_9 and T_{10} which were glass taps greased with BDH high vacuum silicone grease. Tap T_1 was of 'straight through' design to enable the injection of samples

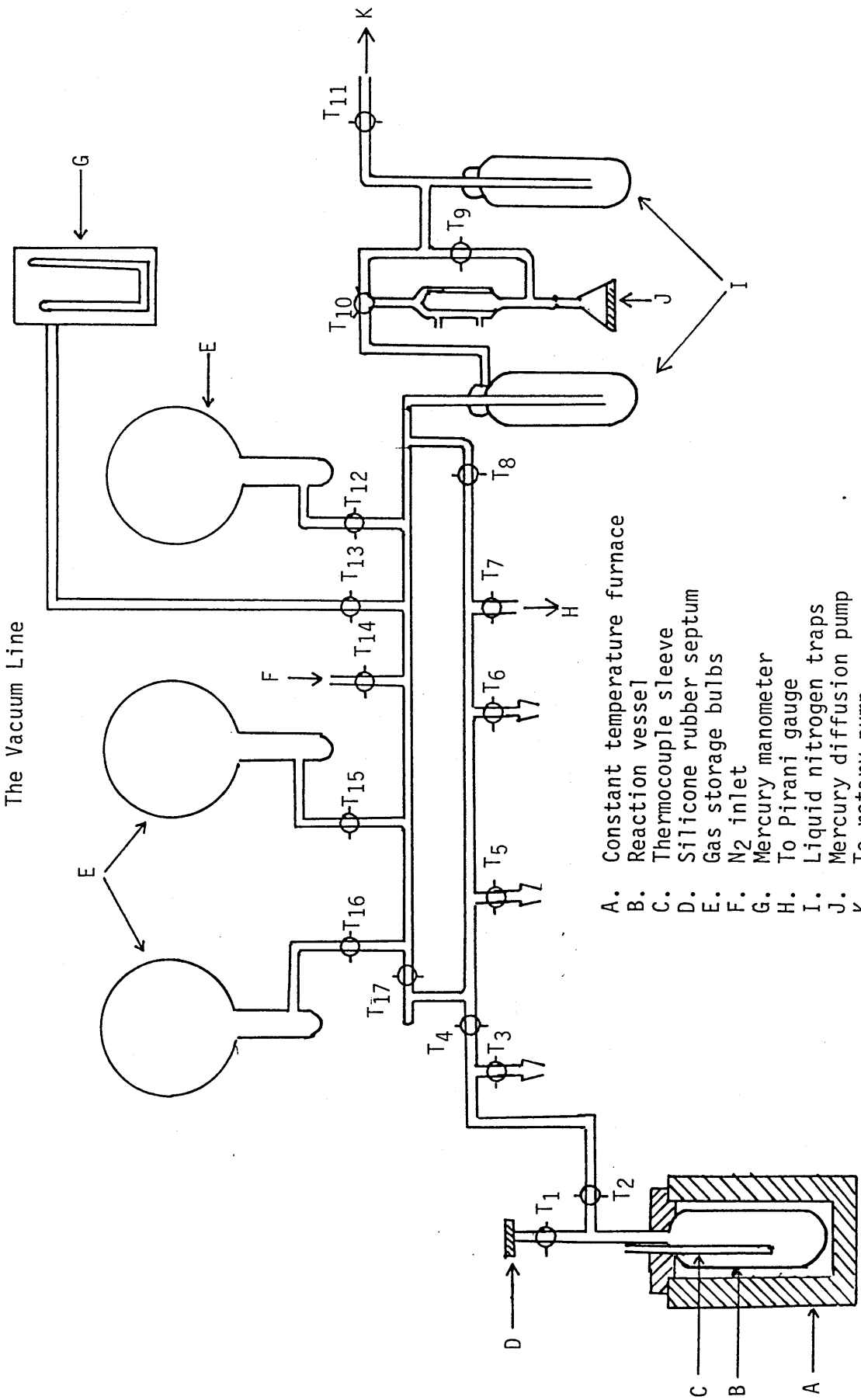

Figure 2.4

The Vacuum Line

directly into the reaction vessel. The reaction vessel was constructed from a pyrex glass tube 5.2cm diameter and 14cm long with hemispherical ends giving an approximate volume of 300cm^3. It was equipped with a ground glass flange above tap T_1 to which a silicone rubber septum was fitted for syringe injection of samples. The vessel was situated within a thermostatted furnace and the tubing above the furnace to tap T_4 was wound with Electrothermal heating tape maintained at 120° to prevent the contents condensing during a run.

The contents of the reaction vessel could be trapped out using a pump through trap of the kind shown in Figure 2.5 which was immersed in liquid nitrogen.

Figure 2.5

Trap for Sampling Vessel Contents

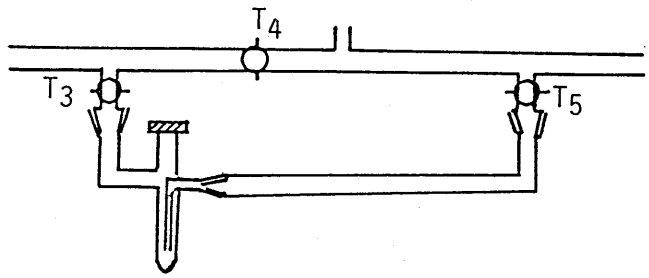

The vacuum line was evacuated by a mercury diffusion pump backed by an Edwards rotary pump, both being protected by cold traps immersed in liquid nitrogen. The pumping system employed enabled the line and reaction vessel to be evacuated to a pressure of $<10^{-4}$ Torr, as measured by an Edwards Pirani gauge.

b) The Furnace and Temperature Control System

The furnace was a cylindrical aluminium block contained within an asbestos box packed with glass fibre wool to minimise heat losses. A centrally bored cavity within the block accommodated the reaction

vessel. The block was heated with a nichrome element wound on sheets of mica around the aluminium. The windings were more closely spaced at the top in order to compensate for the greater heat losses through the top of the furnace. Previous workers[86] using a similar system have shown temperature gradients within the block are small; <0.1°C horizontally and <0.5°C vertically.

The temperature within the vessel was measured with a copper/copper nickel thermocouple inserted into a pyrex finger that penetrated to the centre of the vessel. Temperature variation within the vessel was found to be better than $\pm$ 0.3°C over a period of several days. The furnace temperature was controlled by a C.N.S. Instruments Limited Versicon Type 101 controller coupled to a platinum resistance thermometer which acted as a sensor and was inserted into a hole in the aluminium block.

2.2.2 Gas Chromatography

Product analysis was by gas chromatography using either a Varian 1400 gas chromatograph fitted with $^1/_8$" stainless steel columns or a Pye Unicam 204 gas chromatograph fitted with ¼" glass columns. Both instruments utilised a flame ionisation detector system. A number of columns were prepared for this work and were investigated under various operating conditions to achieve optimum resolution, while retaining a convenient analysis time. Eventually, the columns and operating conditions given in Table 2.3 were used routinely. Quantitative measurements of product ratios were determined by integration of the peaks of interest using a LDC 304 integrator in conjunction with the Varian 1400 chromatograph and a Shimadzu C-R1B Chromatopac integrator for analysis using the Pye Unicam machine. Area ratios were converted to molar ratios by calibrating the GC

response using synthetic mixtures. A number of carefully weighed mixtures were prepared with compositions similar to those of the products, such that the peak area ratios obtained from product analysis were bracketed by the area ratios obtained from the synthetic mixtures. To test for any possible loss of involatile products during the trapping of the vessel contents, samples of the synthetic mixtures were injected into the reaction vessel and trapped out in the same manner as in product sampling. Results obtained from these experiments are given in Table 2.4.

Table 2.3

Gas Chromatography Conditions

Column No:	1		2	
Packing:	2m 10% silicone oil SE52 + 0.5m 10% silicone oil SE30 on Chrom W A.W. DCMS 100 - 120		3m 10% silicone oil SE30 on Chrom W A.W. DCMS 100 - 120	
G.C:	Varian 1400		Pye Unicam 204	
Temperature/°C	100		60	
N_2 Flow Rate/mlmin^{-1}:	25		30	
Retention Times/min:	$nC_5H_{11}I$	5.0	$nC_5H_{11}I$	10.2
	$nC_{10}H_{22}$	6.0	nC_5H_9I	12.6
	$cC_6H_{11}I$	9.3	$nC_{10}H_{22}$	20.5
	$(cC_6H_{11})_2$	25.2	$(cC_5H_9)_2$	34.3

Table 2.4

Comparison of Sampling Techniques for GC Analysis

Compounds	molar ratio	Area Ratio direct sampling	Area Ratio after trapping
$nC_5H_{11}I/cC_6H_{11}I$[a]	2.98	1.42	1.40
$nC_{10}H_{22}/(cC_6H_{11})_2$[a]	13.65	12.16	12.42
$nC_5H_{11}I/cC_5H_9I$[b]	1.69	1.61	1.63
$(cC_5H_9)_2/nC_{10}H_{22}$[b]	1.90	1.91	1.90

(a) analysis by Column no. 1 (b) analysis by Column no. 2

Table 2.4 shows the area ratios obtained were in good agreement, regardless of whether the mixtures were injected directly into the GC or injected after trapping from the reaction vessel. Subsequent calibrations were made by direct injection of synthetic mixtures.

2.2.3 Materials

a) Iodoalkanes

The iodoalkanes used in kinetic measurements were obtained from the suppliers and purified by the methods given in section 2.1.5a.

b) Initiator

The initiator used was di-t-butyl peroxide obtained from Koch Light Laboratories. Gas chromatographic analysis indicated no significant impurities and the material was used as received, other than outgassing on a vacuum line.

c) Alkanes

n-Decane and dicyclohexyl were obtained from BDH and Aldrich Chemical Company respectively. Analysis by gas chromatography indicated purities >99% and they were used as received. Dicyclopentyl was

prepared by a Wurtz synthesis[87] using sodium and bromocyclopentane (Aldrich). The products were fractionated through a 30cm column packed with glass helicies and the fraction boiling between 200 - 202° collected (literature value for boiling point of dicyclopentyl is 189°C @ 753 mmHg[88]. GC analysis indicated a purity of 98%.

2.2.4 General Procedure for a Kinetic Experiment

The two iodoalkanes were carefully weighed into a sample tube, the initiator added, and the contents mixed and flushed with nitrogen. Iodoalkane ratios were chosen to give approximately equal ratios of recombination products, although the ratio was varied by a factor of 10 in some experiments. Prior to an experimental run the vessel was evacuated to $<10^{-3}$ torr with taps T_1 and T_2 open (Figure 2.4). Tap T_2 was then closed and the mixture, typically 0.1 to 0.25ml, was injected into the vessel via the septum from a 0.5ml gas tight syringe equipped with a 12cm needle which passed through tap T_1. Immediately following injection tap T_1 was closed. The reaction was allowed to proceed for between 1 and 15 hours after which the products were trapped out for GC analysis. This was accomplished by placing the trap on the line as shown in Figure 2.5 and evacuating the line to T_2 with taps T_3, T_4 and T_5 open. The trap was then cooled in liquid nitrogen, taps T_4 and T_5 closed, and tap T_1 opened. The products were allowed to condense in the trap for approximately 1 minute then tap T_5 opened for 1 minute. Taps T_3 and T_5 were then closed, air was admitted to the trap by slackening the septum cap and the trap removed from the line, sealed with quickfit stoppers and warmed. Samples for GC analysis were then taken via the septum.

Chapter 3

RESULTS

This chapter gives results obtained from thermochemical and kinetic studies of alkyl radicals by the radical buffer technique.

3.1 Thermochemical Experiments

3.1.1 General Procedures

The results presented in the following sections have been obtained from solution studies of the radical buffer reaction following the procedures given in sections 2.1.2 and 2.1.3. Generally, the most intense line of the ESR spectrum of each radical was scanned, although for some systems studied this was impractical due to line overlap or problems with background signals from the ESR cavity. In such cases a number of less intense lines were scanned. Some experiments were repeated using different lines of the ESR spectra of each radical, to eliminate potential systematic errors which could arise from background signals if only one line was studied.

The mean temperatures of the thermochemical studies were close to 298K and, furthermore, the average ΔCp values for the systems studied were close to zero. As a consequence corrections of enthalpy and entropy data to the thermodynamic standard temperature of 298K were small, being less than 0.4 $kJmol^{-1}$ and 1.6 $JK^{-1}mol^{-1}$ respectively in all cases. Therefore, results presented here are uncorrected, and may be taken as ΔH^{o}_{298} and ΔS^{o}_{298}.

The following results are presented as the mean of a number of individual runs at a particular temperature. More detailed results are given in Appendix 2.

3.1.2 Ethyl/n-Propyl

Equilibrium constants for the reaction

$$C_2H_5I + n\text{-}C_3H_7\cdot \rightleftharpoons n\text{-}C_3H_7I + C_2H_5\cdot$$

were measured over a temperature range of -51 to +51°C using both a static and flow system.

The ethyl radical ESR spectrum consists of 12 lines, relative intensities 1:2:3:1:6:3:3:6:1:3:2:1 arising from two equivalent α protons with couplings of 22.4 Gauss and three equivalent β protons with couplings of 26.9 Gauss.

The n-propyl radical ESR spectrum consists of 9 lines, relative intensities 1:2:2:1:4:1:2:2:1 arising from two equivalent α protons with couplings of 22.1 Gauss and two equivalent β protons with couplings of 29.4 Gauss. Further coupling from the three equivalent γ protons is small and unresolved under the experimental conditions employed in this work as no useful information would be gained and signal intensity would be reduced.

Equilibrium constants were determined using the static system by measuring the variation of intensity with time for lines at 3248 Gauss, representing $^{6}/_{32}$ of the ethyl radical spectrum intensity and 3261 Gauss, representing $^{4}/_{16}$ of the n-propyl radical spectrum intensity. Table 3.1 summarises results obtained from these experiments.

A few experiments to measure equilibrium constants for this system were carried out using the flow system and computer double integration technique described in the previous chapter. Due to a broad background signal from the ESR cavity in the region of the central line of the n-propyl spectrum giving rise to integration problems, two lines, each representing $^{2}/_{16}$ of the n-propyl radical spectrum intensity at 3231 and 3238 Gauss together with the above mentioned ethyl radical line were scanned. The results of these experiments are given in Table 3.2.

Table 3.1

Temperature Dependence of K for the $C_2H_5\cdot/n\text{-}C_3H_7\cdot$ Buffer Reaction : Static System

T/°C	no. of runs	K
-50.7	3	2.86
-40.0	3	2.91
-28.8	4	2.85
-24.8	4	2.82
-20.5	3	2.40
-12.0	1	2.43
-2.3	6	2.38
21.1	10	2.13
25.7	3	1.94
41.0	3	1.94
50.8	3	1.90

Table 3.2

Temperature Dependence of K for the $C_2H_5\cdot/n\text{-}C_3H_7\cdot$ Buffer Reaction : Flow System

T/°C	K
-19.0	2.73
-5.8	2.61
5.9	2.62
18.8	2.37
30.6	2.10
43.0	2.31

From the above data the van't Hoff plot of $^1/_T$ against ln K, shown in Figure 3.1, was constructed. The slope and intercept of the plot give the values of ΔH and ΔS for the reaction, as shown in Table 3.3. The meaning of the two terms 'Second Law Method' and 'Third Law Method' is given in section 4.1.1.

Table 3.3

ΔH and ΔS Values for the $C_2H_5\cdot/n\text{-}C_3H_7\cdot$ Buffer Reaction

Method	$\Delta H/kJmol^{-1}$	$\Delta S/JK^{-1}mol^{-1}$
Second Law	-2.5 $\pm$0.4	-2.0 $\pm$1.3
Third Law	-2.0 $\pm$0.2	0.4

3.1.3 Methyl/Ethyl

Equilibrium constants for the reaction

$$C_2H_5I + CH_3\cdot \rightleftharpoons CH_3I + C_2H_5\cdot$$

were measured over a temperature range of -47 to -3°C using a flow system. It was not possible to measure equilibrium constants at higher temperatures as additional lines appeared in the ESR spectrum due to solvent radicals, presumably arising from abstraction of hydrogen by methyl radicals, as this phenomenon was only observed in systems involving methyl radicals.

The methyl radical spectrum consists of 4 lines, relative intensities 1:3:3:1 arising from 3 equivalent protons with couplings of 23.0 Gauss.

In these experiments one line of the methyl radical spectrum at 3250 Gauss, representing $^3/_8$ of the total methyl radical spectrum intensity, together with two lines of the ethyl radical spectrum at 3248 and

Figure 3.1

van't Hoff Plots for the Ethyl/n-Propyl Buffer Reaction

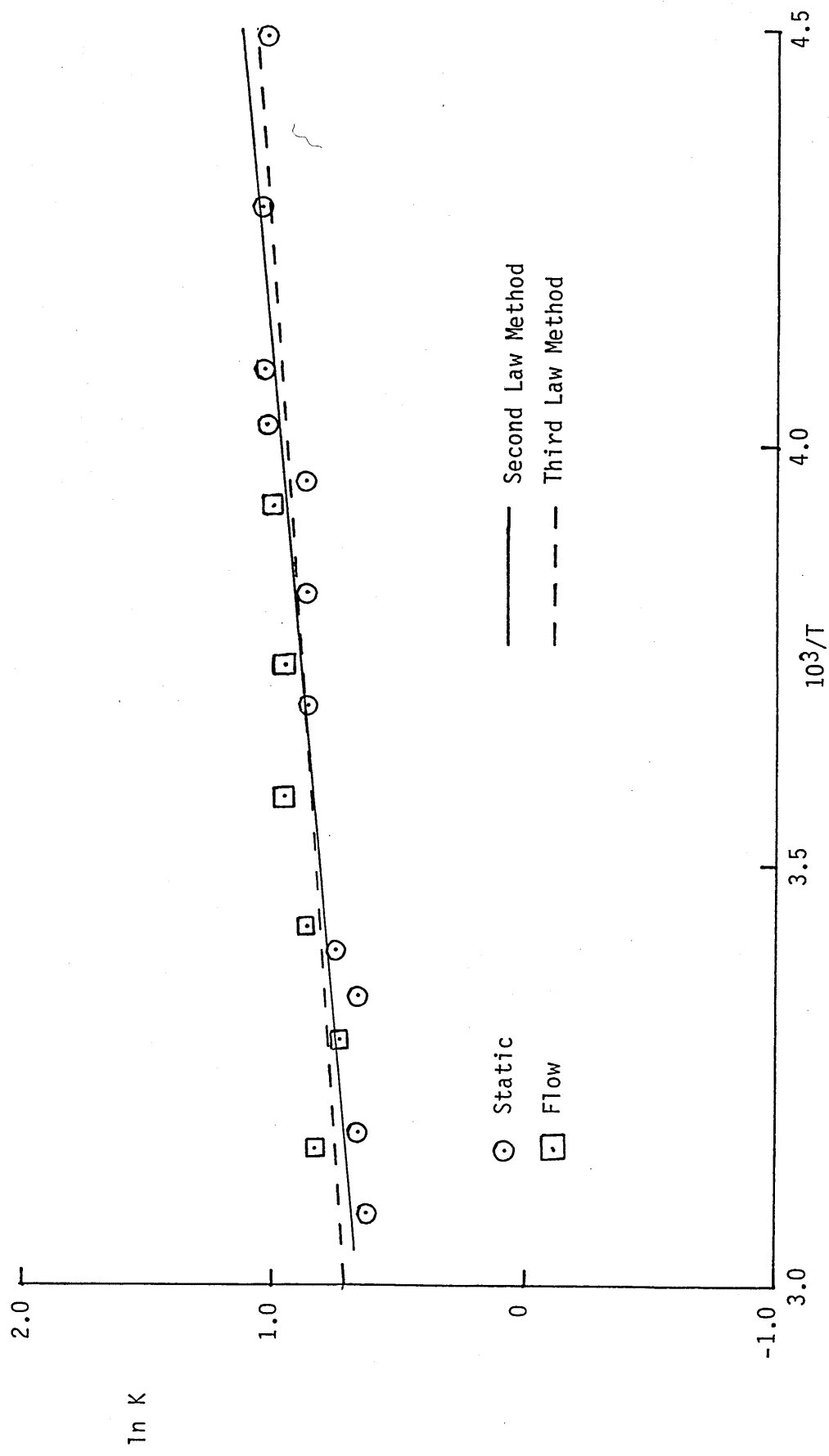

3252 Gauss, representing $^{6}/_{32}$ and $^{3}/_{32}$ respectively of the total ethyl radical spectrum intensity were scanned. A $[CH_3I]:[C_2H_5I]$ ratio of about 20 was necessary to give roughly equal areas under the integrated lines of each radical.

The variation of equilibrium constants with temperature is summarised in Table 3.4.

Table 3.4

Temperature Dependence of K for the $CH_3\cdot/C_2H_5\cdot$ Buffer Reaction

T/°C	no. of runs	K
-47.0	2	31.2
-37.3	2	30.9
-28.6	4	33.1
-19.7	4	32.6
-14.9	2	33.4
-3.5	4	30.7

A van't Hoff plot of these data is shown in Figure 3.2 which yields the values shown in Table 3.5.

Table 3.5

$\triangle H$ and $\triangle S$ Values for the $CH_3\cdot/C_2H_5\cdot$ Buffer Reaction

Method	$\triangle H/kJmol^{-1}$	$\triangle S/JK^{-1}mol^{-1}$
Second Law	0.3 $\pm$0.6	29.8 $\pm$2.4
Third Law	-4.3 $\pm$0.3	10.9

Figure 3.2

van't Hoff Plots for the Methyl/Ethyl Buffer Reaction

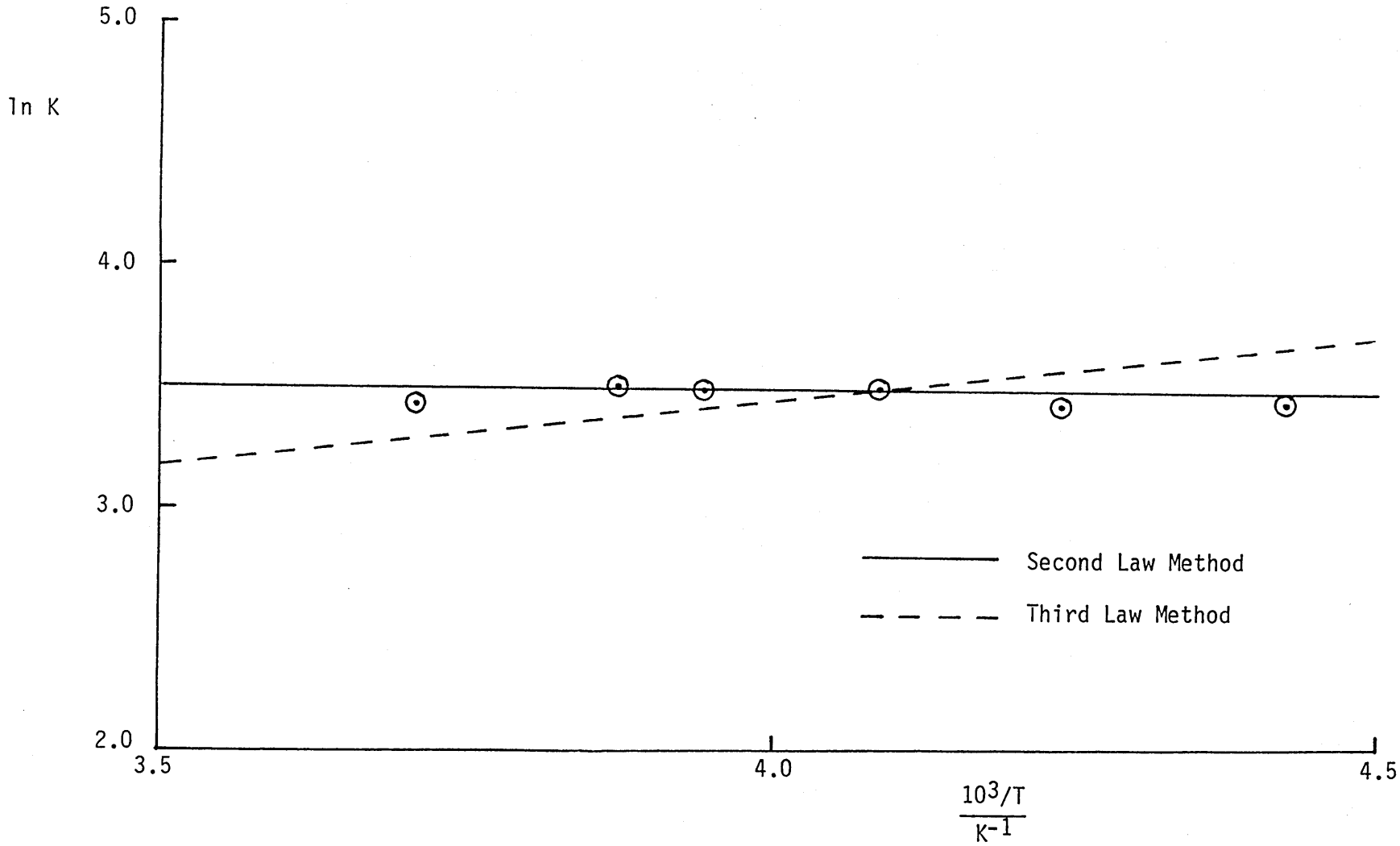

3.1.4 Methyl/n-Propyl

Equilibrium constants for the reaction

$$n\text{-}C_3H_7I + CH_3\cdot \rightleftharpoons CH_3I + n\text{-}C_3H_7\cdot$$

were measured in a flow system over a temperature range of -51 to -4°C. Measurements at higher temperatures were not made for reasons given in the previous section (3.1.3), namely the appearance of solvent radicals.

Two lines of the n-propyl radical spectrum at 3231 and 3238 Gauss, each representing $^2/_{16}$ of the total n-propyl radical spectrum intensity together with one line at 3250 Gauss, representing $^3/_8$ of the total methyl radical spectrum intensity were scanned. $A[CH_3I]:[n\text{-}C_3H_7I]$ ratio of about 8 was necessary to give approximately equal areas under the integrated lines of each radical.

Table 3.6 gives the variation of equilibrium constant with temperature for these experiments.

Table 3.6

Temperature Dependence of K for the $CH_3\cdot/n\text{-}C_3H_7\cdot$ Buffer Reaction

T/°C	no. of runs	K
-51.8	2	11.7
-41.1	2	11.6
-36.9	2	13.6
-27.0	2	14.5
-22.5	2	14.2
-18.2	2	13.9
-12.4	2	14.0
-4.2	2	13.2

A van't Hoff plot of these data, shown in Figure 3.3, yields the values shown in Table 3.7.

Table 3.7

ΔH and ΔS Values for the $CH_3\cdot/n\text{-}C_3H_7\cdot$ Buffer Reaction

Method	$\Delta H/kJmol^{-1}$	$\Delta S/JK^{-1}mol^{-1}$
Second Law	1.7 $\pm$0.8	28.9 $\pm$3.3
Third Law	-2.6 $\pm$0.3	10.5

3.1.5 n-Propyl/iso-Propyl

Equilibrium constants for the reaction

$$i\text{-}C_3H_7I + n\text{-}C_3H_7\cdot \rightleftharpoons n\text{-}C_3H_7I + i\text{-}C_3H_7\cdot$$

were measured over a temperature range of -35 to +45°C using a flow system.

The iso-propyl radical ESR spectrum consists of 14 lines, relative intensities 1:1:6:6:15:15:20:20:15:15:6:6:1:1, arising from an α coupling of 22.1 Gauss and six equivalent β couplings of 24.7 Gauss.

In most of these experiments one line of the n-propyl radical spectrum at 3261 Gauss, representing $^4/_{16}$ of the total spectrum intensity, together with one line of the iso-propyl radical spectrum at 3250 Gauss, representing $^{20}/_{128}$ of the total spectrum intensity were scanned. Experiments at the low end of the temperature range revealed that total iodoalkane concentrations of 2.5 molar were required for the reaction to be at equilibrium, as shown in Table k of Appendix 2. Subsequent experiments were carried out using solutions at least 3 molar in iodoalkanes. $[n\text{-}C_3H_7I]$: $[i\text{-}C_3H_7I]$ ratios of about 35 were used in these experiments. The variation of equilibrium constants with temperature is summarised in Table 3.8.

Figure 3.3

van't Hoff Plots for the Methyl/n-Propyl Buffer Reaction

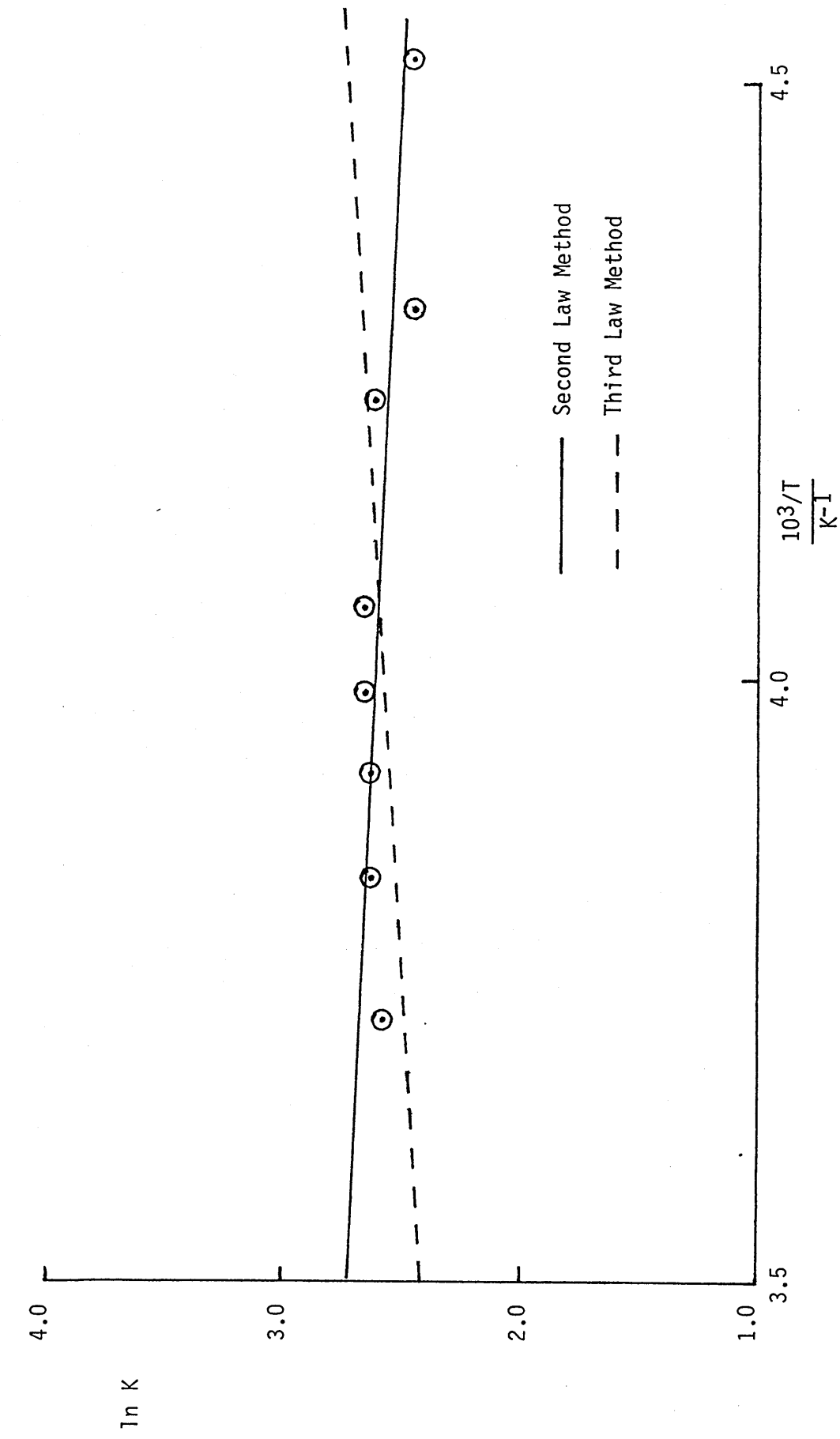

Table 3.8

Temperature Dependence of K for the n-$C_3H_7\cdot$/i-$C_3H_7\cdot$ Buffer Reaction

T/°C	no. of runs	K
-34.6	3	89.6
-16.3	2	77.2
-6.2	2	70.6
6.9	2	72.3
25.4	2	65.3
44.5	2	55.5

A van't Hoff plot of these data, shown in Figure 3.4, yields the values shown in Table 3.9.

Table 3.9

$\triangle$H and $\triangle$S Values for the n-$C_3H_7\cdot$/i-$C_3H_7\cdot$ Buffer Reaction

Method	$\triangle H/kJmol^{-1}$	$\triangle S/JK^{-1}mol^{-1}$
Second Law	-3.4 $\pm$0.4	22.9 $\pm$1.6
Third Law	-5.7 $\pm$0.3	14.0

3.1.6 n-Propyl/Cyclopentyl

Equilibrium constants for the reaction

$$c\text{-}C_5H_9I + n\text{-}C_3H_7\cdot \rightleftharpoons n\text{-}C_3H_7I + c\text{-}C_5H_9\cdot$$

were measured over a temperature range of -50 to +51°C using a flow system.

The cyclopentyl radical ESR spectrum consists of 10 lines, relative

intensities 1:1:4:4:6:6:4:4:1:1, arising from an α coupling of 21.5 Gauss and four equivalent β couplings of 35.2 Gauss. Under the experimental conditions no additional lines due to coupling to the four γ protons were observed.

Experiments were performed by scanning either a) one line of the n-propyl radical spectrum at 3261 Gauss representing $^4/_{16}$ of the total spectrum intensity and one line of the cyclopentyl radical spectrum at 3250 Gauss representing $^6/_{32}$ of the total spectrum intensity, or b) two lines of the n-propyl radical spectrum at 3231 and 3239 Gauss or 3282 and 3289 Gauss, each representing $^2/_{16}$ of the total spectrum intensity, together with one line of the cyclopentyl radical spectrum at 3236 or 3284 Gauss representing $^4/_{32}$ of the total spectrum intensity, or c) one line of the n-propyl radical spectrum at 3231 or 3289 Gauss representing $^2/_{16}$ of the total spectrum intensity, together with one line of the cyclopentyl radical spectrum at 3214 or 3304 Gauss representing $^4/_{32}$ of the total spectrum intensity. Ratios of $[n\text{-}C_3H_7I]:[c\text{-}C_5H_9I]$ were varied between 15 and 45 in these experiments.

The variation of equilibrium constants with temperature is summarised in Table 3.10.

A van't Hoff plot of the data in Table 3.10, shown in Figure 3.5, yields the values shown in Table 3.11.

Figure 3.4

van't Hoff Plots for the n-Propyl/iso-Propyl Buffer Reaction

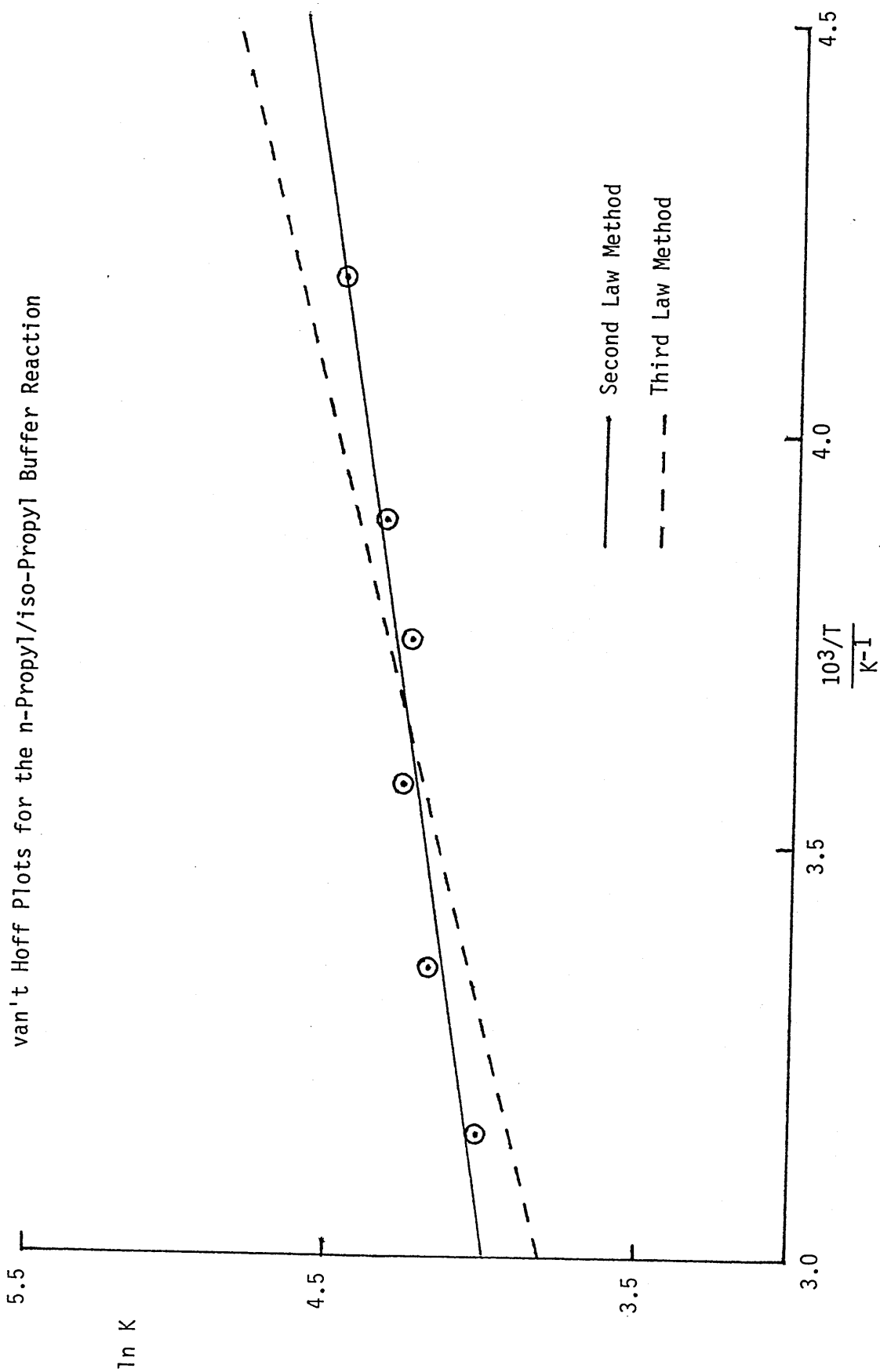

Table 3.10

Temperature Dependence of K for the $n\text{-}C_3H_7\cdot/c\text{-}C_5H_9\cdot$ Buffer Reaction

T/°C	no. of runs	K
-49.2	2	161.0
-44.0	2	145.4
-29.8	3	124.8
-21.1	2	119.0
-15.9	2	118.6
-9.7	3	98.4
9.9	2	76.0
29.1	3	66.3
38.5	2	64.3
44.6	3	51.5
51.0	7	53.5

Table 3.11

$\triangle H$ and $\triangle S$ Values for the $n\text{-}C_3H_7\cdot/c\text{-}C_5H_9\cdot$ Buffer Reaction

Method	$\triangle H/kJmol^{-1}$	$\triangle S/JK^{-1}mol^{-1}$
Second Law	-6.8 ± 0.4	12.3 ± 1.4
Third Law	-9.9 ± 0.4	-1.2

Figure 3.5

van't Hoff Plots for the n-Propyl/Cyclopentyl$^-$ Buffer Reaction

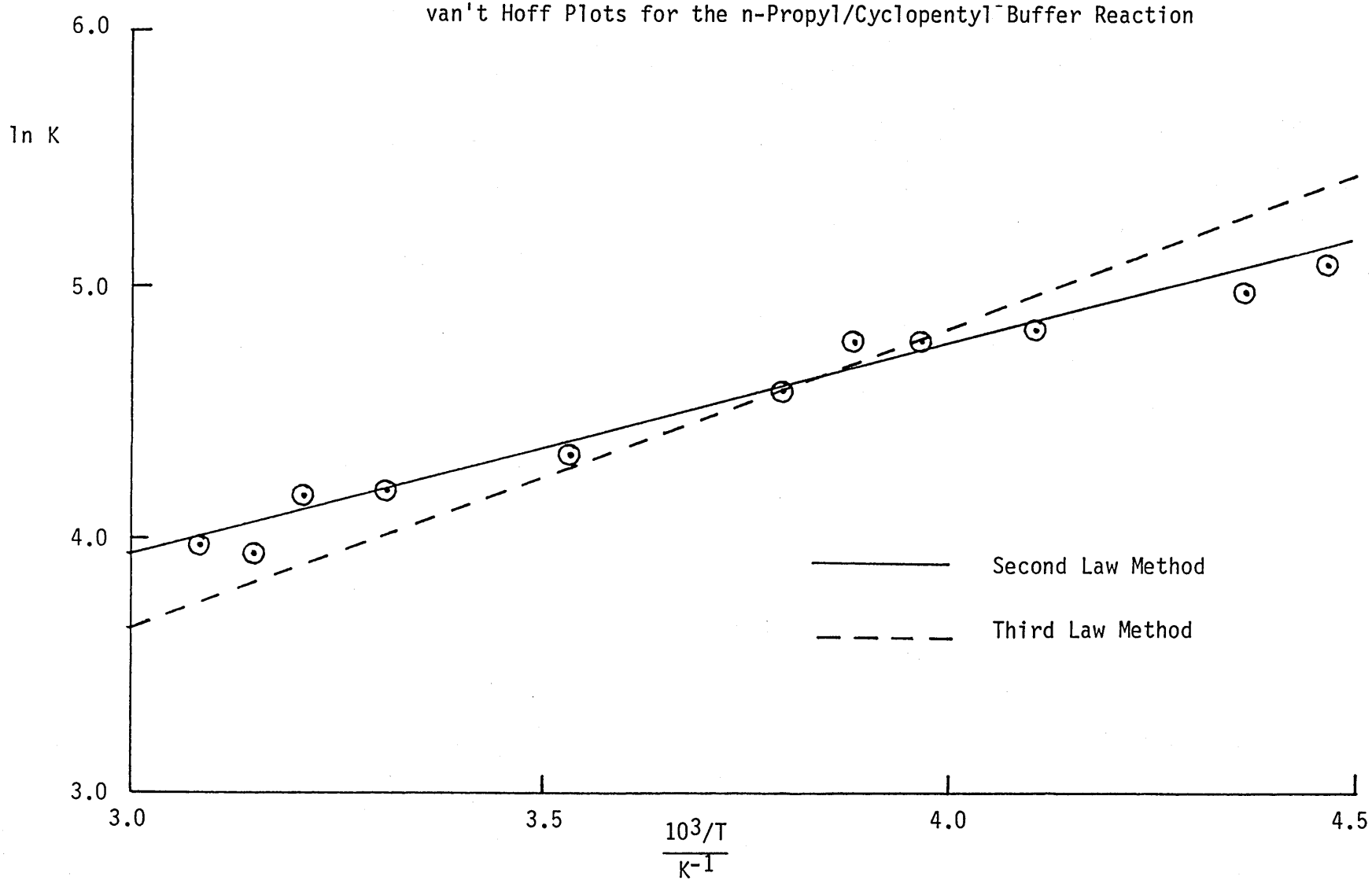

3.1.7 Ethyl/Cyclopentyl

Equilibrium constants for the reaction

$$c\text{-}C_5H_9I + C_2H_5\cdot \rightleftharpoons C_2H_5I + c\text{-}C_5H_9\cdot$$

were measured over a temperature range of -20 to +60°C using a flow system.

Experiments were performed by scanning either a) two lines of the cyclopentyl radical spectrum at 3215 and 3236 Gauss or 3285 and 3306 Gauss each representing $^4/_{32}$ of the total spectrum intensity, together with two lines of the ethyl radical spectrum at 3221 and 3225 Gauss representing $^2/_{32}$ and $^3/_{32}$ respectively of the total spectrum intensity, or the corresponding high field ethyl lines at 3296 and 3301 Gauss, or b) scanning the above ethyl radical lines together with one line from cyclopentyl at 3215 or 3306 Gauss.$[C_2H_5I]$: $[c\text{-}C_5H_9I]$ratios of approximately 40 were used in these experiments.

The variation of equilibrium constants with temperature is summarised in Table 3.12.

A van't Hoff plot of the data in Table 3.12, shown in Figure 3.6, yields the values shown in Table 3.13.

Table 3.12

Temperature Dependence of K for the $C_2H_5\cdot$/c-$C_5H_9\cdot$ Buffer Reaction

T/°C	no. of runs	K
-20.3	2	57.4
-16.7	2	48.1
0.2	3	43.0
3.4	2	46.9
14.1	6	35.8
22.8	4	31.9
35.5	3	29.1
55.7	2	20.9
60.5	2	22.9

Table 3.13

$\triangle$H and $\triangle$S Values for the $C_2H_5\cdot$/c-$C_5H_9\cdot$ Buffer Reaction

Method	$\triangle H/kJmol^{-1}$	$\triangle S/JK^{-1}mol^{-1}$
Second Law	-8.2 $\pm$0.7	1.2 $\pm$2.4
Third Law	-9.0 $\pm$0.2	-1.7

Figure 3.6

van't Hoff Plots for the Ethyl/Cyclopentyl Buffer Reaction

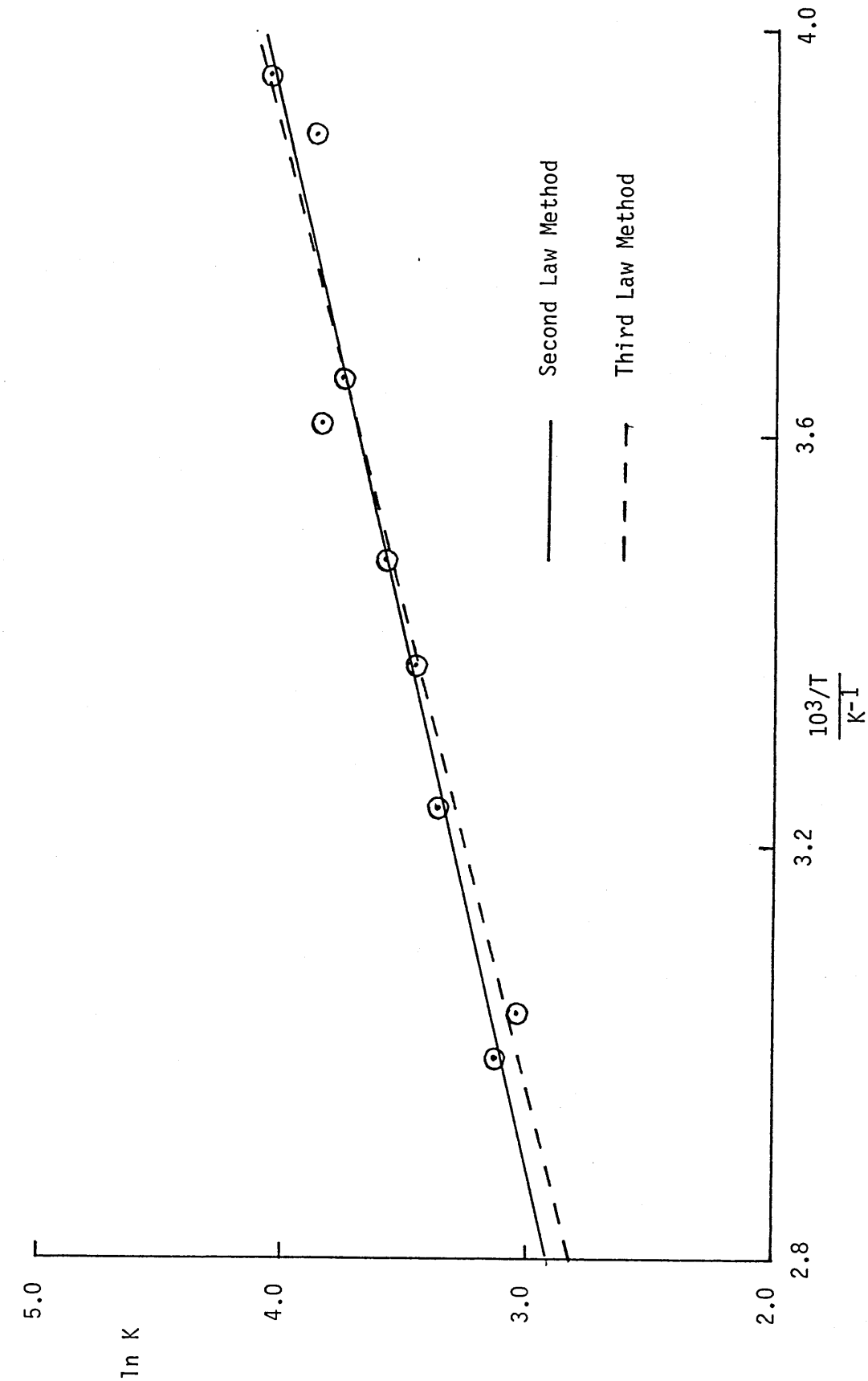

3.1.8 n-Propyl/Cyclohexyl

Equilibrium constants for the reaction

$$c\text{-}C_6H_{11}I + n\text{-}C_3H_7\cdot \rightleftharpoons n\text{-}C_3H_7I + c\text{-}C_6H_{11}\cdot$$

were measured over a temperature range of -32 to +60°C using a flow system.

The cyclohexyl radical ESR spectrum is more complex than other radical spectra studied in this work due to the non-equivalence of the four β protons which have been shown[126] to be equivalent in pairs. Also, due to ring inversion, certain expected lines in the ESR spectrum are broadened to such an extent that they are not observed[126]. This results in a 6 line spectrum, relative intensities 1:1:4:4:1:1 at temperatures between -40 and 0°C. At higher temperatures only the outer wing lines remain invariant as the inner 4 lines become broadened and new lines appear. In these experiments the wing line at either 3207 or 3318 Gauss, representing $^1/_{32}$ of the total cyclohexyl spectrum, together with one line at 3239 or 3289 Gauss, representing $^2/_{16}$ of the n-propyl spectrum were scanned. [nC_3H_7I]:[$c\text{-}C_6H_{11}I$]ratios of approximately $^1/_2$ were used in these experiments.

The variation of equilibrium constant with temperature is given in Table 3.14.

A van't Hoff plot of the data in Table 3.14, shown in Figure 3.7, yields the values shown in Table 3.15.

Table 3.14

Temperature Dependence of K for the n-$C_3H_7\cdot$/c-$C_6H_{11}\cdot$ Buffer Reaction

T/°C	K
-40.0	1.63
-31.7	2.69
-22.5	1.25
-9.5	2.37
-4.0	2.54
31.0	2.37
42.6	2.05
59.4	2.20

Table 3.15

ΔH and ΔS Values for the n-$C_3H_7\cdot$/c-$C_6H_{11}\cdot$ Buffer Reaction

Method	$\Delta H/kJmol^{-1}$	$\Delta S/JK^{-1}mol^{-1}$
Second Law	1.3 ± 1.8	10.9 ± 6.5
Third Law	1.1 ± 0.6	10.0

3.1.9 n-Propyl/Cycloheptyl

Equilibrium constants for the reaction

$$c\text{-}C_7H_{13}I + n\text{-}C_3H_7\cdot \rightleftharpoons n\text{-}C_3H_7I + c\text{-}C_7H_{13}\cdot$$

were measured over a temperature range of -23 to +58°C using a flow system.

The cycloheptyl radical ESR spectrum consists of 10 lines, relative

intensities 1:1:4:4:6:6:4:4:1:1, at temperatures greater than -10° due to 4 equivalent β protons with couplings of 24.7 Gauss and an α coupling of 21.8 Gauss. At lower temperatures the inner 8 lines coalesce in pairs as the β protons become non-equivalent in pairs. This phenomenon did not present a problem in these experiments as two lines of the cycloheptyl radical spectrum at 3272.2 and 3274.5 Gauss representing $^{6}/_{32}$ and $^{4}/_{32}$ respectively of the total spectrum intensity were scanned. These lines are two which coalesce at lower temperatures and experiments showed the sum of their relative intensities to be constant over the above temperature range. These two lines together with two lines of the n-propyl spectrum at 3282 and 3289 Gauss, each representing $^{2}/_{16}$ of the total n-propyl spectrum intensity were scanned. [n-C_3H_7I]:[c-$C_7H_{13}I$]ratios were varied between 80 and 300 in these experiments.

The variation of equilibrium constants with temperature is summarised in Table 3.16.

Table 3.16

Temperature Dependence of K for the n-$C_3H_7\cdot$/c-$C_7H_{13}\cdot$ Buffer Reaction

T/°C	no. of runs	K
-23.0	3	332.4
-16.3	2	252.4
-4.2	2	251.1
10.8	4	238.0
27.7	4	196.2
39.0	2	153.4
58.1	5	115.7

Figure 3.7

van't Hoff Plots for the n-Propyl/Cyclohexyl Buffer Reaction

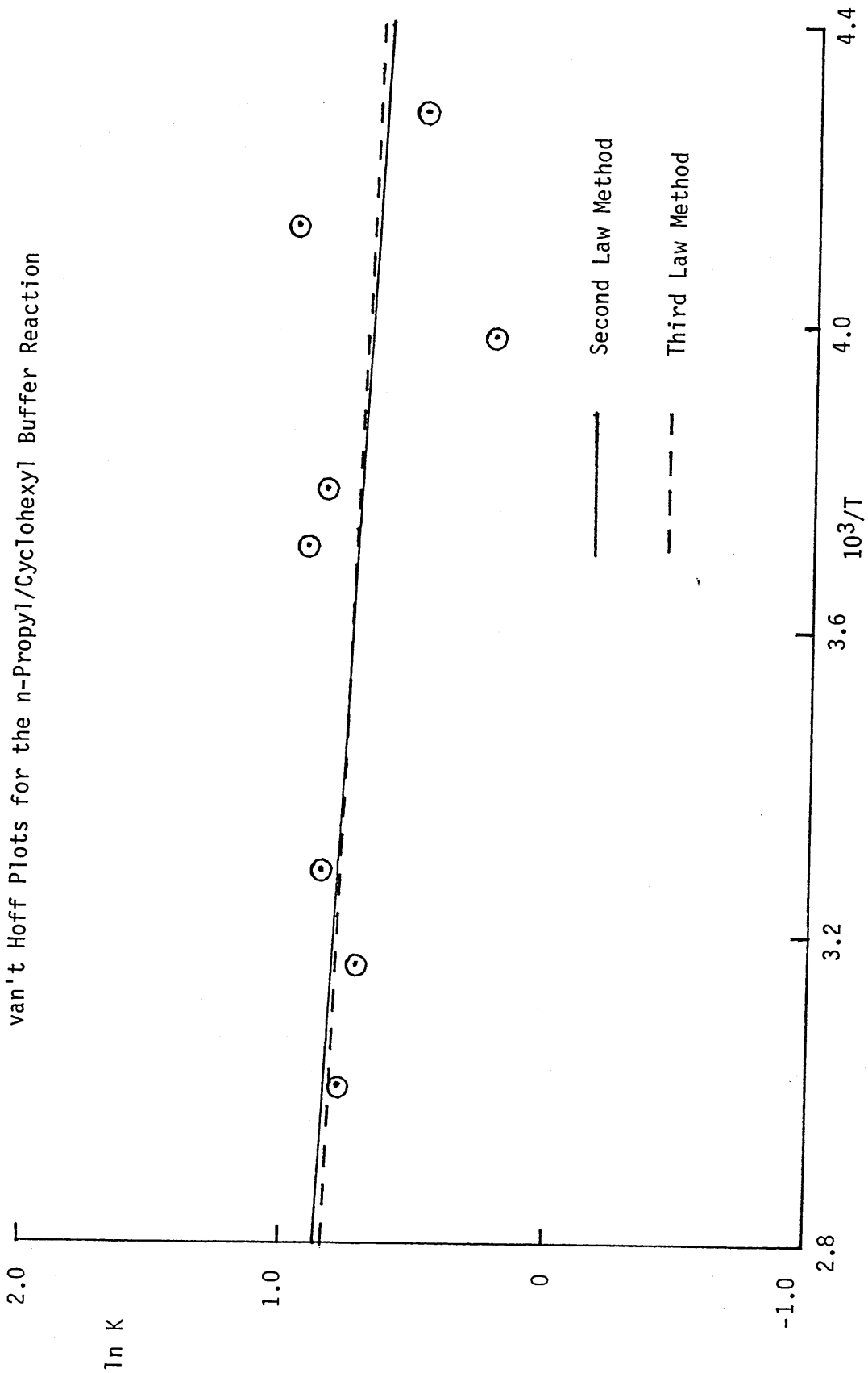

A van't Hoff plot of these data, shown in Figure 3.8, yields the values shown in Table 3.17.

Table 3.17

ΔH and ΔS Values for the n-$C_3H_7\cdot$/c-$C_7H_{13}\cdot$ Buffer Reaction

Method	$\Delta H/kJmol^{-1}$	$\Delta S/JK^{-1}mol^{-1}$
Second Law	-7.7 $\pm$1.1	17.4 $\pm$4.0
Third Law	-11.7 $\pm$0.8	2.0

3.1.10 n-Pentyl/Cyclopentyl

Equilibrium constants for the reaction

$$c\text{-}C_5H_9I + n\text{-}C_5H_{11}\cdot \rightleftharpoons n\text{-}C_5H_{11}I + c\text{-}C_5H_9\cdot$$

were measured over a temperature range of -20 to +47°C using a flow system.

The n-pentyl radical ESR spectrum consists of 9 lines and is essentially identical to the n-propyl radical ESR spectrum regarding line positions and relative intensities.

One line of the cyclopentyl radical spectrum at 3308 Gauss, representing $^4/_{32}$ of the total intensity, and one line of the n-pentyl radical spectrum, representing $^2/_{16}$ of the total intensity, were scanned. [n-$C_5H_{11}I$]:[c-C_5H_9I] ratios of 30 and 40 were used.

Table 3.18 gives the variation of equilibrium constant with temperature.

A van't Hoff plot of the data in Table 3.18, shown in Figure 3.9, yields the data shown in Table 3.19.

Figure 3.8

van't Hoff Plots for the n-Propyl/Cycloheptyl Buffer Reaction

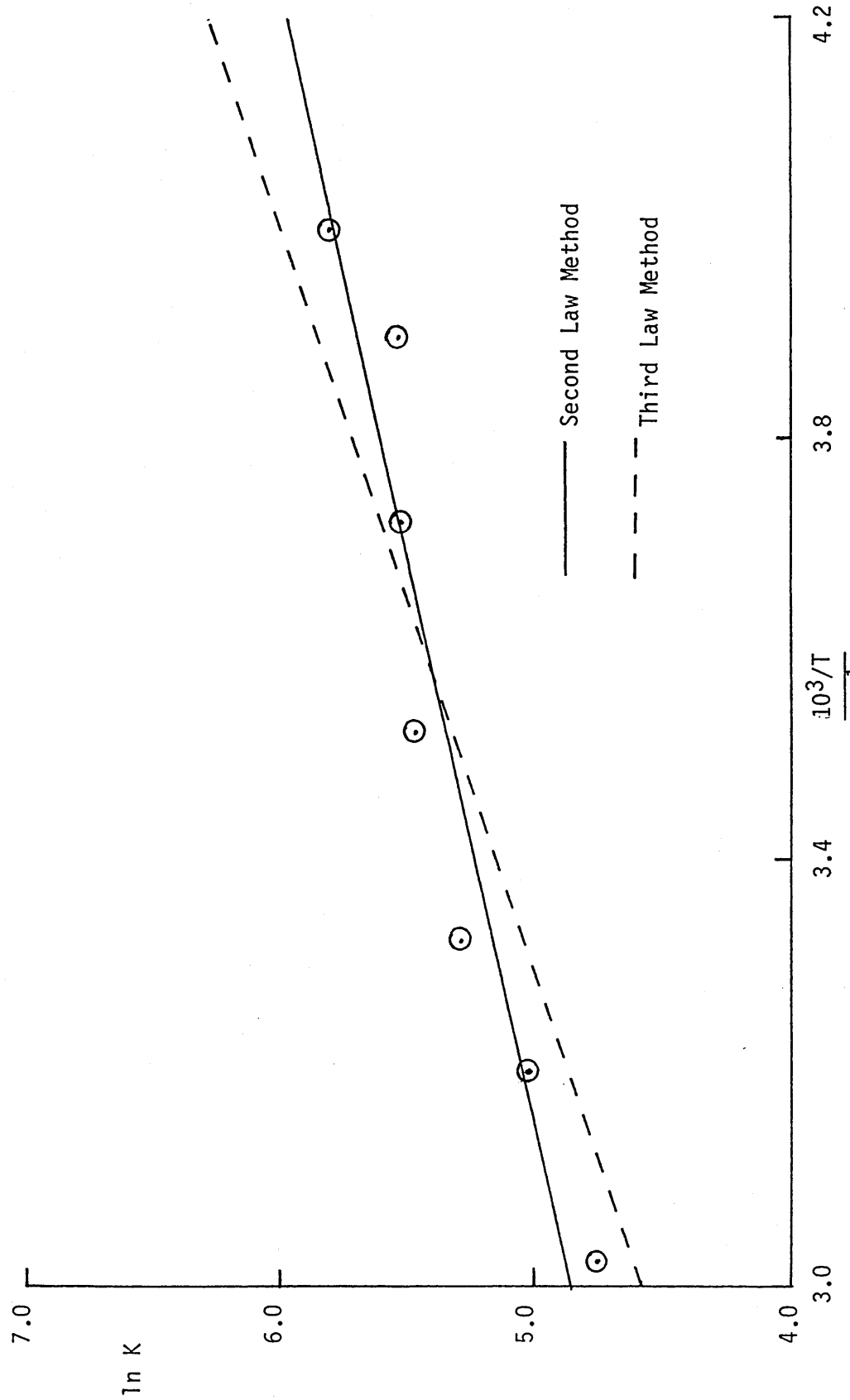

Figure 3.9

van't Hoff Plots for the n-Pentyl/Cyclopentyl Buffer Reaction

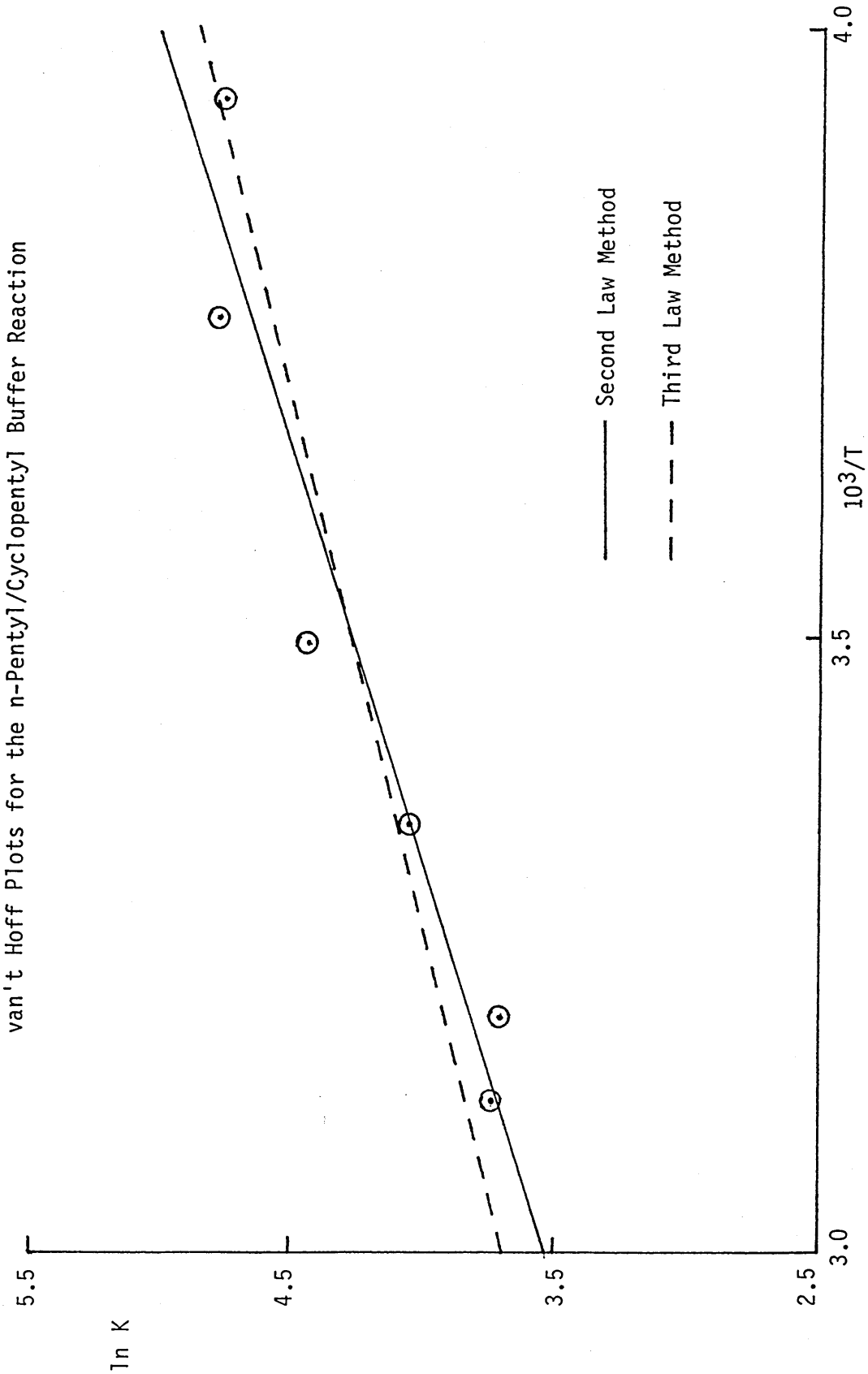

Table 3.18

Temperature Dependence of K for the n-$C_5H_{11}\cdot$/c-$C_5H_9\cdot$ Buffer Reaction

T/°C	K
-19.5	118.6
-7.1	121.4
12.9	84.5
25.5	57.1
40.2	40.2
46.8	41.4

Table 3.19

ΔH and ΔS Values for the n-$C_5H_{11}\cdot$/c-$C_5H_9\cdot$ Buffer Reaction

Method	ΔH/kJmol^{-1}	ΔS/JK^{-1}mol^{-1}
Second Law	-12.4 $\pm$1.7	-7.9 $\pm$5.9
Third Law	-9.7 $\pm$0.6	2.0

3.1.11 n-Pentyl/Cyclohexyl

Equilibrium constants for the reaction

$$c\text{-}C_6H_{11}I + n\text{-}C_5H_{11}\cdot \rightleftharpoons n\text{-}C_5H_{11}I + c\text{-}C_6H_{11}\cdot$$

were measured over a temperature range of 14 to 62°C using a flow system.

One line of the cyclohexyl radical ESR spectrum at 3207 Gauss, representing $^1/_{32}$ of the total intensity, together with one line of the n-pentyl radical ESR spectrum at 3236 Gauss, representing $^2/_{16}$ of the total intensity, were scanned.

Table 3.20 gives the variation of equilibrium constants with temperature.

Table 3.20

Temperature Dependence of K for the n-$C_5H_{11}\cdot$/c-$C_6H_{11}\cdot$ Buffer Reaction

T/°C	K
14.6	2.56
19.1	2.87
37.8	2.30
61.4	2.34

A van't Hoff plot of these data, shown in Figure 3.10, yields the values shown in Table 3.21.

Table 3.21

ΔH and ΔS Values for the n-$C_5H_{11}\cdot$/c-$C_6H_{11}\cdot$ Buffer Reaction

Method	$\Delta H/kJmol^{-1}$	$\Delta S/JK^{-1}mol^{-1}$
Second Law	-2.8 ± 1.9	-1.4 ± 6.1
Third Law	1.6 ± 0.6	13.0

3.2 Kinetic Experiments

3.2.1 General Procedures

The recombination rate constants for cyclopentyl and cyclohexyl radicals were determined relative to the recombination rate constant for n-pentyl radicals using the radical buffer technique in the gas phase. n-Pentyl radicals were chosen as the reference since their recombination product, n-decane, was of similar volatility to the cycloalkyl radical recombination products which simplified gas

Figure 3.10

van't Hoff Plots for the n-Pentyl/Cyclohexyl Buffer Reaction

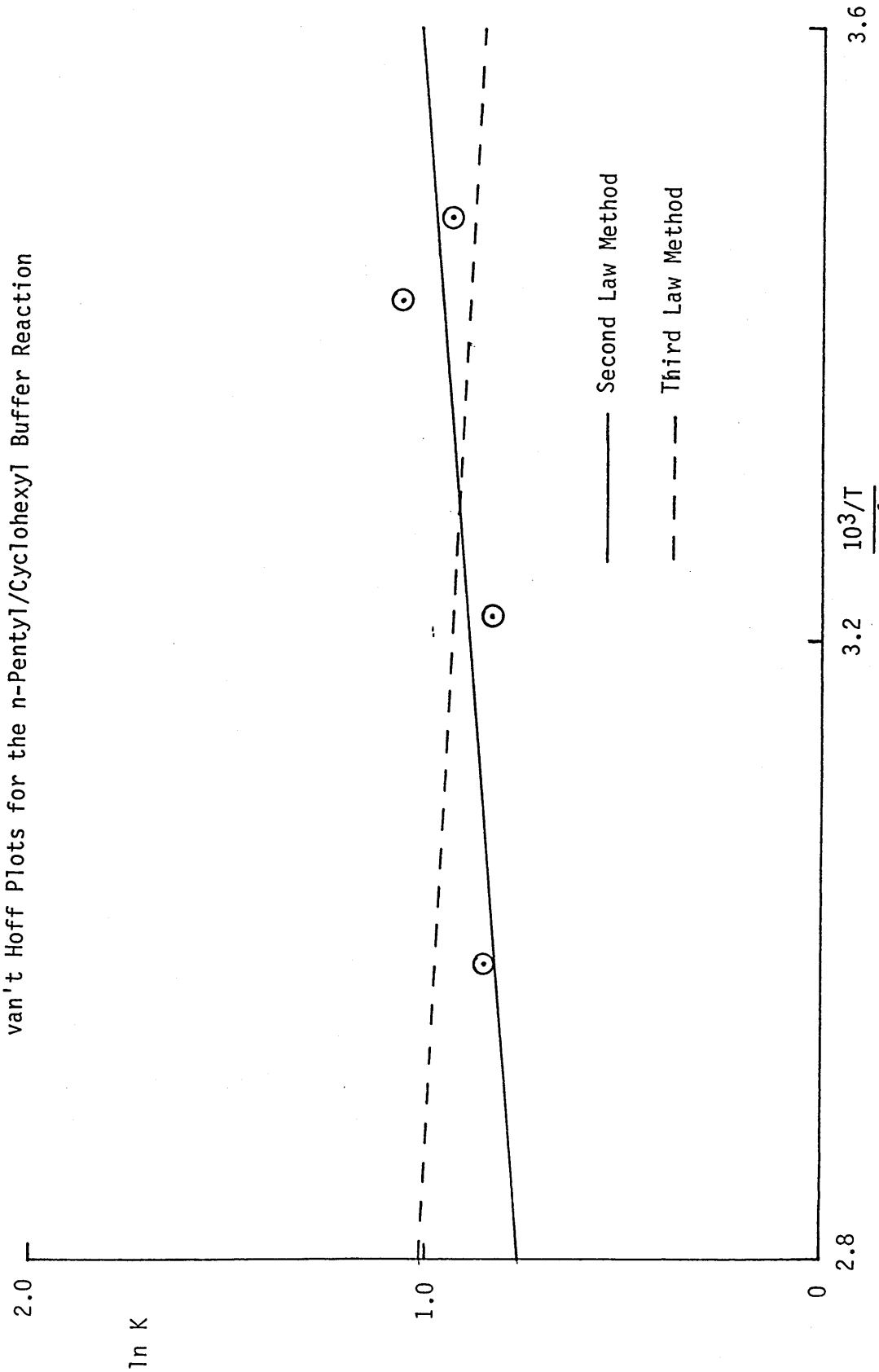

chromatographic analysis.

Details of the experimental techniques are given in Section 2.2.4. Full results for individual experiments are given in Appendix 3.

3.2.2 Cyclohexyl/n-Pentyl

The radical buffer reaction

$$c\text{-}C_6H_{11}I + n\text{-}C_5H_{11}\cdot \rightleftharpoons n\text{-}C_5H_{11}I + c\text{-}C_6H_{11}\cdot$$

was studied in the gas phase at 430K using di^{t}butyl peroxide as an initiator.

The results of the study showed no appreciable dependence on initial iodoalkane ratios when varied by a factor of 16 nor on the total initial pressure. Furthermore, variation of the relative concentration of initiator and differing reaction times led to results consistent to within experimental errors for the analysis.

Averaging the results of the 16 runs shown in Appendix 3(a) gives

$$\frac{k_{ch}}{k_{np}} \cdot K^2_{ch.np} = 0.56 \pm 0.23$$

where k_{ch} and k_{np} are the rate constants for cyclohexyl radical and n-pentyl radical recombination respectively and $K_{ch.np}$ the equilibrium constant for the buffer reaction at 430K. The quoted uncertainty represents ± 1 standard deviation.

The equilibrium constant for the reaction is obtained from the study of the reaction thermochemistry in solution (section 3.1.11). Thus, extrapolation of the second law plot shown in Figure 3.10 to 430K yields

$$K_{ch.np} = 1.85 \text{ at } 430K$$

Therefore

$$\frac{k_{ch}}{k_{np}} = \frac{0.56}{(1.85)^2} = 0.16$$

implying the n-pentyl radical recombination rate constant is approximately 6 times greater than that for cyclohexyl radical recombination.

3.2.3 Cyclopentyl/n-Pentyl

The radical buffer reaction

$$c\text{-}C_5H_9I + n\text{-}C_5H_{11}\cdot \rightleftharpoons n\text{-}C_5H_{11}I + c\text{-}C_5H_9\cdot$$

was studied in the gas phase at 430K using di^{t}butyl peroxide as an initiator.

To within the experimental errors of the analysis the results were independent of initial iodoalkane ratios when varied by a factor of 10 as well as the total initial pressure. Also no variations were observed when the relative amount of initiator and reaction time were altered.

Averaging the results of the 12 runs detailed in Appendix 3(b) gives

$$\frac{k_{cp}}{k_{np}} K_{cp.np}^2 = 36.4 \pm 6.5$$

where k_{cp} and k_{np} are the rate constants for cyclopentyl radical and n-pentyl radical recombination respectively, and $K_{cp.np}$ the equilibrium constant for the buffer reaction at 430K. The quoted uncertainty represents ± 1 standard deviation.

The equilibrium constant is obtained from the study of the reaction thermochemistry in solution (section 3.1.10). Thus, extrapolating the second law plot shown in Figure 3.9 to 430K yields

$$K_{cp.np} = 12.4 \text{ at } 430K$$

Therefore

$$\frac{k_{cp}}{k_{np}} = \frac{36.4}{(12.4)^2} = 0.24$$

implying the n-pentyl radical recombination rate constant is 4 times greater than that for cyclopentyl radical recombination.

Chapter 4

DISCUSSION

The results of thermochemical and kinetic studies of the radical buffer reaction are discussed in this chapter. The revised thermochemical parameters recommended for aliphatic radicals are compared with recent values and the implications of the revisions considered. Thermochemical parameters for cyclic radicals are interpreted by a consideration of ring strain upon radical formation. Finally, radical recombination rate constants for cyclic radicals are discussed and compared with recent determinations.

4.1 Thermochemistry

4.1.1 Internal Consistency of Enthalpy Data

Measurements of the enthalpy change in the buffer reaction for various sets of radicals should demonstrate internal consistency. This can readily be tested by examining these data for three radicals (R_1, R_2, R_3) taken pairwise in three sets of experiments (R_1 with R_2 etc). Experiments were performed in this manner for the majority of radicals studied, and the internal consistency of the enthalpy data evaluated for two methods of data treatment.

The first involves obtaining ΔH values from the van't Hoff equation (equation 1.17) using the range of temperatures over which the experiment was performed (this is subsequently referred to as the second law method). This method also yields ΔS values for the reaction.

In the second method the entropy change for the reaction is calculated from literature values of the entropies of the individual components and included in the van't Hoff plot (subsequently referred to as the third law method). The latter has the advantage of effectively increasing the temperature range of the experiment, thus resulting in a more accurate measure of ΔH for the reaction. Also examination of the data reveals that ΔH is relatively insensitive to small changes in ΔS, a 20 $JK^{-1}mol^{-1}$ change in ΔS causing ΔH to change by only $5kJmol^{-1}$. Furthermore, S° values can usually be estimated[4] to within $2JK^{-1}mol^{-1}$, thus providing ΔH values with an uncertainty of generally less than $2kJmol^{-1}$. Naturally, this method of calculation precludes an experimental determination of ΔS, but since the main emphasis of this work is the determination of BDE's, increased accuracy

in ΔH is sought at the expense of experimental verification of $S°$ for the species concerned.

Data obtained by the second and third law plots are summarised in Table 4.1.

Table 4.1

Thermochemical Data Derived from the Radical Buffer Reaction

$$R'I + R\cdot \rightleftharpoons RI + R'\cdot$$

		Second Law		Third Law	
R·	R'·	ΔH(a)	ΔS(b)	ΔH(a)	ΔS(b,c)
CH_3·	C_2H_5·	0.3 ±0.6	29.7 ±2.4	-4.3 ±0.3	11
CH_3·	n-C_3H_7·	1.7 ±0.8	28.9 ±3.3	-2.6 ±0.3	10
n-C_3H_7·	C_2H_5·	-2.5 ±0.4	-2.0 ±1.3	-2.0 ±0.2	1
n-C_3H_7·	i-C_3H_7·	-3.4 ±0.4	22.9 ±1.6	-5.7 ±0.3	14
C_2H_5·	c-C_5H_9·	-8.2 ±0.7	1.2 ±2.4	-9.0 ±0.2	-2
n-C_3H_7·	c-C_5H_9·	-6.8 ±0.4	12.3 ±1.4	-9.9 ±0.4	-1
i-C_3H_7·	c-C_5H_9·(d)	-2.8 ±0.7	-8.6 ±2.5	-4.4 ±0.4	-15
n-C_3H_7·	c-C_6H_{11}·	1.3 ±1.8	10.9 ±6.5	1.1 ±0.6	10
c-C_5H_9·	c-C_6H_{11}·(e)	13.4 ±2.0	15.2 ±8.2	12.3 ±0.9	11
n-C_3H_7·	c-C_7H_{13}·	-7.7 ±1.1	17.4 ±4.0	-11.7 ±0.8	2
n-C_5H_{11}·	c-C_5H_9·	-12.4 ±1.7	-7.9 ±5.9	-9.7 ±0.6	2
n-C_5H_{11}·	c-C_6H_{11}·	-2.8 ±1.9	-1.4 ±6.1	1.6 ±0.6	13

a) ΔH/kJmol^{-1} ; b) ΔS/JK^{-1}mol^{-1} ; c) From Literature values given in Appendix 1 ; d) T.J. Burkey and D. Griller, private communication ; e) C.J. Harding, private communication.

Quoted errors represent one standard deviation.

Examination of the enthalpy data in Table 4.1 reveals that, by applying Hess's law, better internal consistency is achieved by the third law method than by the second law method. Data which allow an internal consistency check between four radicals reveal agreement to $1 kJmol^{-1}$ using the third law method, compared to $4 kJmol^{-1}$ using the second law method, as demonstrated in Figure 4.1.

Figure 4.1

Internal Consistency of Enthalpy Data for $R\cdot \longrightarrow R\cdot'$ in the Buffer Reaction

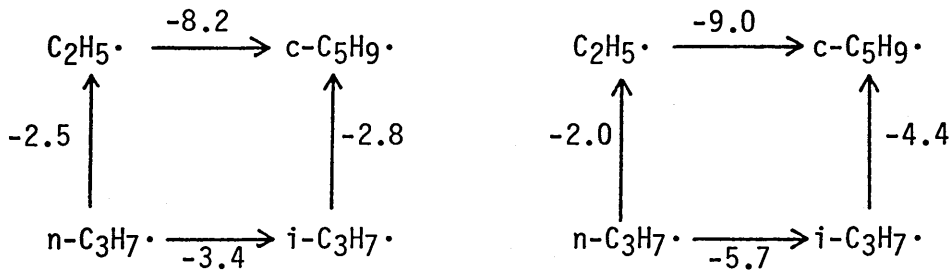

Second Law Data

Third Law Data

All values $\Delta H/kJmol^{-1}$

This demonstrates that the radical buffer technique shows excellent internal consistency and implies that data obtained by the third law method are more accurate than data obtained by the second law method. The technique allows relative enthalpy changes to be measured with high precision, consistent with the estimated errors from the van't Hoff plots.

4.1.2 Derived Thermochemical Data

The enthalpy change, ΔH, obtained from the buffer reaction is the difference in the carbon-iodine bond dissociation energies of the two iodoalkanes, i.e.

$$\Delta H = D(R' - I) - D(R - I) \qquad 4.1$$

Hence, an absolute value of D(R - I) for one iodoalkane provides absolute values for D(R' - I) for other iodoalkanes investigated. Furthermore, given the heats of formation of the iodoalkanes and one radical, the heats of formation of other radicals studied may be derived via equation 4.2.

$$\Delta H = \Delta H_f(RI) + \Delta H_f(R'\cdot) - \Delta H_f(R'I) - \Delta H_f(R\cdot) \qquad 4.2$$

From the $\Delta H_f(R\cdot)$ values so obtained, D(R - H) values may be calculated from the heats of formation of the hydrogen atom and corresponding hydrocarbon since

$$D(R - H) = \Delta H_f(R\cdot) + \Delta H_f(H\cdot) - \Delta H_f(R - H) \qquad 4.3$$

Heats of formation of iodoalkanes and hydrocarbons are available in the literature and are tabulated in Appendix 1. The heat of formation of the methyl radical is used as a standard in this work since this is the most widely studied and best characterised of the alkyl radicals. The value assigned to $\Delta H_f(CH_3\cdot)$ is 146 $\pm$1kJmol^{-1} which encompasses the excellent agreement obtained in recent years by workers using a variety of techniques, as demonstrated in Table 4.2.

Table 4.2

Recent Determinations of $\Delta H_f(CH_3\cdot)$

Technique	$\Delta H_f(CH_3\cdot)$/kJmol^{-1}	Year	Ref
Equilibrium study of $Cl\cdot + CH_4 = \cdot CH_3 + HCl$	147 $\pm$0.6	1979, 1981	62, 63
Pyrolysis of Ethane	147 $\pm$2	1984	90
Measurement of $\Delta H_f(CH_3^+)$	145 $\pm$3	1981	91
Photoionisation of CH_4	146 $\pm$0.5	1976	92

From this value of $\Delta H_f(CH_3\cdot)$ and data given in Appendix 1, the value of $D(CH_3 - I)$ may be calculated and used as a standard D(R - I) value. This is obtained from the enthalpy change of the reaction

$$CH_3I \longrightarrow CH_3\cdot + I\cdot \qquad 4.4$$

Thus

$$D(CH_3 - I) = \Delta H_f(CH_3\cdot) + \Delta H_f(I\cdot) - \Delta H_f(CH_3I) = 237.4 kJmol^{-1} \qquad 4.5$$

Values for D(R - I), $\Delta H_f(R\cdot)$ and D(R - H) calculated from the third law enthalpy data given in Table 4.1, together with the above $D(CH_3 - I)$ value and literature data from Appendix 1, are given in Table 4.3.

The internal consistency of the technique is reflected in the D(R - I) data obtained when radicals are studied in two or more related experiments, as demonstrated in Figure 4.1 Also, the consistency of the $\Delta H_f(R\cdot)$ and D(R - H) data supports the literature values for $\Delta H_f(RI)$ since any errors in these quantities would be observed in these results.

The results given in Table 4.3 are summarised in Table 4.4. These are discussed in relation to literature data later in this chapter.

Table 4.3

Thermochemical Data Derived from the Buffer Reaction using The Third Law Method (a)

R·	R'·	D(R' - I)	ΔH_f(R'·)	D(R' - H)
CH_3·	C_2H_5·	233.1	117.3	419.3
CH_3·	n-C_3H_7·	234.8	95.5	418.3
n-C_3H_7·	C_2H_5·	232.8	117.0	419.0
n-C_3H_7·	i-C_3H_7·	229.1	80.7	403.5
C_2H_5·	c-C_5H_9·	224.0 (b)	104.8 (e)	401.2
n-C_3H_7·	c-C_5H_9·	224.9	105.7	402.1
i-C_3H_7·	c-C_5H_9·	224.7	105.5	401.9
n-C_3H_7·	c-C_6H_{11}·	235.9	78.1	419.4
c-C_5H_9·	c-C_6H_{11}·	236.8 (c)	79.0 (f)	420.3
n-C_3H_7·	c-C_7H_{13}·	223.1	63.2	399.4
c-C_5H_9·	n-C_5H_{11}·	234.2 (c)	56.3 (f)	420.8
c-C_6H_{11}·	n-C_5H_{11}·	234.8 (d)	56.9 (g)	421.4

a) all values/kJmol^{-1} ; b) using D(C_2H_5 - I) = 233.0 kJmol^{-1} ; c) using D(c-C_5H_9 - I) = 224.5 kJmol^{-1} ; d) using D(c-C_6H_{11} - I) = 236.4 kJmol^{-1} ; e) using ΔH_f(C_2H_5·) = 117.2 kJmol^{-1} ; f) using ΔH_f(c-C_5H_9·) = 105.3 kJmol^{-1} ; g) using ΔH_f(c-C_6H_{11}·) = 78.6 kJmol^{-1}

Table 4.4

Thermochemical Data Calculated by The Third Law Method

R·	$\Delta H_f(R\cdot)$/kJmol^{-1}	D(R - I)/kJmol^{-1}	D(R - H)/kJmol^{-1}
$CH_3\cdot$	146.0 (a)	237.4 (a)	438.5 (a)
$C_2H_5\cdot$	117.2	233.0	419.2
n-$C_3H_7\cdot$	95.5	234.8	418.3
n-$C_5H_{11}\cdot$	56.6	234.5	421.1
i-$C_3H_7\cdot$	80.7	229.1	403.5
c-$C_5H_9\cdot$	105.3	224.5	401.7
c-$C_6H_{11}\cdot$	78.6	236.4	419.9
c-$C_7H_{13}\cdot$	63.2	223.1	399.4
Typical Primary		235	420
Typical Secondary		225	400

a) Reference Values

The previous data have all been derived from the third law ΔH values given in Table 4.1 which provide more accurate data. However, use of the second law method allows calculation of S° data for the alkyl radicals by an analogous method to the calculation of $\Delta H_f(R\cdot)$ from equation 4.2.

The S° values given in Table 4.5 are calculated in this manner from the entropies of the iodoalkanes and that of the methyl radical, as given in Appendix 1. Also included in the table are values for $\Delta H_f(R\cdot)$ and D(R - H) calculated by the second law method.

Table 4.5

Thermochemical Data Calculated by The Second Law Method

R·	$S°(R·)/JK^{-1}mol^{-1}$	$\Delta H_f(R·)/kJmol^{-1}$	$D(R - H)/kJmol^{-1}$
$CH_3·$	194 (a)	146.0 (a)	438.5 (a)
$C_2H_5·$	265	121.4	423.4
$n\text{-}C_3H_7·$	309	99.8	422.6
$n\text{-}C_5H_{11}·$	404	66.7	431.2
$i\text{-}C_3H_7·$	318	87.3	410.1
$c\text{-}C_5H_9·$	341	112.2	408.6
$c\text{-}C_6H_{11}·$	353	84.3	426.1
$c\text{-}C_7H_{13}·$	379	71.5	407.7

a) Reference Values

Comparison of the S° values shown in Table 4.5 with those given in Appendix 1, reveals that data obtained by the second law method are in poor agreement with accepted values. Furthermore, the values obtained from the second law method are 5 - 20 $JK^{-1}mol^{-1}$ higher than those in Appendix 1. This is due to the high values obtained for $S°(C_2H_5·)$ and $S°(n\text{-}C_3H_7·)$ which are used as secondary standards in this work. These values are derived from buffer reactions involving methyl radicals which, as shown in Table 4.1, yield ΔS values 20 $JK^{-1}mol^{-1}$ higher than calculated values. A possible explanation for these anomalies is that the temperature range of studies involving methyl radicals was limited, for reasons given in section 3.1.3, namely hydrogen abstraction by methyl from the solvent at high temperatures. Thus, the errors incurred in extrapolation to obtain ΔS values from the van't Hoff plot are increased. It may be noted from Table 4.1 that better agreement between second law

and calculated ΔS values is generally obtained when experiments are carried out over a wider temperature range. The S° values obtained in this work suggest the technique is not particularly suited to the determination of these quantities, due to the restricted temperature range.

The $\Delta H_f(R\cdot)$ and D(R - H) values derived from the second law method are in reasonable agreement with those obtained by the third law method, as shown in Tables 4.5 and 4.4 respectively, although slightly higher values (4 - 10 $kJmol^{-1}$) are obtained from the second law method. This may be due to propagation of errors in secondary standards resulting from the limited temperature range of experiments involving methyl radicals, analogous to the argument regarding $S°(R\cdot)$ values above. However, the higher values obtained from the second law method do not detract from the following discussion which supports an increase in D(R - H) values over those previously accepted.

4.2 Evaluation of the Radical Buffer Technique

4.2.1 Errors

Potential errors in the enthalpy data arise mainly from the heats of formation of the iodoalkanes which generally have uncertainties of the order of 2 $kJmol^{-1}$. Errors in the measurement of equilibrium constants do not contribute significantly to errors in ΔH since these experiments yield data which are reproducible to within 20%, which translates to < 1 $kJmol^{-1}$ uncertainty in ΔH due to the logarithmic relationships involved. Furthermore, since experiments are carried out in the region of 300K, potential errors that may be involved in correcting data to 298K are avoided.

Consideration of the above, and the consistency of the data demonstrated in Table 4.3, suggests $\Delta H_f(R\cdot)$ and D(R - H) values have a maximum uncertainty of $\pm$ 2 kJmol^{-1} when calculated by the third law method.

4.2.2 Assumptions

Thermochemical quantities derived in this work have been in isooctane solution whereas the standard state for these quantities is the gas phase. However, the data may be considered equivalent to gas phase data providing the enthalpy changes of mixing and vaporisation for the radicals and iodoalkanes in the buffer reaction is small.

The first of these conditions is met, assuming the differences in the heats of mixing of alkyl radicals in hydrocarbon solvents are similar to those of the parent alkanes which, together with iodoalkanes, are only weakly solvated in such solvents with heats of mixing of < 0.4 kJmol^{-1} [70]. Since the free energy of solvation for the methyl radical has been measured at only 0.02 kJmol^{-1} in liquid methane[89], this assumption would appear to be valid. Thus, the differences in the heats of mixing of the components of the buffer reaction will be the differences between small values, and therefore, near zero.

The enthalpy change on vaporisation for the components of the buffer reaction should have a very small effect on the measured equilibrium constant in solution, compared to that which would be obtained in the gas phase. This is due to a compensation effect[4] that is exhibited when physical changes occur in a chemical system. Briefly, any change in a system that affects the ΔH of a reaction generally has a comparable effect on $T\Delta S$ and hence, a smaller effect on ΔG.

Since ΔG and K are related via

$$\ln K = - \frac{\Delta G}{RT} \qquad 4.6$$

it is reasonable to assume any changes to K due to vaporisation will be small.

These assumptions are further justified since, as is demonstrated later, good agreement is generally found between data derived in this work and corresponding data obtained from recent gas phase studies. The assumptions made in this technique are comparable to those made in other experimental methods used to determine BDE's such as pyrolysis (section 1.6.1) and iodination studies (section 1.6.2).

4.2.3 Advantages

The prime advantage of the technique is the ability to measure equilibrium constants for the buffer reaction with high precision. This is a result of the direct measurement of radical concentrations by ESR spectroscopy. The use of the buffer reaction in this context is in sharp contrast to its original application by Benson[50], where equilibrium constants were derived from thermochemistry. As a result of the logarithmic relationship between K and ΔH, small errors in K do not contribute significantly to errors in ΔH. For example, if K is measured to within 10% ΔH may be determined with an accuracy of better than 1 $kJmol^{-1}$ [62], providing the ΔS value is known. Conversely, an uncertainty of 4 $kJmol^{-1}$ in ΔH leads to a factor of five uncertainty in K[93]. This demonstrates the value of direct and accurate measurements of equilibrium constants in determining thermochemistry.

4.2.4 Limitations

For the buffer reaction to be at equilibrium, the rate of iodine metathesis must be much greater than the rate of radical recombination (section 1.6.5). This condition has been shown[67] to hold for radicals which are not stabilised by resonance. However, for stabilised radicals such as allyl and benzyl, the requirement is not met. Chemically induced dynamic nuclear polarisation (CIDNP) experiments[67] reveal that the metathesis reaction is too slow, relative to radical combination for these radicals. Thus, the assumption of equilibrium is valid for non-stabilised radicals, as demonstrated in sections 3.1.5 and 3.1.6, but not for stabilised radicals.

To obtain ΔH_f and BDE energies from the technique, literature values of thermodynamic data for iodoalkanes are required. Much of these data have not been experimentally determined, which places a reliance on estimated values, thus introducing some uncertainty. In cases where iodoalkane thermochemistry is unreliable, the technique may be applied to obtain relative D(R - I) values since these are obtained directly from the ΔH of the reaction.

4.3 Literature Values of $\Delta H_f(R\cdot)$ for Acyclic Radicals

The data obtained in this work is in excellent agreement with that obtained from the radical buffer studies of Castelhano and Griller[67]. This is demonstrated in Tables 1.5 and 4.4. These workers used a slightly lower $\Delta H_f(CH_3\cdot)$ value than that recommended here (144 instead of 146 $kJmol^{-1}$) which results in data 2 $kJmol^{-1}$ lower than would be obtained using the recommended value.

Until recently, thermochemical data obtained from the iodination technique[17] has been accepted as the most reliable available, although

recently newer techniques have resulted in an upward revision of these values. The results of this work support this revision, as demonstrated below.

4.3.1 Ethyl Radical

The heat of formation of $C_2H_5\cdot$ has been measured by the iodination technique[17] as 108 kJmol^{-1}. However, the recent studies discussed below support an increase in this value to 117 - 121 kJmol^{-1}, in good agreement with that obtained in this work.

Recently Pilling and co-workers[94] have used a flash photolysis/resonance fluorescence technique to measure the forward and reverse rate constants of the reaction

$$H\cdot + C_2H_4 \rightleftharpoons C_2H_5\cdot \qquad 4.7$$

They obtained an equilibrium constant for the reaction over the temperature range 775 - 825K from which ΔH was calculated using the known entropies of the components. From this ΔH and the heats of formation of ethene and the hydrogen atom, a $\Delta H_f(C_2H_5\cdot)$ value of 118.7 $\pm$1.7 kJmol^{-1} was obtained after heat capacity corrections. This is in good agreement with the value obtained in this work (117.2 kJmol^{-1}) but substantially above the previously accepted value of 108 kJmol^{-1} obtained by the iodination technique[27]. The authors demonstrate that use of the iodination value would result in a discrepancy of a factor of 3 or more between calculated and experimental rate constants for the reverse of equation 4.7. This is much greater than the experimental errors involved, offering support to the higher value of $\Delta H_f(C_2H_5\cdot)$.

Further support for the higher value is found in a study by Pacey

and Wimalasena[90] of the pyrolysis of ethane at 900K. An induction period in the pyrolysis was interpreted as an initial build up of ethyl radicals, from which product analysis enabled determination of the rate constant for ethyl recombination.

$$2\ C_2H_5\cdot \rightleftharpoons C_4H_{10} \qquad 4.8$$

Using literature data for the rate constant for butane decomposition an equilibrium constant for reaction 8 was determined. $\Delta H_f(C_2H_5\cdot)$ was then determined in the usual way as 120 $\pm$4, 119.6 $\pm$2.6, 118.8 $\pm$1.5 or 118.8 $\pm$ 1.6 kJmol^{-1}, depending upon the value used for k_{-8}. These values were rounded to 119 $\pm$2 kJmol^{-1}, in good agreement with the value obtained in this work.

The low values obtained for $\Delta H_f(C_2H_5\cdot)$ by the iodination technique are repeated for other radicals studied by the method. This may be indicative of systematic errors in the method such as a more complicated mechanism than originally proposed or an error in the estimation of activation energies for certain steps (see section 1.6.2). It has been suggested[38] that the errors of 4 kJmol-1 [17] assigned to ΔH_f and BDE's derived from iodination studies may be too low, with 15 kJmol^{-1} being more representative. Since thermochemistry is obtained from differences in activation energies in the iodination method, very accurate kinetic measurements are required. For example, a 20% error at one end of the temperature range in an experiment to determine $\Delta H_f(C_2H_5\cdot)$ leads to a 9 kJmol^{-1} error in the heat of formation[90]. More accurate data is generally obtained if absolute rate constants can be used to yield an equilibrium constant for a reaction since, providing the ΔS value is known for the reaction, a 20% uncertainty in a kinetic measurement gives

only 0.7 kJmol^{-1} uncertainty in ΔH when calculated by the third law method.

4.3.2 n-Propyl Radical

The long accepted value for $\Delta H_f(n\text{-}C_3H_7\cdot)$ has been that of 88 kJmol^{-1} [17], derived from iodination studies. The $\Delta H_f(n\text{-}C_3H_7\cdot)$ value of 95.5 kJmol^{-1} obtained in this work supports the increase suggested in the recent studies discussed below.

Recently, Tsang[38] has obtained a value for $\Delta H_f(n\text{-}C_3H_7\cdot)$ of 100.5 $\pm$2.1 kJmol^{-1} from an assessment of n-propyl radical decomposition data between 500 and 750K.

$$n\text{-}C_3H_7\cdot \rightleftharpoons CH_3\cdot + C_2H_4 \qquad 4.9$$

The experiments yield values for $k_9/(k_{pr})^{\frac{1}{2}}$ where k_{pr} is the rate constant for n-propyl recombination, well established as 10^{10} lmol^{-1}s^{-1}, with no temperature dependence, by kinetic spectroscopy[95]. Thus, k_9 is determined and, since k_{-9} is well established[7], the equilibrium constant for the reaction is obtained. $\Delta H_f(n\text{-}C_3H_7\cdot)$ is then calculated from entropies of the reactant and products and the heats of formation of products.

The iodination technique[17] gives values 12.5 and 7.5 kJmol^{-1} below the values obtained by Tsang[38] and this work respectively. Tsang demonstrates that the iodination value of $\Delta H_f(n\text{-}C_3H_7\cdot)$ leads to a factor of 20 discrepancy at 500K between the calculated and experimentally determined equilibrium constants for reaction 4.9, thus supporting the higher values.

The thermochemistry of the n-propyl radical obtained from iodination studies has also been queried by Marshall and Rahman[96,97]. They

also studied the equilibrium reaction above (reaction 4.9) and, by measuring the yields of ethane and butane, obtained the equilibrium constant via the relationship

$$\frac{Y(C_2H_6)}{Y(C_4H_{10})} = \frac{k_m}{k_{mp}} \cdot \frac{1}{K_9[C_2H_4]} \qquad 4.10$$

where $Y(C_2H_6)$ and $Y(C_4H_{10})$ are the respective yields of ethane and butane, k_m the rate constant for methyl radical recombination and k_{mp} the rate constant for the cross combination of methyl and n-propyl radicals. Initial studies[96] gave an equilibrium constant that required either the $\Delta H_f(n\text{-}C_3H_7\cdot)$ value to be increased by about 8 $kJmol^{-1}$ over the value obtained from group additivity[98], thus giving a value of about 96 $kJmol^{-1}$. Alternatively, the value of $S°(n\text{-}C_3H_7\cdot)$ would have to be reduced by 13 $JK^{-1}mol^{-1}$ from the accepted value[32] of 290 $JK^{-1}mol^{-1}$, a most unlikely revision, especially since this value has been confirmed by recent spectroscopic results[33]. A more detailed study[97] of the reaction over a temperature range 581 - 689K led to a recommendation that $\Delta H_f(n\text{-}C_3H_7\cdot) = 94.6 \pm 4$ $kJmol^{-1}$ and $S°(n\text{-}C_3H_7\cdot) = 282 \pm 13$ $JK^{-1}mol^{-1}$.

These results were obtained from a van't Hoff plot of the equilibrium constants using the best available thermochemistry for methyl radicals and ethene. The value obtained for $\Delta H_f(n\text{-}C_3H_7\cdot)$ is in excellent agreement with that obtained in this work.

4.3.3 i-Propyl Radical

The heat of formation of the i-propyl radical has been investigated by a number of workers in recent years, all of which give a value higher than the 76 $kJmol^{-1}$ derived from iodination studies[17].

Two of the recent studies concern the rate constants for 2,3-dimethylbutane (DMB) decomposition and i-propyl radical recombination

$$(CH_3)_2CHCH(CH_3)_2 \rightleftharpoons 2\ i\text{-}C_3H_7\cdot \qquad 4.11$$

The i-propyl radical recombination rate has been determined by two molecular modulation studies[69,99], by kinetic spectroscopy[95] and by very low pressure pyrolysis[100]. These absolute techniques are essentially in agreement with $k_{-11} \sim 6 \times 10^9$ $lmol^{-1}s^{-1}$ with little or no temperature dependence. DMB decomposition has been studied by shock tube techniques[45] over a temperature range of 1000 - 1200K by Tsang. From an analysis of the decomposition and recombination data in which the rate parameters are varied slightly to accommodate the uncertainties in the results, Tsang[49] concludes that $\Delta H_f(i\text{-}C_3H_7\cdot)$ is 81 - 88 $kJmol^{-1}$. The decomposition reaction has also been studied in the presence of oxygen between 750 and 810K[44]. Values for k_{11} were obtained which, when combined with Tsang's shock tube data, allowed E_{11} to be determined as 319 $\pm$1.5 $kJmol^{-1}$ over the temperature range 750 - 1200K. Combining this value with the zero activation energy for radical recombination and the ΔH_f(DMB) value gave, after heat capacity corrections, $\Delta H_f(i\text{-}C_3H_7\cdot)$ = 79.6 $\pm$2.0 $kJmol^{-1}$. The above results are in agreement with $\Delta H_f(i\text{-}C_3H_7\cdot)$ = 80.7 $kJmol^{-1}$ obtained in this work.

A somewhat higher value has been obtained by Tsang[38] from an analysis of i-propyl decomposition and hydrogen atom addition to propene kinetic data.

$$i\text{-}C_3H_7\cdot \rightleftharpoons C_3H_6 + H\cdot \qquad 4.12$$

The analysis, analogous to that for n-propyl radical decomposition

(section 4.3.2), gives $\Delta H_f(i\text{-}C_3H_7\cdot) = 93.3 \pm 2.5$ kJmol^{-1}. From this value we obtain $D(i\text{-}C_3H_7 - H) = 415.3$ kJmol^{-1} which is only 7 kJmol^{-1} lower than the primary C - H BDE in propane. Other workers[16,27,44], while not agreeing on absolute BDE values, find the difference to be in the region of 15 kJmol^{-1} which implies the above $\Delta H_f(i\text{-}C_3H_7\cdot)$ value may be about 8 kJmol^{-1} too high.

4.4 Some Effects of Revised Thermochemistry

Upward revision of radical heats of formation has generally reconciled previously conflicting kinetic data obtained by absolute methods and methods relying on thermochemistry. Barriers to ring closure in small diradicals have been revised using recent thermochemistry, giving better agreement with theoretical calculations. These effects are considered in detail below.

4.4.1 Thermochemistry and Kinetics of Ethyl Radical Reactions

Absolute techniques used to measure the ethyl radical recombination rate are generally in agreement with $k_{Et} = 1.0 \pm 0.2 \times 10^{10}$ l mol^{-1}s^{-1} [61,69,101]. This value is a factor of 20 higher than that obtained from techniques which depend upon the $\Delta H_f(C_2H_5\cdot)$ when this is taken to be 108 kJmol^{-1}, as previously accepted[17,27].

Thus, Benson's original application of the radical buffer technique[50] gave $k_{Et} = 4.7 \times 10^8$ l mol^{-1}s^{-1} from a study of reaction 4.13 at 415K.

$$CH_3\cdot + C_2H_5I \rightleftharpoons CH_3I + C_2H_5\cdot \qquad 4.13$$

The experiment yields the quantity $K_{13}\,(k_{Et}/k_{Me})^{\frac{1}{2}} = 4.6$, and, since k_{Me} is well established as 3.2×10^{10} l mol^{-1}s^{-1}, k_{Et} is obtained

via the thermochemistry of the reaction. Using $\Delta H_f(C_2H_5\cdot)$ = 117.2 kJmol^{-1}, the value obtained in this work, together with the thermochemical data given in Tables 4.4 and Appendix 1 and the heat capacities given in Reference 50, we obtain K_{13} = 12.6 at 415K. Hence k_{Et} = 0.4 x 10^{10} l mol^{-1}s^{-1}, within a factor of 2 of the value determined absolutely. This agreement is particularly good, considering the propagation of errors, as their exponential and square are included in the result. Hence, a 6 kJmol^{-1} uncertainly in ΔG translates into a factor of 6 in k_{Et}. The thermochemistry used in this calculation is essentially the same as that used by Benson, with the exception of the $\Delta H_f(C_2H_5\cdot)$ value, thus supporting the higher value.

Low values for k_{Et} in the region of 3 x 10^8 l mol^{-1}s^{-1} have also been obtained from the kinetics and thermochemistry of butane dissociation[102,103].

$$C_4H_{10} \rightleftharpoons 2C_2H_5\cdot \qquad 4.14$$

Over the temperature range 895 - 981K Marshall[102] found

$$k_{14/s^{-1}} = 10^{15.3 \pm 0.9} \exp[(-323 \pm 17)\text{kJmol}^{-1}/RT] \qquad 4.15$$

and between 693 and 803K [103]

$$k_{14/s^{-1}} = 10^{15.5} \exp[-331\ \text{kJmol}^{-1}/RT] \qquad 4.16$$

The recombination kinetics was obtained from the thermochemistry of the reaction using equations 1.15 and 1.17a which relate the activation energies and A factors of the reverse process with ΔH and ΔS respectively. Taking $\Delta H_f(C_2H_5\cdot)$ = 108 kJmol^{-1} and accepted values for $S°(C_2H_5\cdot)$ and butane thermochemistry the authors showed

$$k_{Et}/\text{lmol}^{-1}\text{s}^{-1} = 10^{8.33} \exp[4.6\ \text{kJmol}^{-1}/RT] \qquad 4.17$$

over the higher temperature range and

$$k_{Et}/\text{lmol}^{-1}\text{s}^{-1} = 10^{8.3} \exp[1.0\ \text{kJmol}^{-1}/RT] \qquad 4.18$$

over the lower. These results are essentially in agreement and show negligible temperature dependence with $k_{Et} \sim 2.5 \times 10^{8}$ $\text{lmol}^{-1}\text{s}^{-1}$ over the temperature range 693 - 981K. It was concluded that this value and the low value for $\Delta H_f(C_2H_5\cdot)$ was correct since higher values would require increasingly negative activation energies for radical recombination, which is improbable.

However, the $\Delta H_f(C_2H_5\cdot)$ value obtained in this work is compatible with the experimental data of Marshall and co-workers and the absolute value for k_{Et} if absolute rates for butane decomposition, rather than Arrhenius parameters, are considered. Thus, at the mid-points of the temperature ranges

$$k_{14} = 2.24 \times 10^{-3}\ \text{s}^{-1} \quad @ \quad 940\text{K}$$

and

$$k_{14} = 2.79 \times 10^{-8}\ \text{s}^{-1} \quad @ \quad 750\text{K}$$

taking $\Delta H_f(C_2H_5\cdot) = 117.2\ \text{kJmol}^{-1}$, $S°(C_2H_5\cdot) = 248\ \text{JK}^{-1}\text{mol}^{-1}$, $\Delta H_f(C_4H_{10}) = -126.4\ \text{kJmol}^{-1}$ [4] and $S°(C_4H_{10}) = 310\ \text{JK}^{-1}\text{mol}^{-1}$ [4], together with the heat capacaties given in Reference 4, we obtain

$$K_{14} = 2.82 \times 10^{-11}\ \text{atm} \quad @ \quad 940\text{K}$$

and

$$K_{14} = 2.60 \times 10^{-16}\ \text{atm} \quad @ \quad 750\text{K}$$

Since

$$K_{14} = \frac{k_{14}}{k_{Et}} R'T \qquad 1.16$$

we obtain

$$k_{Et} = 6.1 \times 10^9 \text{ lmol}^{-1}\text{s}^{-1} \quad @ \quad 940\text{K}$$

and $$k_{Et} = 6.6 \times 10^9 \text{ lmol}^{-1}\text{s}^{-1} \quad @ \quad 750\text{K}$$

Both these results are in good agreement with the absolute value of 1×10^{10} $\text{lmol}^{-1}\text{s}^{-1}$ giving further support to the higher value of $\Delta H_f(C_2H_5\cdot)$. The negative activation energy that Marshall suggested if $\Delta H_f(C_2H_5\cdot)$ were increased is obviously not required since the results for k_{Et} are in agreement over a 200K temperature range. This suggests a systematic error in the Arrehenius parameters, but not in the absolute rates measured for butane decomposition.

Further argument for a low value for ethyl recombination of 4×10^8 $\text{lmol}^{-1}\text{s}^{-1}$ is found in Marshall and Purnell's consideration[104] of the reaction

$$C_2H_5\cdot + H_2 \rightleftharpoons C_2H_6 + H\cdot \qquad 4.19$$

where the following rate expressions have been experimentally determined at 550K.

$$k_{-19}/\text{lmol}^{-1}\text{s}^{-1} = 10^{11.0} \exp[-38.9 \text{ kJmol}^{-1}/RT] \qquad 4.20$$

and $$\left(k_{19}/k_{Et}^{\frac{1}{2}}\right)/\text{l}^{\frac{1}{2}}\text{mol}^{-\frac{1}{2}}\text{s}^{-\frac{1}{2}} = 10^{4.5} \exp[-57.4 \text{ kJmol}^{-1}/RT] \qquad 4.21$$

Taking $\Delta H_f(C_2H_5\cdot) = 108$ kJmol^{-1} and using standard thermochemical data the authors obtained

$$\Delta H_{19} = 24.7 \text{ kJmol}^{-1} \text{ and } \Delta S_{19} = -36.0 \text{ JK}^{-1}\text{mol}^{-1}$$

from which a rate expression was derived for k_{-19} allowing k_{Et} to be estimated as

$$k_{Et}/\text{lmol}^{-1}\text{s}^{-1} = 10^{9.2} \exp[-12.6 \text{ kJmol}^{-1}/RT] \qquad 4.22$$

The large activation energy implies an error in the Arrhenius parameters and the authors conclude the absolute value of k_{Et} is correct at 1.0×10^8 $lmol^{-1}s^{-1}$.

Using thermochemistry similar to above but with $\Delta H_f(C_2H_5\cdot)$ = 117.2 $kJmol^{-1}$ we obtain, at 550K,

$$\Delta H_{19} = 17.0 \text{ kJmol}^{-1} \text{ and } \Delta S_{19} = -33.8 \text{ JK}^{-1}\text{mol}^{-1}$$

and

$$k_{Et}/\text{lmol}^{-1}\text{s}^{-1} = 10^{9.4} \exp[3.0 \text{ kJmol}^{-1}/RT] \qquad 4.23$$

Examination of equations 4.22 and 4.23 reveals the large positive activation energy implied by using $\Delta H_f(C_2H_5\cdot)$ = 108 $kJmol^{-1}$ becomes a small negative activation energy when $\Delta H_f(C_2H_5\cdot)$ = 117.2 $kJmol^{-1}$ is used. This is a much more likely result, in keeping with the generally accepted near zero activation energy for radical recombination[73]. Also, the recombination rate at 550K is now 4.8×10^9 $lmol^{-1}s^{-1}$, in much better agreement with the absolutely measured rate of 1×10^{10} $lmol^{-1}s^{-1}$.

The higher value of $\Delta H_f(C_2H_5\cdot)$ also resolves a paradox concerning the forward and reverse rate constants for the reaction

$$C_2H_5\cdot \rightleftharpoons H\cdot + C_2H_4 \qquad 4.24$$

A number of studies[37] of the reverse reaction, hydrogen addition to ethene, have determined the temperature dependence of the rate constant and its pressure dependence at 300K. The same quantities have also been determined for ethyl radical dissociation, so the reaction provides a test of RRKM and activated complex theories, since both forward and reverse reactions must proceed via the same

transition state. However, theoretical studies of the reaction revealed that the transition state that accounted for the experimental decomposition rate constant and the pressure dependence of the recombination rate constant overestimated the experimental high pressure recombination rate constant, k_{-24}, by a factor of 10. This has been shown[37] to be due to the use of a dissociation threshold of 193 $kJmol^{-1}$ in previous calculations, derived from a $\Delta H_f(C_2H_5\cdot)$ value of 108 $kJmol^{-1}$. Using $\Delta H_f(C_2H_5\cdot)$ = 118 $kJmol^{-1}$ gives a dissociation threshold of 183 $kJmol^{-1}$ which provides agreement between theory and experiment.

A value of $\Delta H_f(C_2H_5\cdot)$ in the region 117 - 121 $kJmol^{-1}$ is confirmed by a consideration of butane decomposition data by Tsang[49]. It was shown that the radical buffer results of Benson[50,51] which were originally used to give the rate constant for ethyl recombination could be reevaluated to yield a rate constant for butane decomposition at 354 and 415K. The high temperature rate constant is well established by shock tube studies[45] over the temperature range 1000 - 1200K. Since the kinetics of ethyl recombination are well established[69], the thermochemistry of reaction 14 can be used to derive rate parameters for the decomposition reaction at various temperatures. Using $\Delta H_f(C_2H_5\cdot)$ = 117.6 $kJmol^{-1}$ gives $k_{14} = 10^{-35.4}$ and $10^{-27.6}s^{-1}$ at 354 and 415K respectively, in good agreement with the respective radical buffer results of $10^{-35.7}$ and $10^{-28.3}s^{-1}$. However, if the high temperature rate expression is modified to yield a $\Delta H_f(C_2H_5\cdot)$ value of 109 $kJmol^{-1}$ then the calculated k_{14} values are approximately 3 orders of magnitude greater than the experimental values obtained from the radical buffer studies.

The overwhelming evidence appears to be in favour of a $\Delta H_f(C_2H_5\cdot)$ value in the region of 117 $kJmol^{-1}$, as obtained in this work, and not the lower value of 108 $kJmol^{-1}$ accepted until recently[27]. Thus, a value for $D(C_2H_5 - H)$ of 419 $kJmol^{-1}$ is implied.

4.4.2 Ring Closure in Small Cycloalkanes

A particularly elegant demonstration of the use of revised BDE's is found in considering the energetics of the pyrolysis of small cycloalkanes.

Studies of cyclopropane pyrolysis revealed the reaction was unimolecular, yielding propene as the sole product. The biradical trimethylene was proposed as an intermediate[105].

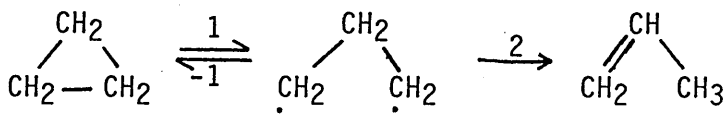

4.25

Further studies[106] using trans-cyclopropane-d_2 revealed that the molecule underwent isomerisation to the cis isomer more rapidly than it formed propene-d_2. This provided evidence of the diradical intermediate, and demonstrated the occurrence of internal rotation within the intermediate. The thermochemical interest in the reaction lies in the existence or otherwise of an energetic barrier to ring closure.

A reasonable reaction profile for Reaction 25 is shown in Figure 4.2.

The activation energy for ring opening, E_1 is approximated[107] by the activation energy for geometrical isomerisation in deuterated cyclopropane (268 $kJmol^{-1}$)[106]. The barrier to ring closure is then obtained providing the enthalpy change of the reaction

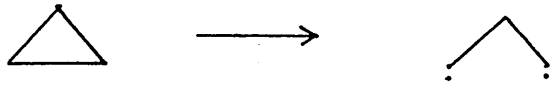

4.26

is known. This is obtained from the scheme

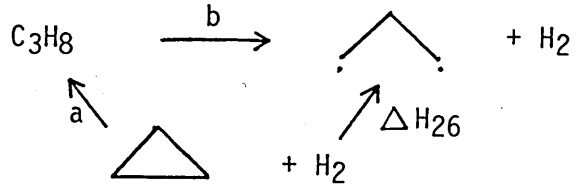

4.27

whereby $\Delta H_{26} = a + b$

$$= [\Delta H_f(C_3H_8) - \Delta H_f(c\text{-}C_3H_6)] + [2D(n\text{-}C_3H_7\text{-}H) - D(H\text{-}H)] \qquad 4.28$$

Figure 4.2

Reaction Profile for Cyclopropane Pyrolysis

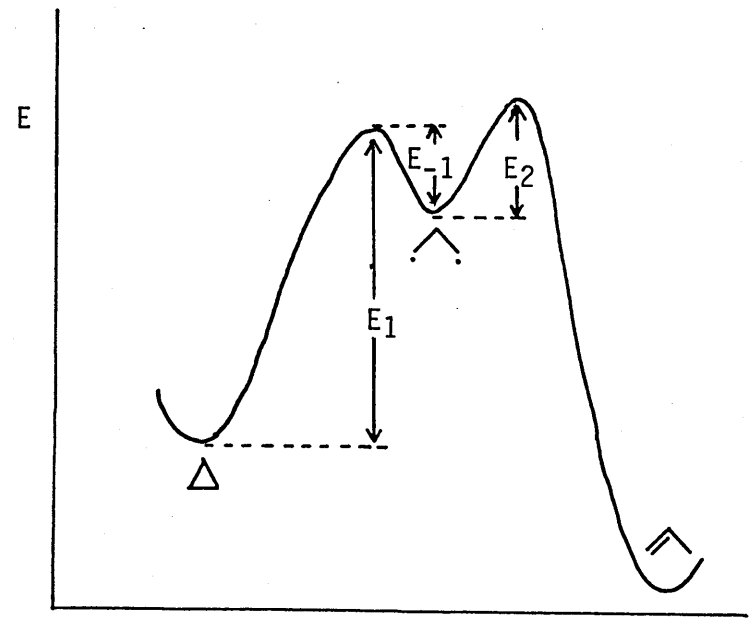

Taking literature values[4] for the first and final 2 terms of Equation 4.28 together with the previously accepted value[17,27] for $D(n\text{-}C_3H_7 - H)$ of 410 $kJmol^{-1}$, we find ΔH_{26} = 227 $kJmol^{-1}$. Therefore, since $E_{-1} = E_1 - \Delta H_{26}$, we obtain

$$E_{-1} = 268 - 227 = 41 \text{ kJmol}^{-1} \qquad 4.29$$

This high barrier to ring closure requires a barrier to internal rotation in the biradical of a similar magnitude[108]. Although the internal rotation barrier in trimethylene is unknown, ESR studies[10] on monoradicals such as n-propyl and isobutyl give values for CH_2 rotation <2 kJmol^{-1}.

If the higher value of D(n-C_3H_7-H) of 418 kJmol^{-1} obtained in this work is used in place of the previous value of 410 kJmol^{-1}, then E_{-1} = 25 kJmol^{-1} which, although still rather high, is more reasonable than the result obtained using a lower value of D(n-C_3H_7-H).

A similar treatment[38] for trans-cis isomerisation of 1,2-dimethylcyclobutane reveals a barrier to ring closure of 6 kJmol^{-1} using D(n-C_3H_7-H) = 422.5 kJmol^{-1} compared to a barrier of 22 kJmol^{-1} using the old thermochemistry. These studies offer further support to the higher values for C-H BDEs.

4.5 Cyclic Radicals

BDEs have been determined for C_5 - C_7 cycloalkanes. The results were found to be compatible with the steric changes occurring in the bond breaking process, as discussed below.

4.5.1 Cyclopentyl Radical

The value for ΔH_f(c-C_5H_9·) obtained in this work (105.6 kJmol^{-1}) is in good agreement with that obtained by Griller and Castelhano[67] who, using a radical buffer technique, found ΔH_f(c-C_5H_9·) = 105.0 kJmol^{-1}. These values imply D(c-C_5H_9-H) = 402 kJmol^{-1}, very similar to that obtained for D(i-C_3H_7-H) and

typical of a secondary C-H bond.

A slightly lower value has been obtained by Benson and co-workers[109] from a study of the kinetics of the reaction

$$I_2 + c\text{-}C_5H_{10} \longrightarrow 2HI + c\text{-}C_5H_8 \qquad 4.30$$

The value obtained for $D(c\text{-}C_5H_9\text{-}H)$ of 397 $kJmol^{-1}$ is in good agreement with that obtained in this work, particularly considering the lack of agreement generally obtained between other results from iodination and radical buffer techniques.

Ferguson and Whittle[110] have studied the photolytic bromination of C_4-C_7 cycloalkanes in a series of competitive experiments and obtained rate parameters for the reaction

$$Br\cdot + c\text{-}RH \longrightarrow HBr + c\text{-}R\cdot \qquad 4.31$$

From the measured activation energy for hydrogen abstraction from cyclopentane, the authors obtain a value for $D(c\text{-}C_5H_9\text{-}H)$ of 391 $kJmol^{-1}$ from an Evans-Polanyi relationship. Other studies have also obtained $D(c\text{-}C_5H_9\text{-}H)$ values via Evans-Polanyi relationships. Abstraction by $CF_3\cdot$ radicals[111] gives a value of 398 $kJmol^{-1}$ and abstraction by $CH_3\cdot$ radicals[111] a value of 391 $kJmol^{-1}$. Whilst these studies are in reasonable agreement, they give values up to 11 $kJmol^{-1}$ lower than that obtained in this work. This may be due, in part, to the questionable validity of Evans-Polanyi relationships to cycloalkanes[16]. The parameters used in the Evans-Polanyi equations are derived from a correlation of activation energies of hydrogen abstraction from aliphatic compounds with BDEs. The activation energies for hydrogen abstraction from cycloalkanes may be affected by the strain energies in

the cycloalkanes and their activated complexes with abstracting radicals, and these effects may be excluded from the parameters obtained from open chain molecules which are used in the Evans-Polanyi equation.

4.5.2 Cyclohexyl Radical

All previously reported values of $D(c\text{-}C_6H_{11}\text{-}H)$ have been obtained from Evans-Polanyi relationships, and therefore this work is the first determination of the quantity by a technique that does not depend upon the general validity of an empirical Evans-Polanyi relationship.

Hydrogen abstraction by Br.[110], CF_3.[111] and CH_3.[111] from cyclohexane lead to $D(c\text{-}C_6H_{11}\text{-}H)$ values of 401, 399 and 395 $kJmol^{-1}$ respectively. These values are typical of a secondary C-H BDE (cf. $D(i\text{-}C_3H_7\text{-}H)$ = 403 $kJmol^{-1}$), whereas the value obtained in this work (420 $kJmol^{-1}$) is closer to that associated with a primary C-H bond. This apparently anomalous result will be considered in a later section.

4.5.3 Cycloheptyl Radical

$D(c\text{-}C_7H_{13}\text{-}H)$ has been determined by the same techniques as $D(c\text{-}C_6H_{11}\text{-}H)$. Evans-Polanyi relationships give values of 384, 396 and 390 $kJmol^{-1}$ for abstraction by Br.[110], CF_3.[111] and CH_3.[111] radicals respectively. These values are somewhat lower than the 399 $kJmol^{-1}$ obtained in this work which is more typical for a secondary C-H bond.

4.6 The Cyclohexane Bond Dissociation Energy

The high value of $D(c\text{-}C_6H_{11}\text{-}H)$ obtained in this work can be accounted for in a semiquantitative manner by considering the strain effects upon forming the cyclohexyl radical from cyclohexane, compared to those involved on forming cyclopentyl and cycloheptyl radicals from their corresponding cycloalkanes.

4.6.1 Relative Strain Energies in Cycloalkanes and Radicals

A qualitative explanation for a higher C-H BDE in cyclohexane, as compared with cyclopentane and cycloheptane, may be found in a consideration of the changes in ring strain and hydrogen eclipsing interactions on forming cyclic radicals from their parent hydrocarbons. First, consider the geometries of cyclopentane and cyclohexane and their corresponding radicals.

Cyclopentane, if planar, would be virtually free of ring strain since the angles of a regular pentagon (108°) are very close to the tetrahedral angle (109° 28'). However, such a structure would have five eclipsing methylene groups, resulting in an eclipsing strain of 60 $kJmol^{-1}$ [115]. To relieve some of this strain, the ring adopts a puckered envelope form or a half chair which, while increasing angle strain by 18 $kJmol^{-1}$, relieves eclipsing strain by 33 $kJmol^{-1}$.

On formation of the cyclopentyl radical, a set of planar trigonal bonds form at the radical centre[127], resulting in an increase in ring strain over that in cyclopentane. However, the introduction of the planar radical centre causes two partially eclipsing methylene interactions to be removed, giving a reduction in eclipsing strain. Thus, on forming the cyclopentyl radical from cyclopentane, the changes in eclipsing and ring strain interactions are in opposition. The geometries of cyclopentane and the cyclopentyl radical are shown in Figure 4.3.

In contrast to the strained cyclopentane molecule, cyclohexane has perfect tetrahedral geometry about the carbon atoms and no ring strain when compared to open chain compounds, as measured by heats of combustion[112]. Also, in its most stable form, the chair, adjacent

methylene groups are fully staggered thus minimising eclipsing interactions.

Figure 4.3

Geometries of Cyclopentane and Cyclopentyl

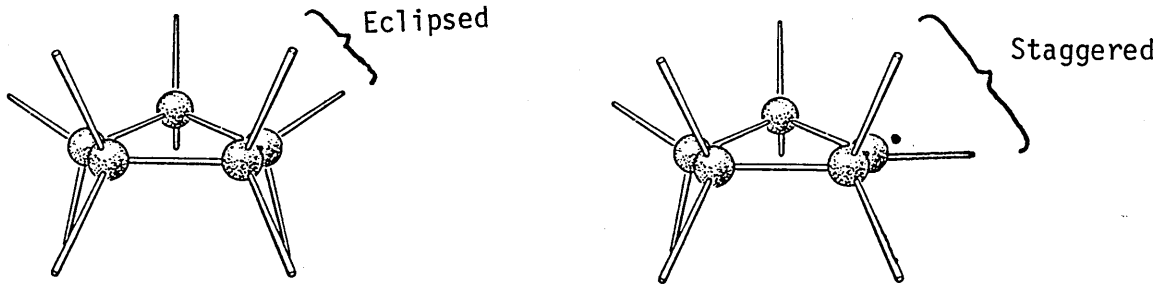

On forming the cyclohexyl radical from cyclohexane ring strain is introduced as the radical centre becomes planar, analogous to the formation of cyclopentyl from cyclopentane. However, whereas two eclipsing interactions are partially relieved on forming cyclopentyl from cyclopentane, for the fully staggered cyclohexane molecule two eclipsing interactions are introduced as the radical is formed and the geometry about the radical centre becomes trigonal[127]. Thus, the two forms of strain incurred on forming the cyclohexyl radical from cyclohexane are working in the same direction, whereas they are opposed for cyclopentyl formation from cyclopentane. The geometries of cyclohexane and cyclohexyl are shown in Figure 4.4.

The formation of cycloheptyl from cycloheptane is somewhat analogous to the formation of cyclopentyl from cyclopentane. Thus, ring strain increases as the trigonal radical centre forms but steric interactions

are relieved. The latter is due, in part, to a reduction of hydrogen interactions across the seven-membered ring, which is somewhat overcrowded[114].

Figure 4.4

Geometries of Cyclohexane and Cyclohexyl

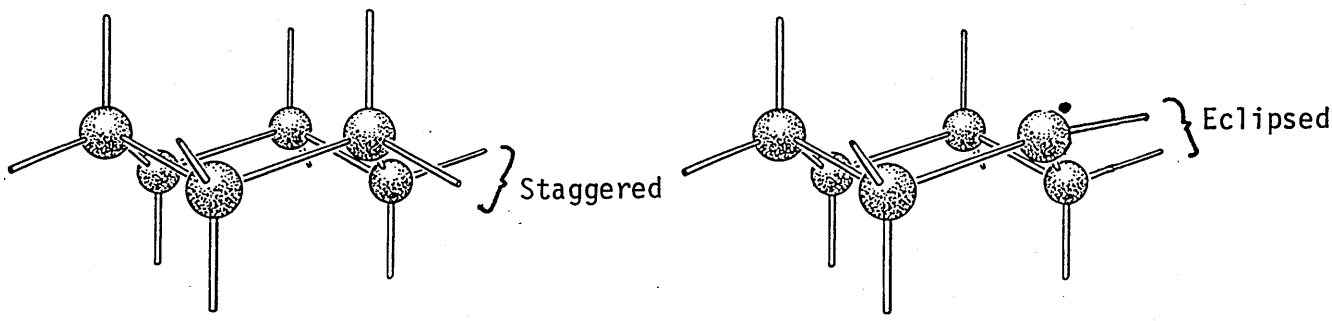

The qualitative arguments regarding the effect of strain on the formation of cyclic radicals reveal that the increase of strain on forming cyclohexyl radicals from cyclohexane is greater than the corresponding strain increases for the formation of cyclopentyl and cycloheptyl radicals. This increase in strain on forming cyclohexyl radicals from cyclohexane will result in a higher $D(c\text{-}C_6H_{11}\text{-}H)$ value than the corresponding values for cyclopentane and cycloheptane.

These qualitative arguments can be considered semi-quantitatively by analogy to hydrogen eclipsing interactions in ethane where a 12 $kJmol^{-1}$ barrier exists to rotation about the C-C bond[112]. This barrier may be represented by the potential energy diagram shown in Figure 4.5

Figure 4.5

Potential Energy Diagram for Ethane

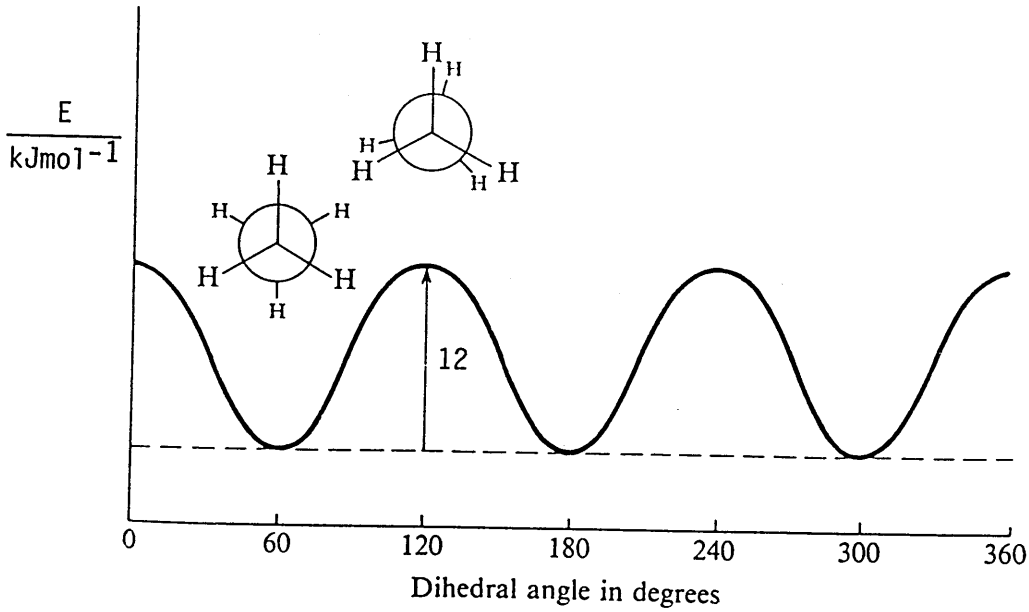

If we assume angular ring strain increases by a similar amount on formation of cyclopentyl and cyclohexyl radicals from their corresponding cycloalkanes, then any differences in total strain will be due to eclipsing interactions. Thus, as cyclopentane relieves eclipsing methylene interaction on forming cyclopentyl we may, by analogy to ethane, assign a relief of 16 $kJmol^{-1}$ of strain since four C-H bonds are no longer eclipsing and three eclipsing C-H bonds in ethane have a 12 $kJmol^{-1}$ barrier to rotation. Similarly, as forming cyclohexyl from cyclohexane involves producing two C-H eclipsing interactions we can assume, by analogy, this adds 8 $kJmol^{-1}$ of strain. This suggests there is an additional 24 $kJmol^{-1}$ of strain incurred on formation of cyclohexyl from cyclohexane over that incurred on forming cyclopentyl from cyclopentane. This difference compares favourably with the observed difference in $D(c\text{-}C_5H_9\text{-}H)$ and $D(c\text{-}C_6H_{11}\text{-}H)$ of 18 $kJmol^{-1}$ obtained from this work, although the difference in strain will probably be slightly lower since the above argument assumes

cyclopentane and cyclohexyl are fully eclipsed which is not the case for the former at least.

4.6.2 Kinetic Evidence to Support High Strain in Cyclohexyl

For any reaction at a ring carbon atom, changes in co-ordination number and hybridisation occur during the motion along the reaction co-ordinate from ground to transition state[112]. If these changes lead to an increase in strain in the transition state, compared to that in an acyclic analogue, then the reaction rate will be retarded, relative to the open chain compound. Conversely, relief of strain leads to a relative acceleration of rate.

These effects will be most pronounced in endothermic reactions where, in accordance with the Hammond Postulate[113], a late transition state occurs in which the C-H bond is broken to a greater extent, leading to a more free radical-like intermediate. Thus, for hydrogen abstraction from cycloalkanes the effect should be pronounced where, for example, bromine is the abstracting radical since current thermochemistry[27] suggests this reaction is endothermic by 30 - 50 $kJmol^{-1}$ for C_5-C_7 cycloalkanes.

Abstraction rates from C_5-C_{12} cycloalkanes have been measured relative to methylene positions in open chain compounds by Bunce and Hadley[114]. Their results for C_5-C_7 cycloalkanes are shown in Table 4.6

These data demonstrate that hydrogen abstraction by bromine from cyclopentane and cycloheptane occurs at a higher rate than abstraction from open chain positions, whereas the converse is true for abstraction from cyclohexane. Where the abstraction reaction is exothermic, as is the case when chlorine is the abstracting radical, then the abstraction reactions occur at similar rates. This effect is as

predicted by the Hammond Postulate since the transition state occurs early in the reaction and presumably shows little or no free radical character.

Table 4.6

Reactivities per Methylene Group of Cycloalkanes Towards Hydrogen Abstraction Relative to Open Chain Methylenes[114].

Abstracting Radical	T/°C	Relative Rates C_5	C_6	C_7
Br·	74.5	1.47	0.47	3.25
Br·	124.5	1.31	0.70	2.83
Cl·	0	1.00	1.00	1.04
Cl·	49.5	1.05	1.02	1.05

From the abstraction data shown in Table 4.6 Bunce and Hadley[114] obtained the relative activation energies of abstraction from cycloalkanes by bromine atoms, relative to open chain positions. These results show abstraction by bromine atoms from cyclopentane and cycloheptane have respective activation energies 2.6 and 3.1 $kJmol^{-1}$ lower than the activation energy of abstraction from open chain compounds. Conversely, the activation energy for abstraction from cyclohexane is 9.2 $kJmol^{-1}$ higher than that from open chain compounds. Thus, the activation energy for abstraction from cyclohexane is approximately 12 $kJmol^{-1}$ higher than the corresponding activation energies of abstraction from cyclopentane and cycloheptane. This value appears to partially reflect the 24 $kJmol^{-1}$ difference in strain between cyclohexyl and cyclopentyl radicals derived in section 4.6.1 by analogy to ethane eclipsing interactions. Also, it is of similar magnitude to the D(R-H) difference (18 $kJmol^{-1}$) between

cyclohexane and cyclopentane obtained in this work.

4.6.3 Comparison with MM2 Results

Heats of formation of cycloalkyl radicals have been determined from MM2 calculations[116,117]. These results are given in Table 4.7

Table 4.7

$\Delta H_f(R\cdot)$ Values from MM2 Calculations [a)]

R·	Allinger and Iman[117]	Courtnedge[116]	This work
$cC_5\cdot$	95.4 (392)	99.2 (396)	105.6 (402)
$cC_6\cdot$	58.6 (398)	58.6 (398)	78.7 (420)
$cC_7\cdot$	50.5 (385)		63.2 (399)

a) All values $kJmol^{-1}$. Numbers in parenthesis are corresponding D(R-H) values.

These results are in accord with previous empirical studies[110,111] in both absolute values of $D(c\text{-}C_6H_{11}\text{-}H)$ and differences between D(C-H) for the 3 compounds. However, the results do not support the 20 $kJmol^{-1}$ difference obtained from this work nor do they conform with the semi quantitative considerations of changes in steric strain and eclipsing interaction upon the formation of the radicals.

However, MM2 calculations offer some quantitative support for the changes in strain energies on forming cycloalkyl radicals from cycloalkanes. The calculated steric energies for cycloalkanes and corresponding radicals are given in Table 4.8.

Table 4.8

Steric Energies From MM2 Calculations[116]

R·	Steric Energy/kJmol^{-1} RH	R·	Δstrain
c-C_5H_9·	47.7	39.5	-8.2
c-C_6H_{11}·	27.4	25.6	-1.8

Thus, the differences in strain (Δ strain) of forming the radical from the corresponding cycloalkane follow the qualitative argument outlined in section 4.6.1. Thus, there is a greater relief of strain on forming cyclopentyl from cyclopentane than on forming cyclohexyl from cyclohexane. One interesting aspect of the calculations is the apparent relief of strain in forming cyclohexyl, in complete contrast to the qualitative argument. The origin of this counter-intuitive result is not known.

4.7 Kinetics of Cyclic Radical Recombinations

4.7.1 Previous Studies

There have been relatively few previous studies of cycloalkyl radical recombination kinetics. Data only exist for termination rates ($k_d + k_c$) in solution[75]. Previous gas phase studies have yielded k_{d/k_c} ratios for cyclopentyl and cyclohexyl radicals[75,118], without obtaining absolute or relative values for k_c.

A previous solution study[119] has indicated that cyclopentyl termination occurs at approximately the same rate as ethyl and iso-propyl recombination. This result is consistent with recombination of simple alkyl radicals occurring at close to the diffusion controlled limit in solution[120] which, in solvents of normal viscosity,

is $\sim 2 \times 10^9$ $lmol^{-1}s^{-1}$.

The self termination rate constant for cyclohexyl radicals in solution also occurs at close to the diffusion controlled rate. In cyclohexane solution $k_d + k_c$ has been measured at 6×10^8 $lmol^{-1}s^{-1}$ by the rotating sector method[121] and at 1.4×10^9 $lmol^{-1}s^{-1}$ by a rotating sector method employing ESR detection[122]. In benzene the rate constant is 3.6×10^8 $lmol^{-1}s^{-1}$ [121], in reasonable agreement with the results in cyclohexane. Disproportionation – to – combination ratios for cyclohexyl radicals in cyclohexane have been determined[123] giving $k_d/k_c = 1.1$. This allows k_c for cyclohexyl radicals to be estimated as $\sim 5 \times 10^8$ $lmol^{-1}s^{-1}$.

Cyclopentyl and cyclohexyl radicals have also been generated by the radiolysis of water vapour containing low concentrations of the cycloalkanes[118]. These studies demonstrate that the geometric mean rule holds for these radicals, i.e.

$$\frac{k_{cp\cdot ch}^2}{k_{cp}k_{ch}} \sim 4$$

where $k_{cp\cdot ch}$ is the rate constant for cross combination of cyclopentyl and cyclohexyl radicals and k_{cp} and k_{ch} the respective self combination rates for cyclopentyl and cyclohexyl radicals. This result suggests there is nothing unusual in the recombination behaviour of either radical. Also, from measurements of recombination products, the same work allows k_{cp}/k_{ch} to be estimated as ~ 1.2.

The above results therefore suggest that the recombination rate constants of cyclopentyl and cyclohexyl radicals are approximately equal and close to the diffusion controlled limit.

However, a study by Tedder and co-workers[124] on the reaction of cyclohexyl radicals with carbon tetrachloride in the gas phase yields results suggesting $k_{ch} < 1 \times 10^7$ $lmol^{-1}s^{-1}$. This very low value is particularly interesting since a study from the same laboratory of the reaction of cyclopentyl radicals with carbon tetrachloride[125] is consistent with $k_{cp} = 6 \times 10^9$ $lmol^{-1}s^{-1}$. Thus, the gas phase recombination rate constant for cyclopentyl radicals is apparently more than two orders of magnitude greater than that for cyclohexyl radicals, a phenomenon not observed in solution studies. These gas phase recombination rate constants have been reinvestigated in this work.

4.7.2 Results Obtained In This Work

Both cyclopentyl and cyclohexyl radical recombination rate constants have been measured relative to n-pentyl radical recombination, using a radical buffer technique in the gas phase at 430K. The results of these studies show

$$\frac{k_{cp}}{k_{np}} = 0.24 \qquad \text{and} \qquad \frac{k_{ch}}{k_{np}} = 0.16$$

where k_{np} is the rate constant for n-pentyl radical recombination. Since it is generally accepted[75] that rate constants for radical recombination are independent of chain length, the recombination rate constant for n-pentyl radical recombination may be equated to that for n-propyl radical recombination which has been measured at 1×10^{10} $lmol^{-1}s^{-1}$ [95]. Therefore,

$$k_{cp} = 2.4 \times 10^9 \text{ lmol}^{-1}\text{s}^{-1} \quad \text{and} \quad k_{ch} = 1.6 \times 10^9 \text{ lmol}^{-1}\text{s}^{-1}$$

and the ratio $k_{cp}/k_{ch} = 1.5$. These results are in good agreement

with those obtained for iso-propyl radical recombination at the same temperature where $k_{i\text{-}pr} = 5 \times 10^9$ $lmol^{-1}s^{-1}$ [69].

Recombination rate constants obtained by the radical buffer technique have previously been questionable. For example, Benson[68] determined the ^{t}butyl recombination rate constant as 2.5×10^5 $lmol^{-1}s^{-1}$ whereas the currently accepted value[69] is 1.5×10^9 $lmol^{-1}s^{-1}$ at 415K. The low value obtained was shown to be due to errors in the radical thermochemistry.

In this work the thermochemistry of the buffer reactions was measured directly and is therefore independent of literature values of thermochemical quantities. Hence, such large errors are unlikely in this work.

The evidence therefore suggests that the low value for cyclohexyl recombination obtained by Tedder[124] is anomalous. The low value was later accounted for[125] by a significant entropy loss in the cyclohexyl radical recombination process, due to restrictions in the bending vibrations of the cyclohexyl radical in the transition state. This effect is not observed in solution studies, however, where 'normal' rates are observed for cyclohexyl recombination. Moreover, there are no other reports of abnormally low rates of radical recombination, including those involving medium and large rings[75]. Only in spin forbidden recombinations are 'low' rates observed, for which good reasons exist[83].

Finally, it is interesting to consider the implications to the thermochemistry of cyclohexyl radicals if k_{ch} was equal to 1×10^7 $lmol^{-1}s^{-1}$. The radical buffer study involving cyclohexyl and n-pentyl radicals in this work gave

$$\frac{k_{ch}}{k_{np}} \quad K^2_{ch\cdot np} \quad = \quad 0.56$$

where $K_{ch\cdot np}$ is the equilibrium constant for the reaction

$$c\text{-}C_6H_{11}I \; + \; n\text{-}C_5H_{11}\cdot \rightleftharpoons n\text{-}C_5H_{11}I \; + \; c\text{-}C_6H_{11}\cdot$$

Taking k_{ch} as 1×10^7 $lmol^{-1}s^{-1}$ and $k_{np} = 1 \times 10^{10}$ $lmol^{-1}s^{-1}$ gives $K_{ch\cdot np} = 23.7$ at 430K. From Appendix 1 $\Delta S = 13$ $JK^{-1}mol^{-1}$ for the above reaction and therefore, from the van't Hoff equation, $\Delta H = -5.7$ $kJmol^{-1}$. Combining this value with the heats of formation for the other components of the buffer reaction which are given in Appendix 1 and Table 4.4 gives $\Delta H_f(c\text{-}C_6H_{11}\cdot) = 71.2$ $kJmol^{-1}$ implying $D(c\text{-}C_6H_{11}\text{-}H) = 413$ $kJmol^{-1}$. Taken together, the kinetic data obtained by Tedder and that described here, lead to the conclusion that the C-H bond in cyclohexane is considerably stronger than a typical secondary C-H bond ($\sim$400 $kJmol^{-1}$). This conclusion, which gives further support to the thermochemical study by ESR spectroscopy and the intuitive arguments concerned with strain, seems inescapable.

Appendix 1

Literature Values of Thermochemical Quantities

R·	$S^o(R\cdot)$ / $JK^{-1}mol^{-1}$	$S^o(RI)$ / $JK^{-1}mol^{-1}$	$\Delta H_f(RI)$ / $kJmol^{-1}$	$\Delta H_f(R\cdot H)$ (h) / $kJmol^{-1}$
$CH_3\cdot$	194 (a)	253 (e)	15.4 ±0.9 (h)	-74.5 ±0.4
$C_2H_5\cdot$	248 (a)	296 (f)	-9.0 ±0.9 (h)	-84.0 ±0.2
n-$C_3H_7\cdot$	290 (a)	339 (g)	-32.5 ±1.7 (h)	-104.8 ±0.3
i-$C_3H_7\cdot$	290 (b)	325 (g)	-41.6 ±1.7 (h)	-104.8 ±0.3
c-$C_5H_9\cdot$	312 (c)	362 (c)	-12.4 ±2.0 (c)	-78.4 ±0.8
c-$C_6H_{11}\cdot$	326 (d)	365 (d)	-51.0 ±4.0 (h)	-123.3 ±0.3
c-$C_7H_{13}\cdot$	345 (d)	392 (d)	-53.1 ±4.0 (d)	-118.2 ±0.6
n-$C_5H_{11}\cdot$	364 (d)	416 (d)	-71.1 ±4.0 (d)	-146.5 ±0.4

	$\Delta H_f(R\cdot)$ / $kJmol^{-1}$
H·	218.0 (i)
I·	106.8 (i)

(a) Reference 32; (b) Reference 38; (c) Reference 109;

(d) From group additivity, Reference 4; (e) E. Gelles and K.S. Pitzer J. Am. Chem. Soc., 75, 5259 (1953); (f) Reference 14;

(g) S. Furuyama, D.M. Golden and S.W. Benson, J. Chem. Thermodynamics, 1, 363 (1969); (h) Reference 15; (i) Codata Bull. No. 28, ICSU Codata, Paris, 1978. J. Chem. Thermodynamics, 10, 903 (1978)

Appendix 2

Results of Thermochemical Experiments

a) Ethyl/n-Propyl

(i) Static System

Run	T/°C	$[n\text{-}C_3H_7I]/[C_2H_5I]$	$[C_2H_5\cdot]/[n\text{-}C_3H_7\cdot]$	K
65	-51	1.00	2.81	2.81
66	-50.5	1.00	2.83	2.83
67	-50.5	1.00	2.95	2.95
23	-40	1.00	2.98	2.98
24	-40	1.00	2.94	2.94
25	-40	1.00	2.82	2.82
45	-27	1.00	2.91	2.91
46	-28	1.00	3.00	3.00
47	-31	1.00	2.67	2.67
48	-29	1.00	2.83	2.83
57	-25	1.00	2.67	2.67
60	-25	1.00	2.81	2.81
61	-24	1.00	2.84	2.84
62	-25	1.00	2.95	2.95
38	-20.8	1.00	2.30	2.30
39	-18.8	1.00	2.32	2.32
40	-21.8	1.00	2.58	2.58
12	-12	1.00	2.43	2.43
9	0	1.00	2.44	2.44
33	0.5	1.00	2.22	2.22
34	-3	1.00	2.20	2.20
35	-3	1.00	2.47	2.47
80	-4	1.00	2.48	2.48
82	-3	1.00	2.46	2.46
6	19	1.00	2.00	2.00
10	22.5	1.00	2.06	2.06
42	22	1.00	2.16	2.16
43	22.5	1.00	2.04	2.04
44	23.5	1.00	2.07	2.07
50	20	1.00	1.99	1.99
51	22	1.00	2.04	2.04
53	21	1.00	2.38	2.38
54	19	1.00	2.31	2.31
55	19	1.00	2.25	2.25
75	26	1.00	2.28	2.28
76	25	1.00	1.74	1.74
77	26	1.00	1.79	1.79
26	41	1.00	1.91	1.91
27	41	1.00	2.07	2.07
28	41	1.00	1.83	1.83
70	51	1.00	1.91	1.91
71	50.5	1.00	1.90	1.90
72	51	1.00	1.89	1.89

(ii) Flow System

Run	T/°C	$[n\text{-}C_3H_7I]/[C_2H_5I]$	$[C_2H_5\cdot]/[n\text{-}C_3H_7\cdot]$	K
249	-19.0	0.50	5.46	2.73
248	-5.8	0.50	5.22	2.61
247	5.9	0.50	5.24	2.62
246	18.8	0.50	4.74	2.37
245	30.6	0.50	4.20	2.10
244	43.0	0.50	4.62	2.31

b) Methyl/Ethyl

Run	T/°C	$[CH_3I]/[C_2H_5I]$	$[C_2H_5\cdot]/[CH_3\cdot]$	K
224a	-46.9	19.44	1.60	31.1
224b	-47.0	19.44	1.61	31.3
228a	-37.5	20.56	1.46	30.1
228b	-37.0	20.56	1.54	31.7
223a	-28.1	19.44	1.71	33.2
223b	-27.0	19.44	1.71	33.2
227a	-30.2	20.56	1.60	32.8
227b	-29.0	20.56	1.62	33.4
221a	-20.0	20.36	1.51	30.7
221b	-18.7	20.36	1.59	32.4
226a	-20.6	20.56	1.57	32.2
226b	-19.5	20.56	1.70	34.9
222a	-15.0	19.44	1.67	32.5
222b	-14.8	19.44	1.76	34.2
220a	-4.0	19.51	1.74	34.0
220b	-3.9	19.51	1.52	29.6
225a	-3.0	20.56	1.40	28.8
225b	-3.0	20.56	1.49	30.6

c) Methyl/n-Propyl

Run	T/°C	$[CH_3I]/[n\text{-}C_3H_7I]$	$[n\text{-}C_3H_7\cdot]/[CH_3\cdot]$	K
234	-53.5	7.49	1.43	10.7
236	-50.0	7.84	1.62	12.7
231a	-41.6	7.55	1.35	10.2
231b	-40.5	7.55	1.72	13.0
241	-38.0	6.89	1.96	13.5
242	-35.7	6.89	1.97	13.6
232a	-27.4	7.55	1.77	13.4
232b	-26.6	7.55	2.05	15.5
239	-23.0	6.89	2.03	14.0
240	-22.0	6.89	2.09	14.4
230a	-18.1	7.55	1.66	12.5
230b	-18.2	7.55	2.04	15.4

Run	T/°C	$[CH_3I]/[n\text{-}C_3H_7I]$	$[n\text{-}C_3H_7\cdot]/[CH_3\cdot]$	K
237	-13.0	6.89	1.80	12.4
238	-11.7	6.89	2.26	15.6
229a	-4.2	7.55	1.67	12.6
229b	-4.2	7.55	1.83	13.8

d) n-Propyl/i-Propyl

Run	T/°C	$[n\text{-}C_3H_7I]/[i\text{-}C_3H_7I]$	$[i\text{-}C_3H_7\cdot]/[n\text{-}C_3H_7\cdot]$	K
207	-35.0	31.58	2.88	91.1
208	-35.0	30.78	2.88	88.5
209	-33.9	39.96	2.23	89.1
210	-16.3	39.96	1.95	77.9
211	-16.3	39.96	1.91	76.4
212	-6.2	39.96	1.75	70.0
213	-6.1	39.96	1.78	71.1
214	6.9	40.37	1.71	69.1
215	6.8	40.37	1.87	75.5
216	25.0	40.37	1.60	64.7
217	25.7	40.37	1.63	65.8
218	44.2	40.37	1.30	52.4
219	44.8	40.37	1.45	58.4

e) n-Propyl/Cyclopentyl

Run	T/°C	$[n\text{-}C_3H_7I]/[c\text{-}C_5H_9I]$	$[c\text{-}C_5H_9\cdot]/[n\text{-}C_3H_7\cdot]$	K
168	-51.2	29.22	6.02	176.0
175	-47.2	30.31	4.82	146.0
181a	-43.9	45.31	3.72	168.7
181b	-44.0	45.31	2.69	122.1
169a	-28.6	29.43	4.35	128.0
169b	-30.5	29.43	3.81	112.0
182b	-30.2	45.31	2.97	134.4
174a	-21.3	30.32	4.06	123.0
174b	-20.8	30.32	3.79	115.0
183a	-15.9	45.31	2.54	115.1
183b	-15.8	45.31	2.69	122.0
173	-10.0	30.30	4.03	122.0
180a	-9.7	30.61	2.71	82.9
180b	-9.4	30.61	2.95	90.4
179a	10.0	30.39	2.49	75.7
179b	9.8	30.39	2.51	76.2
170	28.0	28.76	2.39	68.6
178a	29.3	30.35	2.10	63.8
178b	30.0	30.35	2.19	66.5

Run	T/°C	$[n\text{-}C_3H_7I]/[c\text{-}C_5H_9I]$	$[c\text{-}C_5H_9\cdot]/[n\text{-}C_3H_7\cdot]$	K
171a	38.4	30.34	1.89	57.4
171b	38.6	30.34	2.35	71.2
160	44.5	15.75	3.03	47.8
161	44.7	15.73	4.04	63.5
162	44.7	14.50	2.99	43.3
148	51.3	9.96	6.08	60.6
149	51.6	25.25	1.79	45.2
150	51.7	40.98	1.38	56.4
176a	50.7	30.89	1.74	53.6
176b	51.1	30.89	1.72	53.2
177a	50.1	30.71	1.52	46.6
177b	50.6	30.71	1.92	58.9

f) Ethyl/Cyclopentyl

Run	T/°C	$[C_2H_5I]/[c\text{-}C_5H_9I]$	$[c\text{-}C_5H_9\cdot]/[C_2H_5\cdot]$	K
202a	-19.8	40.86	1.66	67.9
202b	-20.7	40.86	1.15	46.9
191a	-16.7	39.67	1.13	45.0
191b	-16.6	39.67	1.29	51.2
198a	-0.3	41.10	1.07	44.0
201a	0.0	40.86	1.06	43.5
201b	0.9	40.86	1.02	41.5
199a	3.0	41.10	1.33	54.6
199b	3.8	41.10	0.95	39.2
193a	13.7	39.56	0.69	27.4
193b	13.9	39.56	1.09	43.3
194a	13.5	39.35	1.05	41.5
194b	14.5	39.35	0.94	37.0
195a	14.3	39.13	0.87	34.0
195b	14.9	39.13	0.80	31.3
188a	22.0	39.77	0.82	32.8
188b	23.0	39.77	0.79	31.5
189a	22.5	39.45	0.75	29.7
189b	23.7	39.45	0.85	33.4
196a	35.2	41.10	0.82	33.6
197a	35.4	41.10	0.62	25.3
197b	35.8	41.10	0.69	28.4
190a	55.3	39.49	0.44	17.4
190b	56.1	39.49	0.62	24.3
200a	59.7	30.34	0.64	19.3
200b	61.2	30.34	0.87	26.5

g) n-Propyl/Cyclohexyl

Run	T/°C	$[n\text{-}C_3H_7I]/[c\text{-}C_6H_{11}I]$	$[c\text{-}C_6H_{11}\cdot]/[n\text{-}C_3H_7\cdot]$	K
275	-40.0	0.699	2.33	1.63
285	-31.7	0.502	5.36	2.69
276	-22.5	0.501	2.50	1.25
286	-9.5	0.506	4.68	2.37
277	-4.0	0.501	5.07	2.54
279	31.0	0.501	4.73	2.37
284	42.6	0.502	4.08	2.05
274	59.4	0.701	3.14	2.20

h) n-Propyl/Cycloheptyl

Run	T/°C	$[n\text{-}C_3H_7I]/[c\text{-}C_7H_{13}I]$	$[c\text{-}C_7H_{13}\cdot]/[n\text{-}C_3H_7\cdot]$	K
255	-22.5	91.9	4.04	371.0
268	-23.4	336.0	0.81	272.7
269	-23.1	336.0	1.05	353.4
266	-16.2	320.4	0.70	225.2
267	-16.3	320.4	0.87	279.6
264	-3.9	320.4	0.79	252.8
265	-4.5	320.4	0.78	249.5
260	10.6	149.7	1.58	237.0
261	10.5	149.7	1.53	229.0
272	10.9	197.8	1.15	226.6
273	11.0	197.8	1.31	259.5
258	27.2	149.7	1.16	174.0
259	26.9	149.7	1.48	221.3
270	28.1	197.8	0.97	192.3
271	28.6	197.8	1.00	197.3
256	38.7	149.7	0.98	146.8
257	39.2	149.7	1.07	159.9
252	57.8	78.2	1.31	102.4
253	58.3	78.2	1.35	105.8
254	58.6	78.2	1.82	142.3
262	58.0	149.7	0.73	110.0
263	58.0	149.7	0.79	117.9

i) n-Pentyl/Cyclopentyl

Run	T/°C	$[n\text{-}C_5H_{11}I]/[c\text{-}C_5H_9I]$	$[c\text{-}C_5H_9\cdot]/[n\text{-}C_5H_{11}\cdot]$	K
288a	-19.5	38.76	3.06	118.6
289a	-7.1	38.76	3.13	121.4
288b	12.9	38.76	2.18	84.5
287a	25.5	29.91	1.91	57.1
287b	40.2	29.91	1.34	40.2
289b	46.8	38.76	1.07	41.4

j) n-Pentyl/Cyclohexyl

Run	T/°C	$[n\text{-}C_5H_{11}I]/[c\text{-}C_6H_{11}I]$	$[c\text{-}C_6H_{11}\cdot]/[n\text{-}C_5H_{11}\cdot]$	K
291b	14.6	0.493	5.19	2.56
290a	19.1	0.493	5.82	2.87
290b	37.8	0.493	4.67	2.30
291a	61.4	0.493	4.75	2.34

k) Dependence of K on Total Iodoalkane Concentration for the n-Propyl/i-Propyl System

Run	T/°C	$[n\text{-}C_3H_7I]/[i\text{-}C_3H_7I]$	$[i\text{-}C_3H_7\cdot]/[n\text{-}C_3H_7\cdot]$	[RI]	K
205	-35.3	32.45	1.35	0.5	43.8
206	-35.0	31.55	1.78	1.5	56.3
207	-34.8	31.58	2.88	2.5	91.1
208	-33.8	30.78	2.88	3.9	88.5
209	-33.9	39.96	2.23	3.0	89.1

a) Results for the Kinetic Study of the n-Pentyl/Cyclohexyl Buffer Reaction.

Run	Initial Pressure/torr			Total Pressure	Time	$[n\text{-}C_5H_{11}I]/[c\text{-}C_6H_{11}I]$		$\frac{[(c\text{-}C_6H_{11})_2]}{[n\text{-}C_{10}H_{22}]}$	$\frac{k_{ch}}{k_{np}} \cdot K^2_{ch.np}$ (a)
	$c\text{-}C_6H_{11}I$	$n\text{-}C_5H_{11}I$	DTBP	torr	min	Initial	Final		
K1	41.3	41.2	14.6	97.1	180	1.00	1.13	0.384	0.43
K2	66.1	66.0	23.3	155.4	960	1.00	1.66	0.218	0.38
K3	24.8	24.7	17.4	66.9	60	1.00	1.19	0.231	0.28
K5	107.1	25.3	23.3	155.7	1050	0.24	0.32	11.76	0.91
K6	53.5	12.7	11.7	77.9	105	0.24	0.34	5.03	0.42
K7	26.4	105.2	23.3	154.9	30	3.98	3.87	0.064	0.99
K8	13.2	52.6	11.7	77.5	30	3.98	3.89	0.033	0.51
K9	19.8	78.9	17.5	116.2	945	3.98	5.47	0.024	0.54
K10	13.2	52.6	11.7	77.5	240	3.98	4.35	0.033	0.57
K12	31.3	37.4	9.8	78.5	30	1.20	1.30	0.320	0.50
K13	23.0	45.7	9.8	78.5	225	1.20	2.27	0.084	0.38
K14	31.3	37.4	9.8	78.5	1050	1.20	1.98	0.148	0.37
K15	23.0	45.7	9.8	78.5	60	1.99	2.40	0.106	0.51
K16	31.3	37.4	9.8	78.5	210	1.20	1.32	0.255	0.40
K17	18.3	36.6	7.7	62.6	1110	1.99	2.96	0.108	0.66
K18	25.0	29.9	7.7	62.6	8520	1.20	2.35	0.344	1.08

(a) Equal to (average iodoalkane ratio)^2 x alkane ratio ; k_{ch} and k_{np} are the rate constants for cyclohexyl radical and n-pentyl radical recombination respectively, $K_{ch.np}$ the equilibrium constant for the buffer reaction.

b) Results for the Kinetic Study of the n-Pentyl/Cyclopentyl Buffer Reaction.

Run	Initial Pressure/torr			Total Pressure	Time	$[n\text{-}C_5H_{11}I]/[c\text{-}C_5H_9I]$		$\frac{[(c\text{-}C_5H_9)_2]}{[n\text{-}C_{10}H_{22}]}$	$\frac{k_{cp}}{k_{np}} \cdot K^2_{cp.np}$ (a)
	$c\text{-}C_5H_9I$	$n\text{-}C_5H_{11}I$	DTBP	torr	min	Initial	Final		
K19	61.6	59.9	6.5	128.0	217	0.97	0.98	30.36	29.0
K21	14.7	149.6	15.2	179.5	270	10.26	16.21	0.222	38.9
K22	7.4	75.6	7.6	90.6	1035	10.26	24.09	0.180	53.1
K23	11.1	113.4	11.4	135.9	290	10.26	16.32	0.199	35.2
K24	7.4	75.6	7.6	90.6	110	10.26	15.39	0.177	29.1
K25	24.5	158.1	18.2	200.8	60	6.45	8.06	0.589	31.0
K26	49.6	99.5	15.0	164.1	870	2.00	3.24	5.343	36.6
K27	9.8	63.2	7.3	80.3	255	6.45	11.10	0.417	32.1
K28	37.2	74.6	11.2	123.0	135	2.00	2.58	6.529	34.2
K29	19.6	126.5	14.8	160.9	60	6.45	8.22	0.596	32.1
K30	62.1	124.4	18.7	205.2	165	2.00	2.23	9.806	43.8
K32	24.8	49.7	7.5	82.0	360	2.00	2.77	5.957	33.9

(a) Equal to (average iodoalkane ratio)^2 x alkane ratio ; k_{cp} and k_{np} are the rate constants for cyclopentyl radical and n-pentyl radical recombination respectively, $K_{cp.np}$ is the equilibrium constant for the buffer reaction.

References

1. M. Gomberg, J. Am. Chem. Soc., 22, 757 (1900)
2. F. Paneth and W. Hofeditz, Berichte, 62, 1335 (1929)
3. F.C. James and J.P. Simons, Int. J. Chem. Kin., 6, 887 (1974)
4. S.W. Benson, 'Thermochemical Kinetics', 2nd Ed., Wiley, New York (1976)
5. H.M. Frey and R. Walsh, Chem. Rev., 69, 103 (1969)
6. P.D. Pacey and J.H. Purnell, J. Chem. Soc., Faraday Trans. 1, 68, 1462 (1972)
7. J.A. Kerr and M.J. Parsonage, 'Evaluated Data on Gas Phase Addition Reactions', Butterworth, London (1972)
8. R.W. Fessenden and R.H. Schuler, J. Chem. Phys., 39, 2147 (1963)
9. D.C. Nonhebel, J.M. Tedder and J.C. Walton, 'Radicals', Cambridge University Press, Cambridge (1979)
10. H. Fischer in 'Free Radicals', (Ed. J.K. Kochi), Vol. II, Chapter 19, Wiley, New York (1973)
11. S.W. Benson, J. Chem. Ed., 42, 502 (1965)
12. D.A. Johnson, 'Some Thermodynamic Aspects of Inorganic Chemistry' 2nd Ed., Cambridge University Press, Cambridge (1982)
13. JANAF Thermochemical Tables 2nd Ed., Ed. D.R. Stull, H. Prophet, NSDRS, NBS-37, U.S. Government Printing Office, Washington D.C. (1971)
14. J.D. Cox and G. Pilcher, Thermochemistry of Organic and Organometallic Compounds, Academic Press, London (1970)
15. J.B. Pedley and J. Rylance, Sussex - NPL Computer Analysed Data: Organic and Organometallic Compounds, University of Sussex, England (1977)
16. J.A. Kerr, Chem. Rev., 66, 465 (1966)

17. D.M. Golden and S.W. Benson, Chem. Rev., 69, 125 (1969)

18. H.E. O'Neal and S.W. Benson, 'Kinetic Data on Gas Phase Unimolecular Reactions', National Reference Data Service, NSRDS - NBS 21, U.S. Dept. of Commerce (1970)

19. Arrehenius, 2. Phys. Chem., 4, 226 (1889)

20. J.H. van't Hoff, 'Etudes de Dynamique Chemique', F. Muller and Co., Amsterdam (1884)

21. S.W. Benson, 'The Foundations of Chemical Kinetics', McGraw-Hill Book Co. Inc., New York (1960)

22. F.O. Rice and K.F. Herzfeld, J. Am. Chem. Soc., 56, 284 (1934)

23. J.E. Wertz and J.R. Bolton, 'Electron Spin Resonance, Elementary Theory and Practical Applications', McGraw-Hill, New York (1972)

24. F. Daniels and P.L. Veltman, J. Chem. Phys., 7, 756 (1939)

25. A.T. Blades and G.W. Murphy, J. Am. Chem. Soc., 74, 6219 (1952)

26. W. Tsang, J. Chem. Phys., 41, 2487 (1964)

27. D.F. McMillen and D.M. Golden, Ann. Rev. Phys. Chem., 33, 493 (1982)

28. A. MacColl, J. Chem. Soc., 964 (1955)

29. O. Sackur, Ann. Physik, 36, 598 (1911); 40, 67 (1913)

30. H. Tetrode, Ann. Physik, 38, 434 (1912)

31. G.N. Lewis and M. Randall, 'Thermodynamics', McGraw-Hill, New York (1961)

32. J.H. Purnell and C.P. Quinn, J. Chem. Soc., 4049 (1964)

33. J. Pacansky, D.E. Horne, G.P. Gardini and J. Bargon, J. Phys. Chem., 81, 23 (1977)

34. J. Pacansky and H. Coufal, J. Chem. Phys., 72, 3298 (1980)

35. J. Pacansky and J.S. Chang, J. Chem. Phys., 74, 5539 (1981)

36. J. Pacansky and B. Schraeder, J. Chem. Phys., 78, 1033 (1983)

37. W.L. Hase and H.B. Schlegel, J. Phys. Chem., 86, 3901 (1982)

38. W. Tsang, J. Am. Chem. Soc., 107, 2872 (1985)

39. M. Szwarc, Chem. Rev., 47, 75 (1950)

40. G.L. Estban, J.A. Kerr and A.F. Trotman-Dickenson, J. Chem. Soc., 3873, 3879 (1963)

41. J.R. McNesby and A.S. Gordon, J. Am. Chem. Soc., 79, 4593 (1951)

42. R.R. Baldwin, R.W. Walker and R.W. Walker, J. Chem. Soc., Far. Trans. I, 76, 825 (1980)

43. G. Atri, R.R. Baldwin, G.A. Evans and R.W. Walker, J. Chem. Soc., Far. Trans., I, 74, 366 (1978)

44. R.R. Baldwin, G.R. Drewery and R.W. Walker, J. Chem. Soc., Far Trans. I, 80, 2827 (1984)

45. W. Tsang, J. Chem. Phys., 43, 352 (1965)

46. W. Tsang, J. Chem. Phys., 41, 2487 (1964)

47. W. Tsang, Int. J. Chem. Kin., 1, 245 (1969)

48. W. Tsang, J. Chem. Phys., 44, 4283 (1966)

49. W. Tsang, Int. J. Chem. Kin., 10, 821 (1978)

50. R. Hiatt and S.W. Benson, J. Am. Chem. Soc., 94, 25 (1972)

51. R. Hiatt and S.W. Benson, J. Am. Chem. Soc., 94, 6886 (1972)

52. R. Hiatt and S.W. Benson, Int. J. Chem. Kin., 4, 151 (1972)

53. R. Hiatt and S.W. Benson, Int. J. Chem. Kin., 4, 479 (1972)

54. M.H. Baghal-Vayjooee, A.J. Colussi and S.W. Benson, J. Am. Chem. Soc., 101, 3214 (1978)

55. M.J. Rossi and D.M. Golden, Int. J. Chem. Kin., 11, 969 (1979)

56. R. Walsh, Acc. Chem. Res., 14, 246 (1981)

57. A.S. Rodgers, 'ACS Symposium Series 66', Ed. J.W. Root, Am. Chem. Soc., Washington D.C., (1978)

58. G.N. Spokes and S.W. Benson, J. Am. Chem. Soc., 89, 2525 (1967)

59. G.N. Spokes and S.W. Benson, Agnew Chem. Int. Ed., 12, 534 (1973)

60. P.J. Robinson and K.A. Holbrook, 'Unimolecular Reactions', Wiley Interscience, London (1972)

61. D.M. Golden, K.Y. Choo, M.J. Perona and L.W. Piszkiewicz, Int. J. Chem. Kin., 8, 381 (1976)

62. M.H. Baghal-Vayjooee, A.J. Colussi and S.W. Benson, Int. J. Chem. Kin., 11, 147 (1979)

63. S.P. Heneghan, P.A. Knoot and S.W. Benson, Int. J. Chem. Kin., 13, 677 (1981)

64. M.G. Evans and M. Polanyi, Trans. Far. Soc., 34, 11 (1938)

65. K.D. Bartle, P.G. Butcher, C.J. Harding and D.R. Roberts, J. Chem. Ed., 55, 742 (1978)

66. A.L. Castelhano, P.R. Marriott and D. Griller, J. Am. Chem. Soc., 103, 4262 (1981)

67. A.L. Castelhano and D. Griller, J. Am. Chem. Soc., 104, 3655 (1982)

68. R. Hiatt and S.W. Benson, Int. J. Chem. Kin., 5, 385 (1973)

69. D.A. Parkes and C.P. Quinn, J. Chem. Soc., Faraday 1, 72, 1952 (1976)

70. J. Wisniak and A. Tamir, Physical Sciences Data Journal, 'Mixing and Excess Thermodynamic Properties', Elsevier, New York (1978)

71. S.W. Benson and J.H. Buss, J. Chem. Phys., 29, 546 (1958)

72. S.W. Benson, F.R. Cruickshank, D.M. Golden, G.R. Haugen, H.E. O'Neal, A.S. Rodgers, R. Shaw and R. Walsh, Chem. Rev., 69, 279 (1969)

73. J.A. Kerr, 'Free Radicals', Ed. J.K. Kochi, John Wiley, New York (1973)

74. J.A. Hawari, S. Davis, P.S. Engel, B.C. Gilbert and D. Griller, J. Am. Chem. Soc., 107, 4721 (1985)

75. M.J. Gibian and R.C. Corley, Chem. Rev., 73, 441 (1973)

76. G.M. Burnett and H.W. Melville, 'Technique of Organic Chemistry', Ed. Weissberger, 2nd Edn., Vol. 8, Part 2, Wiley (1963)

77. A. Shepp, J. Chem. Phys., 24, 939 (1956)

78. D.A. Parkes, D.M. Paul and C.P. Quinn, J. Chem. Soc., Far. 1, 72, 1935 (1976)

79. R.G.W. Norrish and G. Porter, Nature, 164, 685 (1950)

80. N. Basco, D.G.L. James and R.D. Stuart, Int. J. Chem. Kin., 2, 215 (1970)

81. H.E. van den Berg, A.B. Callear and R.J. Norstrom, Chem. Phys. Letters, 4, 101 (1969)

82. A.V. Cunliffe, 'Internal Rotations in Molecules', Ed. W.J. Orville-Thomas, Wiley, London (1974)

83. J. Troe, Ann. Rev. Phys. Chem., 29, 223 (1978)

84. M.H. Baghal-Vayjooee and S.W. Benson, J. Am. Chem. Soc., 101, 2838 (1979)

85. G.A. Olah, S.C. Narrang, B.G. Balaram Gupta and R. Malhotra, J. Org. Chem., 44, 1247 (1979)

86. A. Maccoll, J. Chem. Soc., 247 (1955)

87. A. Vogel, A Textbook of Practical Organic Chemistry, Including Qualitative Organic Analysis, 3rd Ed., Longman, New York (1956)

88. W. Meiser, Berichte, 32, 2049 (1899)

89. R.M. Stratt and S.G. Desjardins, J. Am. Chem. Soc., 106, 256 (1984)

90. P.D. Pacey and J.H. Wimalasena, J. Phys. Chem., 88, 5657 (1984)

91. J.C. Traeger and R.G. McLoughlin, J. Am. Chem. Soc., 103, 3647 (1981)

92. K.E. McCulloh and V.H. Dibeler, J. Chem. Phys., 64, 4445 (1976)

93. S.W. Benson, 'Frontiers of Free Radical Chemistry', Ed. W.A. Pryor, Academic Press, New York (1980)

94. M. Brovard, P.D. Lightfoot and M.J. Pilling, J. Phys. Chem., 90, 445 (1986)

95. H. Adachi and N. Basco, Int. J. Chem. Kin., 13, 367 (1981)

96. R.M. Marshall and L. Rahman, J. Chem. Soc. Chem. Comm., 614 (1976)

97. R.M. Marshall and L. Rahman, Int. J. Chem. Kin., 9, 705 (1977)

98. H.E. O'Neal and S.W. Benson, Int. J. Chem. Kin., 1, 221 (1969)

99. P. Arrowsmith and L.J. Kirsch, J. Chem. Soc., Far. Trans. I, 74, 3016 (1978)

100. D.M. Golden, L.W. Piszkiewicz, M.J. Perona and P.C. Beadle, J. Am. Chem. Soc., 96, 1645 (1974)

101. H. Adachi, N. Basco and D.G.L. James, Int. J. Chem. Kin., 11, 995 (1979)

102. D.G. Hughes, R.M. Marshall and J.H. Purnell, J. Chem. Soc. Faraday I, 70, 594 (1974)

103. D.G. Hughes and R.M. Marshall, Int. J. Chem. Kin., 7, 413 (1975)

104. R.M. Marshall and J.H. Purnell, J. Chem. Soc. Chem. Comm., 764 (1972)

105. T.S. Chambers and G.B. Kistiakoswky, J. Am. Chem. Soc., 56, 399 (1934)

106. B.S. Rabinovitch, E.W. Schlag and K.B. Wiberg, J. Chem. Phys., 28, 504 (1958)

107. R.G. Bergman, 'Free Radicals, Chapter 5', Ed. J.K. Kochi, John Wiley, New York (1973)

108. W. von E. Doering, Proc. Nat. Acad. Sci. USA, 78, 5279 (1981)

109. S. Furuyama, D.M. Golden and S.W. Benson, Int. J. Chem. Kin., 2, 83 (1970)

110. K.C. Ferguson and E. Whittle, J. Chem. Soc. Faraday Trans., 68, 2618 (1971)

111. S.H. Jones and E. Whittle, Int. J. Chem. Kin., 2, 479 (1970)

112. E.L. Eliel, 'Stereochemistry of Carbon Compounds', McGraw-Hill Book Co., New York (1962)

113. G.S. Hammond, J. Am. Chem. Soc., 77, 334 (1955)

114. N.J. Bunce and M. Hadley, J. Org. Chem., 39, 2271 (1974)

115. E.L. Eliel, N.L. Allinger, S.J. Angyal and G.A. Morrison, 'Conformational Analysis', John Wiley, New York (1965)

116. J. Courtnedge, Private Communication

117. M.R. Imam and N.L. Allinger, J. Mol. Struct., 126, 345 (1985)

118. N. Fujisaki and T. Gaumann, Int. J. Chem. Kin., 14, 1059 (1982)

119. D. Griller and K.U. Ingold, Int. J. Chem. Kin., 6, 453 (1974)

120. K.U. Ingold, 'Free Radicals', Vol. I, Ed. J.K. Kochi, Wiley, New York (1973)

121. R.D. Burkhart, J. Phys. Chem., 73, 2703 (1969)

122. D.J. Carlsson and K.U. Ingold, J. Am. Chem. Soc., 90, 7047 (1968)

123. W.A. Cramer, J. Phys. Chem., 71, 1171 (1967)

124. J. Currie, H. Sidebottom and J. Tedder, Int. J. Chem. Kin., 6, 481 (1974)

125. I. Matheson, J. Tedder and H. Sidebottom, Int. J. Chem. Kin., 15, 905 (1983)

126. S. Ogawa and R.W. Fessenden, J. Chem. Phys., 41, 994 (1964)

127. J.K. Kochi, 'Advances in Free-Radical Chemistry', Ed. G.H. Williams, 5, 189, Eleck Science, London (1975)